Social Resilience to Flooding: A Case Study of Material Stocks in Surrey, British Columbia

by

Stephanie Vong

A thesis
presented to the University of Waterloo
in the fulfillment of the
thesis requirement for the degree of
Master of Science
in
Geography

Waterloo, Ontario, Canada, 2024

© Stephanie Vong 2024

Author's Declaration

I hereby declare I am the sole author of this thesis. This a true copy of the thesis, including any required final revisions, as accepted by my examiners.

I understand that my thesis may be electronically available to the public.

Abstract

The United Nations 2030 Agenda for Sustainable Development is a call for international action towards social, economic, and environmental sustainability. The integration of different sustainable development goals can alleviate the impacts of climate change and advance the development of more sustainable infrastructure and resilient communities. One of the core impacts of warmer global temperatures is rising sea levels and increased severity and frequency of storms. As part of the Sustainable Development Goals (SDG) 9, 11 and 13 is to strengthen infrastructure and community resilience to improve the adaptive capacity of cities related to climate hazards.

This research presents a methodology based on a spatial approach to model flooding and sea level rise in the City of Surrey. It further identifies vulnerable regions and infrastructure (i.e. buildings and roads) that would be impacted. LiDAR data was used to create a Digital Elevation Model for identifying inundated areas, which improves the accuracy of current flood modelling approaches. To assess the amount of material stocks that would be potentially lost to flooding and sea level rise, this research applies a bottom-up approach using Geographic Information Systems (GIS) for quantifying and analyzing material stocks associated with buildings and roads. This enhanced understanding of the spatial distribution of material stocks and estimated the quantity that could be lost to different flood scenarios. A social flood resilience index was created using census data and the previous flood analysis to inform disaster risk management and climate change adaptation efforts. This was created by applying a combination of GIS and statistical analysis.

Results of this study indicate that a 1/100 return period could affect nearly 12.59% of buildings and 27.17% of roads. Combined with a sea level rise of 1.0 m, this would affect most roads and buildings in Crescent Beach, Cloverdale, Colebrook, Mud Bay, Nico-Wynd and Semiahmoo First Nation. At a 1/10 return period, the total amount of building material stocks impacted is 87,039.20 t/capita compared to 87,574.74 t/capita at a 1/100 scenario. Compared to a 1 metre rise in sea level, the total amount of building material stocks impacted is 1,192,606.43 t/capita and 3,445,953.29 kt at a 2.5 metre sea level rise scenario. As for roads, a 1/10 return

period had an estimate of 8,209.83 t/capita impacted compared to 8,232.09 t/capita at a 1/100 return period. Compared to a 1 metre sea level rise scenario had an estimate of 905,479.07 t/capita impacted and 790,506.45 t/capita at a 2.5 metre sea level rise scenario.

The social resilience analysis found that areas with low resilience and high flood risk were highly concentrated in Cloverdale and South Surrey. Areas with high resilience and low flood risk had the highest concentration in Newton and Fleetwood. Social indictors attributed with low resilience were an older population (65 years and over), high immigration status, no knowledge of official languages, low income, and high unemployment rate. Indicators attributed to high resilience were greater percentage of home ownership, high household income, and high value of dwelling. This study demonstrates the value of linking social resilience to flooding as it can inform planning and policy to address underlying social factors and inform future actions to build resilience.

Keywords: Flooding, Sea Level Rise, Geographic Information Systems (GIS), Digital Elevation Model (DEM), Light Detection and Ranging (LiDAR), Material Stock Analysis (MSA), Social resilience, Social Resilience Index (SoRI)

Acknowledgements

First and foremost, I would like to express my sincere gratitude to my supervisor, Dr. Su-Yin Tan, for your unconditional support, enthusiasm, and invaluable guidance throughout this research. I am especially grateful for your motivation as without it this thesis would not have been possible.

I would like to thank my committee members, whose work demonstrated to me the importance of climate impact assessments and the potential of material stocks for informing infrastructure resilience to endure climate change. Thank you for inspiring me to pursue and contribute to a meaningful and growing area of research.

A special thanks to my sister, Cherry and my best friend Evelyn for your immense encouragement, smiles, and support during this long and challenging journey. My deepest gratitude goes to my parents for their love and believing in me as I pursued my graduate studies. Thank you sharing in my ups and downs and for the sacrifices you have made in support of my education.

Table of Contents

Author's Declaration ii
Abstract iii
Acknowledgements v
List of Tables ix
List of Figures x
Introduction 1
1.1 Background 1
1.1.1 Flooding and Material Stocks 3
1.1.2 Flooding and Social Resilience 8
1.2 Overview of Research Design and Questions 11
1.3 Study Area 12
1.4 Structure of Thesis 14
1.4 References 15
2.0 Development of a GIS-based Method to Evaluate Flood Risk and Sea Level Rise Impacts . 24
2.1 Introduction 24
2.2 Background of flooding and sea level rise in Surrey 24
2.3 Methods to forecast flooding and sea level rise 25
2.3.1 Types of Remote Sensing Technologies 26
2.3.2 Sea Level Rise 29
2.4 Methodology 32
2.4.1 The Bluespot Model 32
2.4.2 Preparing the data 32
2.4.3 Identifying bluespots – Tool Outputs 33
2.4.4 Flood Scenarios 33
2.5 Results 36
2.5.3 Temporal analysis of buildings and roads 37
2.5.1 Risk Maps of Critical Infrastructure 38
2.6 Discussion 41
2.7 Limitations 43
2.8 References 45
3.0 Connecting Manuscript 1 and 2 52
4.0 Accounting for building and road material stocks for the City of Surrey, British Columbia. 53

4.1 Introduction 53
4.1.1 Socioeconomic Metabolism 53
4.2 Methodology 56
4.2.1 Data Collection and Creating a Geodatabase 57
4.2.2 System Boundary and Data Sources 57
4.2.3 Material Intensities 58
4.3 Assigning Building Occupancy Classes 58
4.3.1 Physical Size of Buildings 59
4.3.2 Material Intensities for Buildings 59
4.3.3 Building Material Stocks 62
4.4 Assigning Road Classes 62
4.4.1 Road Pavement Structures 63
4.4.2 Physical Size of Road 63
4.4.3 Material Intensities for Roads 64
4.4.5 Road Material Stocks 65
4.5 Results 66
4.5.1 Material Stock (MS) in buildings 66
4.5.2 Material Stocks in Roads 73
4.5.3 Temporal Changes of Material Stock 79
4.5.4 Spatiotemporal analysis of material stocks 82
4.6 Discussion 87
4.6.1 Building and road material stocks in the City of Surrey 87
4.6.2 Temporal and spatial distribution of building and road material stocks 89
4.6.3 Vulnerability of Material Stocks to Flooding and Sea Level Rise 91
4.7 Limitations 92
4.8 References 94
5.0 Connecting Manuscript 2 and 3 99
6.0 Mapping social resilience to flooding 100
6.1 Introduction 100
6.1.1 Census Data: Social and Spatial Indicators 101
6.1.2 The Social Resilience Index 103
6.2 Methodology 104
6.2.1 SoRI scores and principal component analysis 105
6.2.2 Social Resilience Mapping 106

6.2.3 Social Resilience and Flood Risk Matrix 107
6.3 Results & Findings 107
6.3.1 City of Surrey 108
6.3.2 Spatial Distribution of SORI 111
6.4 Spatial Distribution of Social Resilience to Flood Exposure 114
6.5 Discussion 117
6.6 Limitations 119
6.7 References 122
7.0 Conclusions 125
7.1 Development of a GIS-based Method to Evaluate Flood Risk and Sea Level Rise Impacts 125
7.2 Accounting for building and road material stocks for the City of Surrey, British Columbia 126
7.3 Mapping social resilience to flooding 126
7.4 Contributions of the study 127
7.5 Future Study Directions 129
Appendix A. Supplementary Information for the City of Surrey Study Data Sources 132
A.1 Classification of Building Codes 132
A.2 Building Types 133
A.3 Equations for measuring material intensities 136
A.4 Material Intensity Summary 138
Appendix B Principal Components Analysis (PC) Procedure 139
B.1 Suitability of PCA 139

List of Tables

Table 1. Amount of precipitation for four different return periods in the City of Surrey
Table 2. Quantity of buildings and roads impacted by flooding in Surrey
Table 3. Quantity of buildings and roads impacted by sea level rise in Surrey
Table 4. Material Intensity Calculation break down of materials and material intensity classes in kg/m3
Table 5. Final material intensities summarized within each building occupancy class (kg/m3)
Table 6. Material Intensity Calculation break down of materials and material intensity classes in kg/m3
Table 7. Building material stocks by material type
Table 8. Breakdown of material stock per capita in building use-types by material category
Table 9. Percentage of breakdown of material stock per capita in building use-types by material category
Table 10. Road Material stocks by Material type
Table 11. Quantity of building material stocks impacted by flooding in tonnes per capita
Table 12. Quantity of road material stocks impacted by flooding in tonnes per capita
Table 13. Quantity of building material stocks impacted by sea level rise in tonnes per capita
Table 14. Quantity of road material stocks impacted by sea level rise in tonnes per capita
Table 15. Social Resilience Index (SoRI) variables
Table 16. Flood risk matrix comparing social vulnerability and flood exposure extents
Table 17. Summary of PCA results for the City of Surrey

List of Figures

Figure 1. Map of Surrey
Figure 2. Number of buildings constructed between 1990 and 2022
Figure 3. Number or roads constructed between 1942 and 2017 (Update chart)
Figure 4. Map of buildings and roads exposed to flooding
Figure 5. Map of buildings and roads exposed to sea level rise
Figure 6. Map of dykes exposed to flooding
Figure 7: Socio-economic metabolism conceptual diagram (modified from De Kroon, 2020; Krausmann, 2018; Wiedenhofer et al., 2015)
Figure 8. Percentage of building material stocks by material type
Figure 9. Map of building material stock distribution by community in Surrey
Figure 10. Map of building material stock distribution by dissemination area in Surrey
Figure 11. Road material sock distribution (break down of five materials) by dissemination area in Surrey
Figure 12. Percentage of road material stocks by material type
Figure 13. Map of road material stock distribution by community in Surrey
Figure 14. Map of road material stock distribution by dissemination area in Surrey
Figure 15. Road material sock distribution (break down of five materials) by dissemination area in Surrey
Figure 16. Temporal change in material stocks in buildings between 1900 and 2022
Figure 17. Temporal change in material breakdown in buildings between 1900 and 2022
Figure 18. Temporal change in material stocks in roads between 1900 and 2022
Figure 19. Temporal change in material breakdown in roads between 1900 and 2022
Figure 20. Spatial distribution in material stocks in buildings in 1999 and 2022
Figure 21. The Social Resilience Index (SoRI) for City of Surrey based on 2016 census data
Figure 22. SoRI breakdown by demographic, household composition, economic, and employment by dissemination area in Surrey
Figure 23. Map of social resiliene and flood risk by disemination are in Surrey

Introduction

1.1 Background

Over the past decade, there has been a rise in the occurrence and severity of flooding disasters worldwide, driven by the acceleration of global warming and rapid urbanization (Bouwer et al., 2010), Khosravi, 2018, Khosravi et al., 2016, Luu et al., 2018, Nardi et al., 2006, Rahmati et al., 2016). Densely populated areas are particularly vulnerable to urban flooding, as these regions become inundated due to heavy rainfall exceeding the capacity of urban drainage systems (Bouwer et al., 2010). This phenomenon is now a common and significant natural hazard in many cities worldwide, especially those experiencing rapid population growth or struggling with outdated and insufficient drainage systems and flood protection infrastructure.

In Canada, urban flooding presents an ongoing and escalating challenge for municipalities, insurance providers, and homeowners. The damage caused by these events often reach tens to hundreds of millions of dollars. For instance, major flooding in Vancouver from November 13-15, 2021 caused damages estimated at $7.5 US billion and led the province to declare a state of emergency (Slepian, 2021). The flood displaced thousands of residents from their homes and resulted in numerous injuries (Slepian, 2021). Highway infrastructure including roads and bridges were heavily impacted by the water, resulting in several main access routes into the province being cut off (Ministry of Transportation and Infrastructure, 2022). The total rainfall recorded for November 2021 was a record breaking 312 mm and had an estimated return period of 45 and 100 years (Gillet et. al, 2022). A separate incident in 2004 where a severe storm hit Edmonton, Alberta, resulted in insured damages of approximately $166 million, in which $143million was attributed to sewer backup (Sandink, 2007). Moreover, municipalities often find themselves experiencing multiple urban flood events occurring in relatively close succession. The City of Hamilton encountered over ten instances of widespread basement flooding linked to extreme rainfall between August 2009 and September 2010 (Sandink, 2013). These examples highlight the significant financial and infrastructural impact that flooding can have on urban areas.

Undoubtedly, flooding presents a multifaceted challenge as they impact human lives, cause substantial economic losses, and rank among the most recurrent and overwhelming natural hazards (Pradhan 2009; Khan et al. 2011; Uddin et al. 2013). Furthermore, flood risks are expected to persist and potentially worsen due to the onset of climate change (Jonkman & Dawson 2012; Korah & López 2015). However, the adverse effects of flooding can be mitigated through accurate susceptibility analysis. Over the years, the literature has employed various methods to evaluate and construct flood hazard maps (Tehrany et al. 2015; Rahmati et al. 2016). A susceptibility analysis takes into account a multitude of geographic factors, such as hydrological data (i.e. precipitation, streamflow, evaporation) and topographic data (i.e. elevation, slope, terrain to provide a comprehensive assessment of the surrounding area. (Subyani and Al-Dakheel 2009). GIS techniques play a crucial role in flood modeling and determining the extent of flood-affected areas (Pradhan et al. 2014; Tehrany et al. 2014). It integrates spatially referenced data and enables the simultaneous assessment of multiple data types, enhancing the accuracy of the analysis (Fernandez and Lutz 2010; Malczewski 2004; Yang et al. 2013).

The accuracy of flood risk mapping could help identify vulnerable areas and inform early warning, evacuation, and mitigation plans. GIS techniques play a pivotal role in flood modeling and delineating flood-prone areas, due to their effectiveness of integrating spatially referenced data across different environments. Flood susceptibility mapping involves a diverse array of both qualitative and quantitative methods. Cai et al., integrated a hydrodynamic model to investigate the risk of flooding in the urban area of Yifeng, Jiangxi Province, China, whereas Pradhan (2019) and Tehrany et al., (2014) adopted statistical models to construct flood scenario maps, employing historical data and statistical relationships to predict potential flood scenarios. More recently, numerous studies have turned to multicriteria evaluation methods (Malczewski, 2004; Marpaung et al., 2022; Yang et al. 2013). The Multicriteria Decision Analysis (MCDA) method has been widely used to combine, integrate, and evaluate factors related to flood risk. The consideration of criteria is a crucial step in the assessment process, as the inclusion or exclusion of specific criteria can significantly influence the final results. For example, Phung et al. (2016) conducted a study where they integrated flood susceptibility and health factors to create a flood consequence map for Vietnam. Their findings primarily focused on assessing the consequences

of human health factors on flooding (Phung et al., 2016). This involved incorporating variables such as population density, poverty rates, healthcare facilities, and land use to gauge the impact of flooding on these factors (Phung et al., 2016). Marpaung et al. (2022) undertook a study that combined flood susceptibility with economic factors to assess the risk posed to various goods and services. The results aimed to identify services and sectors that would be most vulnerable to economic consequences resulting from future flooding events (Marpaung et al., 2022). These two studies offer different perspectives on the multifaceted nature of flood risk assessment, highlighting the importance of considering various criteria to gain a comprehensive understanding of the potential impacts of flooding.

1.1.1 Flooding and Material Stocks

Floods often leave an enormous quantity of debris from damaged buildings and infrastructure. Estimating losses in construction material would be valuable for rebuilding and recovery after a disaster. Construction materials, essential for national economies, are sourced from the natural environment (Fischer-Kowalski et al., 2011). Materials such as fossil fuels and biomass are not typically considered part of material stocks because they are consumed rapidly and used for energy rather than being integrated into long-lasting infrastructure. Metals contribute significantly to material stocks due to their durability, long-term use, and recyclability. Non-metallic minerals also contribute to material stocks by being integral to construction and infrastructure. They have a long-term presence in material stocks but are less commonly recycled compared to metals. While fossil fuels and biomass contribute to the flow of materials in the economy, metals and non-metallic minerals build and sustain the material stock due to their long-term applications and integration into infrastructure and products. Material stocks (MS) represent in-use stocks such as machinery, buildings, and infrastructure and provide physical services for basic human needs like mobility, transport, shelter, and health (Tanikawa et al., 2015; Wiedenhofer et al., 2015; Huang et al., 2017). Given the increasing demand for buildings, numerous studies concentrate on urban material stock (Olaya et al., 2017).

The United Nations' Sustainable Development Goals (SDGs), established in 2012, emphasize the importance of sustainable material consumption in the built environment and resource management (United Nations, n.d.). These principles are reflected in SDG 13.1, which

aims to strengthen resilience to climate hazards and natural disasters, SDG 11 focusing on creating inclusive, safe, resilient, and sustainable cities and human settlements, and SDG 9.1 aiming to develop sustainable and resilient infrastructure (United Nations, n.d.). The reconstruction or replacement of structures with greater resilience—defined as the capacity of a system to absorb disturbance and still retain its basic function and structure—following a disaster would require substantial quantities of construction materials (Tabata et al., 2018). A thorough understanding of the quantity of materials stored in buildings and infrastructure is crucial for attaining these goals. These materials serve as potential secondary resources after building decommissioning (Tirado et al., 2021). They provide an environmentally sustainable solution by reducing reliance on virgin resources when extensively integrated into reuse practices within demolition waste flows (Tirado et al., 2021). This research aligns with these SDGs by identifying vulnerable infrastructure and their specific material compositions susceptible to flooding and sea level rise. Additionally, it assesses the social resilience of neighborhoods in Surrey to effectively respond and adapt to such disasters. The insights gained from this study can guide future research on sustainable construction materials and the development of resilient communities.

Recently, many studies have attempted to trace material flows and evaluate the accumulation of materials (Gontia et al., 2018; Guo, Miatto, Shi, & Tanikawa, 2019; Kleemann, Lederer, Rechberger, & Fellneret al., 2016). Most previous studies have utilized material flow and stock accounting and analysis (MFA). For instance, Tanikawa and Imura (2001) used statistical data to estimate trends in MS contained in residential buildings in Japan. Mesta et al. (2019) used a GIS model to store information about different building types, classify building stock, and map the spatial accumulation of materials in a Peruvian city. Similarly, other studies employed material stock analysis (MSA) which involves assessing and quantifying the amount, type, and flow of materials within a particular system or environment (Tanikawa et al., 2014; Tanikawa et al., 2015; Wiedenhofer et al., 2016). Tanikawa and colleagues (2009) examined MS for road networks in all Japanese prefectures. These studies provide comprehensive insights into the temporal changes and spatial distributions of accumulated MS. These analysis helps decision makers understand how processes and activities such as construction, transportation, consumption, and waste disposal are linked systematically together with inputs and outputs (Tanikawa et al., 2015). The analysis can be applied to improving resource efficiency, reducing

waste, and minimizing environmental impacts in buildings and construction. Previous MSA research highlights two main types of approaches: top-down stock analysis and bottom-up stock analysis.

The top-down approach considers the overall material flows, stocks, and trends over a long period of time (Augiseau & Barles, 2017). This analysis involves evaluating the entire system in which materials are used or managed such as studying the material flows within an organization or city (Tanikawa et al., 2015; Augiseau & Barles, 2017). There have been different applications of this approach throughout the literature, from looking at material flows and stocks at the macro level compared to looking at more specific materials, industries or applications. Using historical data, Müller (2006) incorporated population and lifestyle considerations into the MSA calculation, examining their impact on MS in the residential building sector. Other studies focus on specific sectors or industries to understand material flows with them. For instance, Hatayama et al. examined the entire life cycle of steel from extraction to manufacturing and end-of-life disposal, providing a comprehensive view of its material flows (Hatayama et al., 2010). At a more granular level, Peled and Fishman (2021) performed a material stock analysis on buildings and infrastructure in Europe. Other top-down approaches consider resource efficiency strategies and policies at the national or regional level. Volk et al. (2014) integrates regional building and infrastructure material stock and flow modelling with stakeholders, policy measures, their impacts and mutual interactions.

In contrast, the bottom-up approach starts at the level of individual components or products and aggregating upward to provide a comprehensive view of material stocks (MS) within a system or area (Tanikawa et al., 2015). This approach involves detailed data collection and measurement of materials at the micro-level, such as buildings, infrastructure components, or products, and then scaling up to understand material flows and stocks at various higher levels of aggregation (Lichtensteiger & Baccini, 2008). For instance, Bradshaw et al. (2020) conducted a material stock study at a local level on Trinket Island, utilizing the bottom-up technique to construct a comprehensive account of local material stocks for two consecutive years. They categorized the existing infrastructure on the island into ten distinct types and devised a typology based on material intensity (MI), derived from a representative sample (Bradshaw et al., 2020).

The assessment of the built area of these structures was accomplished by multiplying the physical number of objects with the material content required for a single unit of objects, quantified as MI (Heeren and Fishman, 2019). The bottom-up material stock approach is commonly used in sectors like construction, infrastructure management, and product lifecycle assessment to track and manage material usage, understand resource consumption, and support sustainability initiatives. For instance, Khumvongsa et al. (2023) adopted a bottom-up strategy to quantify the quantity of MS within the transportation infrastructure of Bangkok. It was discovered that the increase in vehicle ownership and the resultant CO2 emissions was due to a large accumulation of transportation MS (Khumvongsa et al., 2023). The study emphasizes the importance of effective urban planning as a means to prevent short-term urban redevelopment, which, in turn, can help mitigate unnecessary material consumption and associated environmental impacts, such as CO2 emissions (Khumvongsa et al., 2023).

Other approaches to material stock (MS) estimation leverage remote sensing and Geographic Information Systems (GIS) (Gontia et al., 2018; Ortlepp et al., 2016). These technologies are integrated through a computer system for collecting, managing, processing, and presenting spatial data (Ortlepp et al., 2016). It offers researchers the capability to conduct analyses at various scales, locate areas with intensive human activities and development, and compare MS across different locations and time periods (Lanau et al., 2019). For instance, Tanikawa et al. (2015) utilized GIS databases to develop a comprehensive, long-term material stock account for Japan, showcasing the accumulation of material stocks in different prefectures over time. GIS incorporates a 3D dimension encompassing latitude, longitude, and height to calculate the overall volume of buildings (Tanikawa et al., 2015). The association of building composition and the quantification of material stocks can then be linked to their corresponding locations (Tanikawa et al., 2015). This information is valuable for identifying areas characterized by higher material composition, potentially making them more susceptible to destruction, or pinpointing locations where substantial amounts of construction waste can be recycled. Satellite images and orthophotos serve as valuable tools for examining the distribution of material stocks (MS). Satellite images, by nature, capture a specific moment and location, offering a 'snapshot' perspective on stocks and flows (Lanau et al., 2019). For instance, Peled & Fishman (2021) employed radiance values from nighttime lights data extracted from satellite imagery to estimate

the total material stocks in Europe. This innovative approach addresses the challenge of limited material stock data availability and offers advantages such as spatial comparability and the potential for frequent updates. For this study, a static bottom-up approach was selected as it was considered more suitable for a local scale and efficient utilization of GIS (Lanau et al., 2019).

Few studies to date have evaluated the stock of buildings and infrastructure lost as a result of major natural disasters (Tanikawa et al., 2014). The scarcity of research in investigating the connection between environmental hazards and material stocks can be attributed to several factors. One primary reason is the limited availability of detailed data regarding the damage incurred by individual buildings, a process that demands substantial effort to collect (Thomsen & van der Flier, 2009). An exhaustive examination of the impact on individual buildings necessitates a comprehensive understanding of their structural characteristics, mechanical properties of construction materials, and their current state of preservation (Aksözen et al., 2016). Tanikawa et al. conducted a study on the repercussions of an earthquake and tsunami in Japan, focusing on the losses of building and infrastructure materials (2014). They employed GIS databases and statistical methods to estimate the spatial distribution and quantity of materials lost and the amount required for the rehabilitation of disaster-affected areas. Nonetheless, gathering this information, along with the computational effort needed, proves to be exceptionally challenging, particularly when assessing flood risk on a large building stock. In addressing this research gap, Milanesi (2018) and colleagues developed a framework aimed at defining the vulnerability of buildings to flooding based on their construction type and materials. This framework categorizes buildings into four vulnerability classes, each associated with a distinct vulnerability curve depicting the relationship between water depth and the extent of damage (Milanesi et al., 2018).

Natural disasters, such as earthquakes, tsunamis, and floods, result in significant human casualties and generate substantial disaster waste. It is crucial to have a comprehensive understanding of the quantity and composition of disaster waste to effectively implement disaster waste management measures (Maryono et al., 2015). A widely used method for estimating disaster waste involves Material Intensity Coefficients (MIC), which quantify disaster waste generation per housing unit (Kung et al., 2012; Xiao et al., 2012; Nakayama et al., 2013). This

estimation is then computed by multiplying the MIC with damage functions, contingent on the specific natural disaster type and its severity (Tanikawa et al., 2015). Typically, past disaster data are utilized for this purpose, however, several limitations exist in this approach. MIC values change over time due to technological advancements in housing, such as building materials (Heeren & Fishman, 2019). Additionally, rural housing typically has a larger floor area compared to urban housing, making MIC values calculated for urban areas unsuitable for rural applications (Lanau et al., 2020). To address these issues, this study employs Geographic Information System (GIS), which allows for the identification of housing location, type, and quantity without the need for historical MIC values (Miatto et al., 2017; Nguyen et al., 2019; Symmes et al., 2019; Tanikawa & Hashimoto, 2009). This method offers the advantage of estimating disaster waste directly from map data and can be applied to areas of any scale, as long as cartographic data is available (Tanikawa et al., 2014).

1.1.2 Flooding and Social Resilience

Resilience in the face of natural disasters has emerged as a pivotal concept in the realm of disaster management and climate adaptation. Natural disasters, ranging from floods and earthquakes to wildfires and hurricanes, pose significant threats to communities, often resulting in devastating consequences. The Sixth Assessment Report of the Intergovernmental Panel on Climate Change (IPCC) defines resilience as: "The capacity of social, economic and ecosystems to cope with a hazardous event or trend or disturbance, responding or reorganising in ways that maintain their essential function, identity and structure as well as biodiversity in case of ecosystems while also maintaining the capacity for adaptation, learning and transformation" (IPCC, 2023, pg 128). It articulates resilience as the collective ability of social systems, economic systems, and ecosystems to confront and deal with various types of threats, challenges, or disturbances. These threats can range from natural disasters and climate-related events to broader trends and changes (Cutter et al., 2010). The essence of resilience lies in the capacity of these systems to react to these disturbances or challenges in a manner that allows them to continue functioning and maintaining their core features (Chang et al., 2015). Importantly, resilience is not just about bouncing back to the way things were before a disturbance but also about adapting, learning, and sometimes undergoing transformation (IPCC, 2023). This means that resilient systems have the ability to not only recover but also to evolve and adjust in

response to the changing conditions (Cutter et al., 2010). In doing so, they can better prepare for future challenges and maintain their functionality, identity, and structure.

Similarly, social resilience reflects the capacity of communities to effectively respond to disasters, to support one another, and to adapt in ways that minimize harm and promote recovery (United Nations, n.d.). This multidimensional concept encompasses not only physical preparedness but also the strength of social connections, community cohesion, and the effectiveness of institutions in safeguarding lives and livelihoods (Cutter, 2011). Communities that are more informed and prepared will have a greater opportunity to recover quickly from weather and climate-related events (Morrow, 2008). The focus on resilience has become increasingly prominent to aid disaster risk reduction and management (100RC, 2019; The Heinz Center, 2009; The Royal Society, 2014; The World Bank, 17 2015). The exploration of social resilience is essential for understanding how societies can build the robustness needed to confront the growing challenges presented by a changing climate and an increasingly vulnerable world.

In recent years, international policy frameworks, such as the United Nations' 2015 Sendai Framework for Disaster Risk Reduction, have incorporated the concept of disaster resilience (Prevention Web, n.d.). The Sendai Framework recognizes that reducing disaster risk is critical for sustainable development and sets out key priorities for action in order to build resilience to natural and human-made hazards (Li et al, 2023). It presents a comprehensive approach to disaster risk reduction, employing 38 indicators to monitor and evaluate the progress of efforts to prevent and mitigate disaster risks (Li et al, 2023). Disaster resilience studies often employ a combination of social and physical indicators to provide a thorough evaluation of a community's capacity to withstand and recover from natural disasters (Cutter et al., 2008). Social indicators offer insights into aspects like community cohesion, preparedness, and adaptability, while physical indicators scrutinize the resilience of the built environment, infrastructure, and land use planning (Briguglio, 2003). Together, these indicators provide invaluable information for well-informed disaster risk reduction and response planning, ultimately contributing to the safeguarding of lives, property, and the environment (Oulahen et al., 2015).

Many studies have incorporated various indicators of resilience (Cutter et al., 2008; Cutter et al., 2014; Cutter, 2016; Morrow, 2008) and metrics to quantify resilience (Cutter et al., 2010; Damude et al., 2015; Joakim et al., 2016). The Social Resilience Index is a critical tool in disaster management and community development, providing a comprehensive assessment of a community's ability to withstand and recover from various shocks and stresses (Cutter et al., 2000, Cutter et al., 2008). Prior research has concentrated on evaluating resilience by employing social indicators like income, household composition, demographics, and educational attainment. Socioeconomic factors are commonly utilized to depict vulnerability and resilience to environmental risks (Cutter et al., 2000). These factors play a crucial role in guiding and prioritizing disaster risk management and climate change adaptation efforts (Cannon, 1994; Cutter, 1996; Buckle et al., 2000; Cutter et al., 2000; Oulahen et al., 2015; Rickless et al., 2019; Tapsell et al., 2002). By examining the socioeconomic characteristics, it is possible to compare populations, such as those with greater access to resources that enhance their resilience compared to populations lacking in these same attributes (Cannon, 1994; Cutter, 1996; Cutter et al., 2003; Frerks et al., 2011; Sayers et al., 2017; Sevoyan et al., 2013). By combining various socioeconomic and demographic factors, communities that are at higher risk and require targeted interventions for disaster risk reduction and response can be identified. Assessing the spatial patterns of social resilience can provide valuable insights for disaster management, policy formulation, and contribute to more effective disaster preparedness and resilience-building efforts (Morrow, 2008).

Quantitative indicators, typically drawn from sources like census data, are frequently utilized to capture socioeconomic characteristics. These indicators help explore the distribution of social and financial resources that could be accessible in the event of a disaster (Buckle et al., 2000; Cutter et al., 2003; Cutter et al., 2008; Oulahen et al., 2015; Prouse et al., 2014). Census data contains both attribute and geographic information which allows analysis of both the underlying population characteristics as well as its spatial distribution and patterns (Carrington et al., 2018; Dorling, 1993). These data may be compiled into aggregation units that represent individual socioeconomic characteristics (Mendelson, 2001). Across Canada, Statistics Canada is responsible for conducting and disseminating the census program (Statistics Canada, 2012). The census is conducted once every five years, with the most recent censuses conducted in 2016 and

2011 (Statistics Canada, 2012). Census tracts (CTs) are small, relatively stable geographic units that generally have a population between 2,500 to 8,000 people (Statistics Canada, 2012). Dissemination areas (DAs) are the smallest standard census geography units comprising of populations between 400 to 700 people (Statistics Canada, 2012). DAs are contained within CTs, such that their boundaries must respect those of the bounding CT unit (Statistics Canada, 2012). Census data helps in understanding the social fabric of a community, including social networks, community engagement, and cohesion (UNISDR, 2015). These factors play a significant role in determining the physical and social aspects of a community that can impact its ability to respond to and recover from disasters (Cutter, Boruff & Shirley, 2003). The data helps prioritize areas that may be more susceptible to certain risks and guides the allocation of resources for resilience-building efforts (Rickless et al., 2019; Sayers et al., 2017).

1.2 Overview of Research Design and Questions

Recognizing that the built environment and community dynamics are intricately linked, this study addresses a significant gap in current literature. It bridges the gap between material stocks and social resilience, to provide a more holistic understanding of the impacts of flooding on the physical and social aspects that make up the fabric of society. The research is twofold, beginning with an exploration into the vulnerability of material stocks in buildings and infrastructure to flooding events. By employing advanced modeling techniques and considering diverse scenarios, the study aims to map and quantify the potential losses and damages to these critical material resources. Simultaneously, the research conducts an analysis on the social resilience within communities affected by flooding. Leveraging a Social Resiliency Index (SoRI) and census variables, the study seeks to measure and visualize the capacity of neighborhoods to respond and adapt to the challenges posed by flooding. This dual focus on material stocks and social resilience provides a comprehensive understanding of the holistic impact of flooding, offering valuable insights for disaster preparedness, urban planning, and the development of resilient communities in the face of environmental uncertainties.

This thesis adopts a manuscript style, comprising three distinct manuscripts. The study is guided by three primary objectives:

1. *How can the influence of climate change on flooding be spatially represented in Surrey, British Columbia? How can the impacts of flooding be quantified in terms of neighborhoods and infrastructure affected?*

The first manuscript investigates this research question by developing a flood model using a LiDAR derived digital elevation model. The objective is to map at risk areas according to four different return periods and four sea level rise scenarios.

2. *Where are the concentrations of materials used in buildings and roads located in Surrey, British Columbia? How can the amount of material stocks impacted by flooding be quantified?*

The second manuscript investigates these research questions by conducting a material stock analysis of the City of Surrey. The objectives are to map and quantify current material stocks contained in buildings and roads and analyze the impacts of flooding and sea level rise to these material stocks.

3. *How might the social resiliency of communities to flooding be measured? How might this research contribute to creating more sustainable and resilient communities?*

The third manuscript investigates the resiliency of communities to flooding through conducting a social resiliency index (SoRI). Census variables are used to represent socio-economic indicators influencing the resiliency of a neighborhood. The results of the SoRI are mapped by dissemination areas to visualize spatial patterns of social resilience and compare resiliency against flooding maps.

1.3 Study Area

Surrey is a city in the province of British Columbia and located south of the Fraser River. It is the province's second largest with a population of 568, 322 and comprises of seven neighbourhoods (City of Surrey, 2022). Surrey's coastal floodplain makes up about 20% of Surrey's entire land area, stretching from Boundary Bay and Mud Bay along the Nicomekl and Serpentine rivers towards Cloverdale and Newton (City of Surrey, 2022). The floodplain also

includes the Campbell River area and Semiahmoo First Nation (City of Surrey, 2022). The floodplain is home to more than 2500 residents, over $1.5 billion in assessed property value, 13 kilometres of provincial highways, 31 kilometres of railway, over 60 square kilometres of agricultural land, recreational areas, and significant natural areas with very high biodiversity (City of Surrey, 2022). These areas are at risk to both coastal and river flooding as well as future sea level rise.

As Surrey is vulnerable to flooding due to its proximity to rivers, coastal areas, and low-lying terrain, this makes it an important area for studying flood risk and resilience. Analyzing flood risk and resilience in an urban context allows for exploration of the interplay between social, economic, and environmental factors shaping vulnerability and resilience in densely populated areas (Cutter et al., 2003). Additionally, Surrey's proactive approach to climate change adaptation and disaster risk reduction adds policy relevance to the case study (City of Surrey, 2022). The research findings can directly inform policy development and decision-making processes, fostering a more adaptive and proactive approach to managing flood risks and enhancing the overall resilience of urban areas. The availability of comprehensive geospatial data, including LiDAR elevation data, land use maps, infrastructure inventories, and demographic information, further facilitates detailed modeling and analysis of flood risk and resilience.

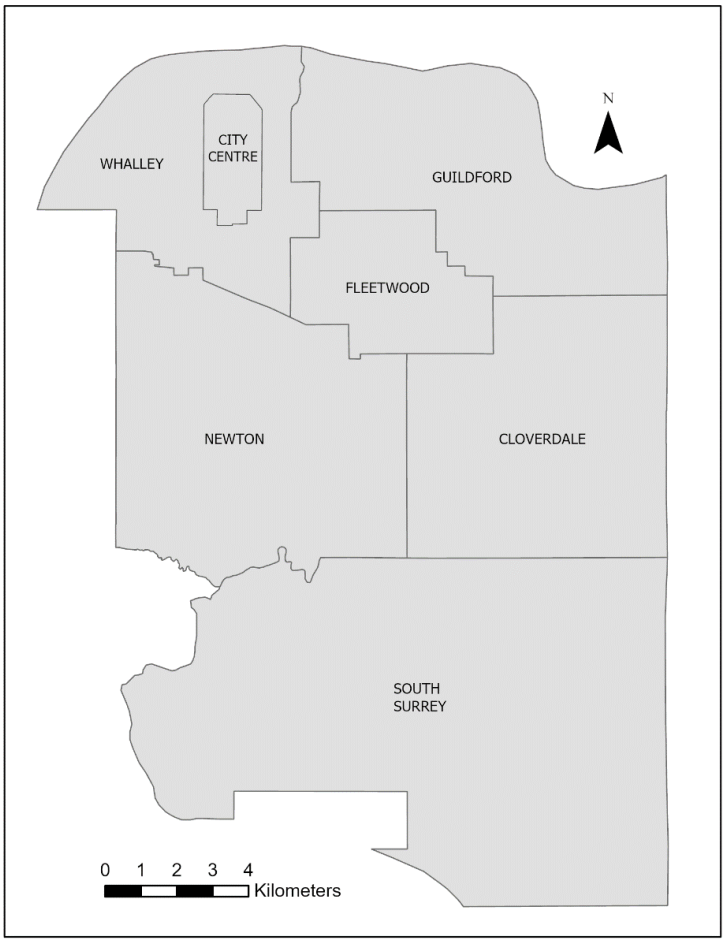


Figure 1. Map of Surrey

1.4 Structure of Thesis

This thesis is written following the manuscript option, where each of the chapters 2, 4 and 6 is a separate manuscript. The manuscripts are meant to stand alone, but together answer the broader research questions. Chapters 2 investigates the vulnerability of buildings and roads to potential flooding and sea level rise. Chapter 4 builds upon this by conducting a material stock analysis of buildings and roads for the City of Surrey. It further investigates the implications of potential flooding and sea level rise to these material stocks. Chapter 6 explores the social resilience of neighbourhoods in the City of Surrey to flooding. Chapters 3 and 5 provide linkages to connect the three manuscripts. The thesis concludes with chapter 7, which summarizes the contributions of the overall thesis and recommendations for future study directions.

1.4 References

100 Resilient Cities. (2019). *Resilient Cities, Resilient Lives – Learning from the 100RC Network*. New York, London, Mexico City, Singapore: 100 Resilient Cities.

Aksözen, M., Hassler, U., Rivallain, M., & Kohler, N. (2016). Mortality analysis of an urban building stock. *Building Research & Information, 0*, 1-19. https://doi.org/10.1080/09613218.2016.1152531

Augiseau, V., & Barles, S. (2017). Studying construction materials flows and stock: A review. Resources, *Conservation and Recycling, 123*, 153–164. https://doi.org/10.1016/j.resconrec.2016.09.002

Bouwer, L. M., Bubeck, P., & Aerts, J. C. J. H. (2010). Changes in future flood risk due to climate and development in a Dutch polder area. *Global Environmental Change, 20*(3), 463-471. https://doi.org/10.1016/j.gloenvcha.2010.04.002

Bradshaw, J., Jit Singh, S., Tan, S. Y., Fishman, T., & Pott, K. (2020). GIS-based material stock analysis (MSA) of climate vulnerabilities to the tourism industry in Antigua and Barbuda. *Sustainability, 12*(19), 8090.

Briguglio, L. (2003). The Vulnerability Index and Small Island Developing States - A Review of Conceptual and Methodological Issues. Malta: University of Malta.

Bubeck, P., Botzen, W. J. W., Suu, L. T. T., & Aerts, J. C. J. H. (2012). Do flood risk perceptions provide useful insights for flood risk management? Findings from central Vietnam. *Journal of Flood Risk Management, 5*(4), 295-302. https://doi.org/10.1111/j.1753-318X.2012.01151.x

Carrington, A., Rahman, N., & Ralphs, M. (2018). The Modifiable Areal Unit Problem: Research Planning. (*NSMAC 11, 11th Meeting of the National Statistics Methodology Advisory Committee*). South Wales: Office for National Statistics.

Chang, S. E., Yip, J. Z. K., van Zijll de Jong, S. L., et al. (2015). Using vulnerability indicators to develop resilience networks: a similarity approach. *Natural Hazards, 78*(5), 1827–1841.

Cutter, S. L., Burton, C. G., & Emrich, C. T. (2010). Disaster Resilience Indicators for Benchmarking Baseline Conditions. *Journal of Homeland Security and Emergency Management, 7*(1). https://doi.org/10.2202/1547-7355.1732

Dorling, D. (1993). Map design for census mapping. *The Cartographic Journal, 30,* 167-183.

Fernandez DS, Lutz MA. (2010). Urban flood hazard zoning in Tucumán Province, Argentina, using GIS and multicriteria decision analysis. *Eng Geol 111*, 90–98.

Fischer-Kowalski, M., Swilling, M., Von Weizsacker, E. U., Ren, Y., Moriguchi, Y., Crane, W., ... & Sewerin, S. (2011). Decoupling: natural resource use and environmental impacts from economic growth. United Nations Environment Programme.

Frerks, G., Warner, J., & Weijs, B. (2011). The Politics of Vulnerability and Resilience. *Ambiente & Sociedade, 14*(2), 105-122.

Gontia, P., Nägeli, C., Rosado, L., Kalmykova, Y., & Österbring, M. (2018). Material intensity database of residential buildings: A case-study of Sweden in the international 126 context. *Resources, Conservation and Recycling, 130*(December 2017), 228–239. https://doi.org/10.1016/j.resconrec.2017.11.022

Hatayama, H., Daigo, I., Matsuno, Y., & Adachi, Y. (2010). Outlook of the World Steel Cycle Based on the Stock and Flow Dynamics. *Environmental Science & Technology, 44*(16), 6457–6463. https://doi.org/10.1021/es100044n

Hatayama, H., Daigo, I., Matsuno, Y., & Adachi, Y. (2010). Outlook of the world steel cycle based on the stock and flow dynamics. *Environmental Science and Technology, 44*(16), 6457–6463. https://doi.org/10.1021/es100044n

Heeren, N., & Fishman, T. (2019). A database seed for a community-driven material intensity research platform. *Scientific Data, 6*, 23.

Huang, C., Han, J., & Chen, W.-Q. (2017). Changing patterns and determinants of infrastructures' material stocks in Chinese cities. Resources, *Conservation and Recycling, 123*(Supplement C), 47-53.

Hutter, G. Organizing social resilience in the context of natural hazards: a research note. *Nat Hazards 67*, 47–60 (2013). https://doi-org.proxy.lib.uwaterloo.ca/10.1007/s11069-010-9705-4

ICLEI (2019). Resilient cities, thriving cities: The evolution of urban resilience. Bonn, Germany. Intergovernmental Panel on Climate Change [Core Writing Team, H. Lee and J. Romero (eds.)]. (2023). Climate Change 2023: Synthesis Report. Contribution of Working Groups I, II and III to the Sixth Assessment Report of the Intergovernmental Panel on Climate Change. IPCC, Geneva, Switzerland. https://doi.org/10.59327/IPCC/AR6-9789291691647

Jonkman SN, Dawson RJ. (2012). Issues and challenges in flood risk management-editorial for

the special issue on flood risk management. *Water 4*, 785–792.

Khan SI, Hong Y, Wang J, Yilmaz KK, Gourley JJ, Adler RF, Brakenridge GR, Policelli F,

Habib S, Irwin D. (2011). Satellite remote sensing and hydrologic modeling for flood ınundation mapping in Lake Victoria basin: implications for hydrologic prediction in ungauged basins. *IEEE Trans Geosci Remote Sens 49*, 85–95.

Khosravi, K., et al. (2018). A comparative assessment of decision trees algorithms for flash flood susceptibility modeling at Haraz watershed, northern Iran. *Science of The Total Environment, 627*, 744-755.

Khosravi, K., Pourghasemi, H. R., Chapi, K., & Bahri, M. (2016). Flash flood susceptibility analysis and its mapping using different bivariate models in Iran: A comparison between Shannon's entropy, statistical index, and weighting factor models. *Environmental Monitoring and Assessment, 188*(12), 656.

Khumvongsa, K., Guo, J., Theepharaksapan, S., Shirakawa, H., & Tanikawa, H. (2023). Uncovering urban transportation infrastructure expansion and sustainability challenge in Bangkok: Insights from a material stock perspective. *Journal of Industrial Ecology, 27*(2), 476-490. https://doi.org/10.1111/jiec.13342

Korah PI, López FMJ. (2015). Mapping flood vulnerable areas in Quetzaltenango. Guatemala using GIS Journal of Environment and Earth Science *5*(6), 132–143.

Kung, H. Y., Chen, C. H., & Ku, H. H. (2012). Designing intelligent disaster prediction models and systems for debris–flow disasters in Taiwan. *Expert Systems with Applications, 39*(5), 5838-5856.

Lanau, M., Liu, G., Kral, U., Wiedenhofer, D., Keijzer, E., Yu, C., & Ehlert, C. (2019). Taking Stock of Built Environment Stock Studies: Progress and Prospects. Environmental Science and Technology, 53(15), 8499–8515. https://doiorg.proxy.lib.uwaterloo.ca/10.1021/acs.est.8b06652

Li, B., Gong, A., Liu, L., Li, J., Li, J., Li, L., Pan, X., et al. (2023). An Earth Observation Framework in Service of the Sendai Framework for Disaster Risk Reduction 2015–2030. *ISPRS International Journal of Geo-Information, 12*(6), 232. MDPI AG. Retrieved from http://dx.doi.org/10.3390/ijgi12060232

Li, X., Song, L., Liu, Q., Ouyang, X., Mao, T., Lu, H., Liu, L., Liu, X., Chen, W., Liu, G. (2023). Product, building, and infrastructure material stocks dataset for 337 Chinese cities between 1978 and 2020. *Scientific Data, 10*(1). https://doi.org/10.1038/s41597-023-02143-w

Li, Z., Zhu, Q., & Gold, C. (2004). Digital terrain modeling: Principles and methodology (1st ed.). Boca Raton: CRC Press.

Lichtensteiger, T., & Baccini, P. (2008). Exploration of urban stocks. *Journal of Environmental Engineering and Management, 18*(1), 41-48.

Lichtensteiger, T., & Baccini, P. (2008). Exploration of urban stocks. *Detail, 5*(6), 16.

Luu, C., Von Meding, J., & Kanjanabootra, S. (2018). Assessing flood hazard using flood marks and analytic hierarchy process approach: a case study for the 2013 flood event in Quang Nam Vietnam. *Natural Hazards, 90*(3), 1031-1050.

Malczewski J. (2004). GIS-based land-use suitability analysis: a critical overview. *Prog Plan 62*(1), 3–65.

Marpaung, F., Fernando, D., Setyaningrum, N., Lestari, S., Sulistyowati, R., & Dinanta, G. P. (2023). Multi-Criteria Decision Analysis (MCDA) for estimating economic valuation for flood risk in DKI Jakarta Province. *IOP Conference Series: Earth and Environmental Science, 1190*, 012030. https://doi.org/10.1088/1755-1315/1190/1/012030

Maryono, Nakayama, H., & Shimaoka, T. (2015). Identification of factors affecting stakeholders' intentions to promote preparedness in disaster waste management: a structural equation modeling approach. Memoirs Faculty of Engineering, *Kyushu University, 74*, 79-98.

Matsuba, M., Tanaka, Y., Yamakita, T., Ishikawa, Y., & Fujikura, K. (2020). Estimation of tsunami debris on seafloors towards future disaster preparedness: Unveiling spatial varying effects of combined land use and oceanographic factors. *Marine Pollution Bulletin, 157*, 111289. https://doi.org/10.1016/j.marpolbul.2020.111289.

Mazzorana, B., Simoni, S., Scherer, C., Gems, B., Fuchs, S., & Keiler, M. (2014). A physical approach on flood risk vulnerability of buildings. *Hydrology and Earth System Sciences, 18*(9), 3817-3836.

Mendelson, R. (2001). *Geographic Structure as Census Variables: Using Geography to Analyze Social and Economic Processes*. Statistics Canada Geography Working Paper Series Catalogue no. 92F0138MIE. Ottawa: Statistics Canada.

Miatto, A., Schandl, H., Wiedenhofer, D., Krausmann, F., & Tanikawa, H. (2017). Modeling material flows and stocks of the road network in the United States 1905–2015. *Resources, Conservation and Recycling, 127*(June), 168–178. https://doi.org/10.1016/j.resconrec.2017.08.024

Milanesi, L., Pilotti, M., Belleri, A., Marini, A., & Fuchs, S. (2018). Vulnerability to Flash Floods: A Simplified Structural Model for Masonry Buildings. *Water Resources Research, 54*(10), 7177-7197. https://doi.org/10.1029/2018WR022577

Morrow, B. H. (2008). Community Resilience: A Social Justice Perspective. CARRI Initiative: Oak Ridge National Laboratory.

Morrow, B. H. (2008). *Community Resilience: A Social Justice Perspective*. Oak Ridge: Community and Regional Resilience Initiative (CARRI). Retrieved from https://www.researchgate.net/publication/280611548_Community_resilience_A_social_justice_perspective

Müller, D. B. (2006). Stock dynamics for forecasting material flows—Case study for housing in The Netherlands. *Ecological economics, 59*(1), 142-156.

Nakayama, H., Shimaoka, T., Omine, K., Patsaraporn, P. M., & Siriratpiriya, O. (2013). Solid waste management in Bangkok at the 2011 Thailand floods. *Journal of Disaster Research,* 456-464.

Nardi, F., Vivoni, E. R., & Grimaldi, S. (2006). Investigating a floodplain scaling relation using a hydrogeomorphic delineation method. *Journal of Water Resources Research, 42*(9).

Nguyen, T. C., Fishman, T., Miatto, A., & Tanikawa, H. (2019). Estimating the Material Stock of Roads: The Vietnamese Case Study. *Journal of Industrial Ecology, 23*(3), 663–673. https://doi.org/10.1111/jiec.12773

Olaya, Y., Vásquez, F., & Müller, D. B. (2017). Dwelling stock dynamics for addressing housing deficit. Resources, *Conservation and Recycling, 123*, 187-199.

Ortlepp, R., Gruhler, K., & Schiller, G. (2016). Material stocks in Germany's non-domestic buildings: a new quantification method. *Building Research and Information, 44*(8), 840–862. https://doi.org/10.1080/09613218.2016.1112096

Oulahen, G., Mortsch, L., Tang, K., & Harford, D. (2015). Unequal Vulnerability to Flood Hazards: "Ground Truthing" a Social Vulnerability Index of Five Municipalities in Metro Vancouver, Canada. *Annals of the Association of American Geographers, 105*(3), 473-495.

Peled, Y., & Fishman, T. (2021). Estimation and mapping of the material stocks of buildings of Europe: a novel nighttime lights-based approach. Resources, *Conservation and Recycling, 169,* 105509. https://doi.org/10.1016/j.resconrec.2021.105509

Peled, Y., & Fishman, T. (2021). Estimation and mapping of the material stocks of buildings of Europe: a novel nighttime lights-based approach. *Resources, Conservation and Recycling, 169*, 105509.

Phung, D., Rutherford, S., Dwirahmadi, F., et al. (2016). The spatial distribution of vulnerability to the health impacts of flooding in the Mekong Delta, Vietnam. *Int J Biometeorol 60*, 857–865. https://doi-org.proxy.lib.uwaterloo.ca/10.1007/s00484-015-1078-7

Pradhan B, Hagemann U, Shafapour Tehrany M, Prechtel N. (2014). An easy to use ArcMap based texture analysis program for extraction of flooded areas from TerraSAR-X satellite image. *Comput Geosci 63*, 34–43.

Pradhan, B. (2009). Flood susceptible mapping and risk area delineation using logistic regression, GIS and remote sensing. *J Spat Hydrol 9*(2), 1–18.

PreventionWeb. (n.d.). Sendai Framework for Disaster Risk Reduction. Retrieved from https://www.preventionweb.net/sendai-framework/sendai-framework-for-disaster-risk-reduction

Prouse, V., Ramos, H., Grant, J. L., & Radice, M. (2014). How and when scale matters: the modifiable areal unit problem and income inequality in Halifax. *Canadian Journal of Urban Research, 23*(1), 61-82.

Rahmati O, Pourghasemi HR, Zeinivand H. (2016). Flood susceptibility mapping using frequency ratio and weights-of-evidence models in the Golastan Province Iran. *Geocarto Int 31*(1), 42–70.

Rahmati, O., Pourghasemi, H. R., & Zeinivand, H. (2016). Flood susceptibility mapping using frequency ratio and weights-of-evidence models in the Golastan Province, Iran. Geocarto *International, 31*(1), 42-70. https://doi.org/10.1080/10106049.2015.1041559 Sandink, D. (2007). Sandink, D. (2007). Sewer Backup: Homeowner perception and mitigative behaviour in Edmonton and Toronto (ICLR research paper series No. 44). Institute for Catastrophic Loss Reduction. Retrieved from https://www.iclr.org/wp-content/uploads/PDFS/sewer-backup.pdf

Rickless, D. S., Yao, X. A., Orland, B., & Welch-Devine, M. (2019). Assessing Social Vulnerability through a Local Lens: An Integrated Geovisual Approach. *Annals of the American Association of Geographers, 0*(0), 1-20.

Sandink, D. (2013). Urban flooding in Canada: Lot-side risk reduction through voluntary retrofit programs, code interpretation, and by-laws (ICLR research paper series No. 52). Institute for Catastrophic Loss Reduction. Retrieved from https://www.iclr.org/wp-content/uploads/PDFS/urban-flooding-in-canada.pdf

Sayers, P. B., Horritt, M., Penning Rowsell, E., and Fieth, J. (2017). Present and future flood vulnerability, risk and disadvantage: A UK scale assessment. A report for the Joseph Rowntree Foundation. Watlington: Sayers and Partners LLP.

Sayers, P.B., Horritt, M., Penning Rowsell, E., & Fieth, J. (2017). *Present and future flood vulnerability, risk and disadvantage: A UK scale assessment*. A report for the Joseph Rowntree Foundation. Watlington: Sayers and Partners LLP.

Sevoyan, A., Hugo, G., Feist, H., Tan, G., McDougall, K., Tan, Y., & Spoehr, J. (2013). Impact of Climate Change on Disadvantaged Groups: Issues and Interventions. Adelaide: National Climate Change Adaptation Research Facility.

Subyani AM, Al-Dakheel AM. (2009). Multivariate geostatistical methods of mean annual and seasonal rainfall in southwest Saudi Arabia. *Arab J Geosci 2*(1), 19–27.

Symmes, R., Fishman, T., Telesford, J. N., Singh, S. J., Tan, S. Y., & De Kroon, K. (2019). The weight of islands: Leveraging Grenada's material stocks to adapt to climate change. *Journal of Industrial Ecology,* 1–14. https://doi.org/10.1111/jiec.12853

Tabata, T., Morita, H., & Onishi, A. (2018). What is the quantity of consumer goods stocked in a Japanese household? Estimating potential disaster waste generation during floods. Resources, *Conservation and Recycling, 133*, 86-98.

Tanikawa, H., & Hashimoto, S. (2009). Urban stock over time: Spatial material stock analysis using 4d-GIS. *Building Research and Information, 37*(5–6), 483–502. https://doi.org/10.1080/09613210903169394

Tanikawa, H., & Hashimoto, S. (2009). Urban stock over time: Spatial material stock analysis using 4d-GIS. *Building Research and Information, 37*(5–6), 483–502. https://doi.org/10.1080/09613210903169394

Tanikawa, H., Fishman, T., Okuoka, K., & Sugimoto, K. (2015). The weight of society over time and space: A comprehensive account of the construction material stock of Japan, 1945-2010. *Journal of Industrial Ecology, 19*(5), 778–791. https://doi.org/10.1111/jiec.12284

Tanikawa, H., Fishman, T., Okuoka, K., & Sugimoto, K. (2015). The weight of society over time and space: A comprehensive account of the construction material stock of Japan, 1945–2010. *Journal of Industrial Ecology, 19*(5), 778-791.

Tanikawa, H., Managi, S., & Lwin, C. M. (2014). Estimates of lost material stock of buildings and roads due to the Great East Japan Earthquake and tsunami. *Journal of Industrial Ecology, 18*(3), 421-431.

Tanikawa, H.; Fishman, T.; Okuoka, K.; Sugimoto, K. The weight of society over time and space: A comprehensive account of the construction material stock of Japan, 1945–2010. J. Ind. *Ecol. 2015, 19*, 778–791.

Tehrany MS, Pradhan B, Jebur MN. (2014a). Flood susceptibility mapping using a novel ensemble weights-of-evidence and support vector machine models in GIS. *J Hydrol 512*, 332–343.

Tehrany MS, Pradhan B, Mansor S, Ahmad N. (2015). Flood susceptibility assessment using GIS-based support vector machine model with different kernel types. *Catena 125*, 91–101.

The Heinz Centre. (2009). *Resilient Coasts: A Blueprint for Action*. Washington: The H. John Heinz III Center for Science, Economics and the Environment. Retrieved from https://www.travelers.com/iw-documents/travelers-institute/ResilientCoastsBlueprint.pdf

The Royal Society. (2014). *Resilience to extreme weather*. London: The Royal Society. Retrieved from https://royalsociety.org/-/media/policy/projects/resilience-climate-change/resilience-fullreport.pdf

The World Bank. (2015). *Investing in Urban Resilience - Protecting and Promoting Development in a Changing World*. Washington: Office of the Publisher, The World Bank.

Thomsen, A., & van der Flier, K. (2009). Replacement or renovation of dwellings: the relevance of a more sustainable approach. *Building Research & Information, 37*(6), 649-659.

Tirado, R., Aublet, A., Laurenceau, S., Thorel, M., Louërat, M., & Habert, G. (2021). Component-Based Model for Building Material Stock and Waste-Flow Characterization: A Case in the Île-de-France Region. *Sustainability, 13*(23), 13159. https://doi.org/10.3390/su132313159

Uddin K, Gurung DR, Giriraj A, Shrestha B. (2013). Application of remote sensing and GIS for flood hazard management: a case study from Sindh province, Pakistan. *Am J Geogr Inf Syst 2*(1), 1–5. https://doi-org.proxy.lib.uwaterloo.ca/10.5923/j.ajgis.20130201.01

United Nations. (n.d.). Sustainable Development Goals. Retrieved from https://sdgs.un.org/goals

Volk, R., Stengel, J., Schultmann, F. (2014). Building Information Modeling (BIM) for existing buildings—Literature review and future needs. *Autom. Constr. 2014, 38,* 109–127.

Wiedenhofer, D., Steinberger, J. K., Eisenmenger, N., & Haas, W. (2015). Maintenance and expansion: modeling material stocks and flows for residential buildings and transportation networks in the EU25. *Journal of Industrial Ecology, 19*(4), 538-551.

Wiedenhofer, D., Steinberger, J. K., Eisenmenger, N., & Haas, W. (2015). Maintenance and expansion: modelling material stocks and flows for residential buildings and transportation networks in the EU25. *Journal of Industrial Ecology, 19*(4), 538-551.

Xiao, J., Xie, H., & Zhang, C. (2012). Investigation on building waste and reclaim in Wenchuan earthquake disaster area. Resources, *Conservation and Recycling, 61*, 109-117.

Y. Olaya, F. Vásquez, D.B. Müller. (2017). Dwelling stock dynamics for addressing housing deficit. *Resour. Conserv. Recycl., 123*, 187-199.

Yang XL, Ding JH, Hou H. (2013). Application of a triangular fuzzy AHP approach for flood risk evaluation and response measures analysis. *Nat Hazards 68*, 657–674.

2.0 Development of a GIS-based Method to Evaluate Flood Risk and Sea Level Rise Impacts

2.1 Introduction

Floods are a major severe natural catastrophe experienced in many countries around the world. In Canada, floods are one of the most frequently occurring hazards (Public Safety Canada, 2022). Hydrologic processes such as snowmelt and ice jams, hydro-meteorological factors such as short duration intense rainfall, rain on snow, or structural failures such as dam breaks influence the occurrence and severity of flooding (Environment and Climate Change Canada, 2013). Ecological systems including climate, surface water, groundwater, riparian and wetland ecosystems, vegetation patterns, geomorphology, and others also influence the characteristics of flooding (Seiler, 2002). These ecological systems are influenced by human activity, including land-use and economic development, and by individual behaviours and systems of government (Wheater and Evans, 2009). Complex interactions within and between hydrological, ecological and social systems combine to influence the risk posed to society by floods (Alfieri et al., 2016).

Floods are also one of the costliest natural disasters. Severe flooding events have been recorded in some of the most populous Canadian cities in the recent years such as: Vancouver in 2021, Montreal in 2017 and 2012, Thunder Bay in 2012, Calgary in 2013 and 2010, Winnipeg in 2009, and Toronto in 2005 and 2013 (Sandink, 2013). The enormous costs of Vancouver floods () in 2020, Calgary floods in 2013 (over $5 billion) and Toronto floods in 2005 ($587 million) and 2013 ($1.2 billion) provide some examples of costs associated with urban flooding in Canada (Sandink, 2013).

2.2 Background of flooding and sea level rise in Surrey

The two principal causes of increased flooding in Surrey's coastal floodplain are increased magnitude and intensity of rain and sea level rise. Changing climate will bring more extreme weather conditions. Surrey's winters are expected to have fewer wet day, but rainfall amounts will be significantly greater than the past on wet days (City of Surrey, 2022). This will result in increased flooding, as more runoff flows into the Nicomel, Serpentine and Campbell Rivers. The frequency and intensity of storm events with heavy precipitation are also expected to increase. In

addition, global sea level is rising due to rising temperatures that are melting glaciers and increasing the average temperature of ocean waters causing them to expand. The effects of sea level rise are anticipated to be greater than those of rainfall in Surrey's coastal floodplain. In the short-term, Surrey can expect more frequent and severe flooding from storm surges, higher sea levels, more erosion of the coastline, impacts on infrastructure, loss of beaches and coastal ecosystems, soil salinization, and groundwater pooling.

2.3 Methods to forecast flooding and sea level rise

Several approaches have been used to simulate flood magnitudes and assess flooding frequencies in catchments across the globe. Remote sensing is commonly used in flood studies as it can quickly collect data over large areas, improving forecasting accuracy and allowing for flood modelling and monitoring of flood events in real time (Klemas, 2015). It is especially useful in areas where it is challenging to collect data on the ground. For instance, in Somalia, a community-based early warning system was developed using remotely managed river gauges and an SMS alert system (Sadiq et al., 2022). This combination of technology enabled text alerts to be sent out when river levels reached a threshold point (Sadiq et al., 2022). Remote sensing technology is also useful in assessing the effectiveness of flood mitigation strategies like levees or flood barriers (Berchum et al., 2018). Aerial imagery during a flooding event can identify whether these flood mitigation structures are performing accurately and identify areas of weakness, overspill, or potential failure (Klemas, 2015).

In the past decade, there has been increasing research studies in this area, but the full potential of remotely sensed data in enhancing flood mapping, modelling and prediction has yet to be unlocked. Remote sensing technologies have some limitations regarding robustness and consistency as environmental conditions such as cloud cover, fog, rain, and pollution can affect the results (Munawar et al., 2022). Data collection and processing remotely sensed data is also time consuming and expensive (Munawar et al., 2022). However, the widespread adoption of remote sensing techniques from various airborne and spaceborne platforms will undoubtedly enhance the quality and increase the spatial and temporal coverage of such data (Yang et al., 2022). This offers new opportunities to foster understanding of flood dynamics and the ability to map and monitor floods at both local and global scales.

2.3.1 Types of Remote Sensing Technologies

Remote sensing technologies can be categorized into two types which are active and passive (Hafiz et al., 2022). Active remote sensors use their light source to gain data from the target located on the surface of the Earth, while passive remote sensing methods rely on natural light or the sun to gain this data (Hafiz et al., 2022). Active remote sensors include technologies such as Radio Detection and Ranging (Radar) and Light Detection and Ranging (LiDAR), whereas passive remote sensors use satellites to capture imagery of the target on Earth (Hafiz et al., 2022). Passive satellite sensors include spectral image acquisition methods which are divided into two main techniques: hyperspectral imaging and multispectral imaging (Hafiz et al., 2022).

2.3.1.1 Passive Remote Sensing: Spectral Image Acquisition Methods

Spectral images are three-dimensional (3-D) in nature, with two spatial dimensions and one spectral dimension (Fan et al., 2019). The hyperspectral technique acquires images with numerous continuous wavebands, while the multispectral technique acquires images with a few discrete wavebands. Sentinel-2, Landsat 7, Landsat 8, and MODIS are satellites that have used these techniques to perform different flood analysis and prediction. For instance, Wieland and Martinis (2019) presented a framework to perform flood prediction using multispectral data gained from Landsat TM and Sentinental-2 images. A convolutional neural network (CNN) was trained using these data to perform segmentation to determine water extent levels (Shengxin et al., 2015). Another study used Advanced Scatterometer (ASCAT) to develop a rain-fall-runoff model that forecasts floods (Massari et al, 2018). The direct association between the satellite, soil moisture and rainfall are utilized in the model to make decisions regarding the future occurrence of flood. Using multispectral data acquired from the Sentinel-1 satellite, Shahabi et al. (2020) identified flood-prone areas through a machine learning method. These technologies are useful for accurate flood mapping and analysis.

2.3.1.2 Active Remote Sensing: Radar

Another remote sensing technology, radar, uses radio waves to find various characteristics of objects such as their direction, speed, location, and range. Radar sensors used for flood monitoring include European Remote-Sensing Satellite (ERS-1), Japanese Earth Resources Satellite (JERS-1), RADARSAT, Environmental Satellite (ENVISAT), Phased Array L-Band Synthetic Aperture Radar (PAL-SAR), Radar Imaging Satellite (RISAT), and Sentinel 1. Radar

sensors are able to penetrate through cloud cover and are unaffected by severe rain and atmospheric haze during flooding events (Vincente, 2011). The data collected are able to provide accurate real-time flood damage assessment since they discriminate land and water precisely (Matgen et al., 2007). The flat surface of water reflects the signals away from the senor causing a decrease in the intensity of returned radiation as compared to the incident radiation causing a darker pixel in the image (Kalantar et al., 2021). Thus, areas with water show dark pixels as compared to the pixels formed by the deflection through land areas.

Radar data revolutionized data extraction since data can be collected even during extreme weather conditions. This technology has been useful in monitoring flood conditions and estimating flood damage (Janizadeh et al., 2021). For instance, one study applied a change detection methodology to determine the extent of flooding using radar images captured during a winter flood event in Yorkshire, UK (Clement et al., 2018). Results were validated against a Sentinel-2 optical image, with both polarisations producing a total accuracy of 97%. Ground-based radar such as the US Next Generation Weather Radar (NEXRAD) has been used to quantitatively measure precipitation on US territory since 1990s and has been widely applied to monitoring precipitation locally and regionally worldwide. Those precipitation products greatly improve hydrological simulation and flood prediction due to their large coverage and relatively high spatial resolution.

2.3.1.3 Active Remote Sensing: LiDAR

LiDAR uses laser pulses to measure the distance of an object present on Earth from the sensor (Cenci et al., 2017; Oglive et al., 2018; Shatnawi and Goodall, 2010). It uses the data obtained to create a 3D model which represents the properties of the Earth's shape and surface. A more common application of LiDAR technology is to generate Digital Elevation Models (DEMs) that can be used in geographic information systems (GIS). DEMs can be used to visualize the interface of floodwater with the elevation of the ground surface (Zhang et al., 2014). Moreover, DEMs are an important indicator in determining the flood inundation and flood depth (Zhang et al., 2014; Grimaldi et al., 2019; Ahmad and Afzal, 2019). LiDAR DEM data best performs compared to other DEM sources (Haile, Schumann et al). Several studies revealed that LiDAR DEM have many advantages which make it suitable for flood modelling. Ghimire (2013) found that LiDAR provides detailed topographic information that is widely used

in flood plain mapping. Furthermore, LiDAR is characterized by rapid data collection capability, high degree of automation, high point density, high level of accuracy, and cost efficiency (Haile, 2005; Turner et al., 2013; Ma, 2005). LiDAR DEM is highly suitable for flood modelling particularly in flat areas and complex urban environments. LiDAR can be used to determine water course and water depth of inundated areas (Ghimire, 2013; Klemas, 2014).

LiDAR has also been used for flood risk assessment in several studies. Lamichhane and Sharma (2017) developed a flood warning system using a DEM derived from LiDAR data. The acquired LIDAR data were also integrated with some field data related to flooding in the target area to determine the evacuation time required by the people. Similarly, Makinano and Santillan (2016) integrated data from LiDAR, an open-source flood model, meteorological data, real-time hydrologic data and geographic visualization tools to construct an early flood warning system. Both studies used a HEC-RAS tool, a software that allows the processing of geospatial data in ArcGIS, to construct a hydraulic model and produce accurate flood risk maps. The flood risk maps were then combined with digital orthographic maps to construct a real-time online flood warning system for the public.

Using LiDAR also presents some challenges for flood modelling. The process of identifying and classifying ground from non-ground points for Digital Terrain Models (DTMs) has proven to be a challenging and often time-consuming task. Haile and Rjentes (2005) found that the filtering process took about 60-80% of the data processing time. Filtering methods are subject to commission errors that classifies non-ground points as ground measurements and omission errors that remove ground points mistakenly. Furthermore, filtering LiDAR data in urban areas are particularly challenging due to complex urban landscape (Bodoque et al., 2016, Turner et al., 2013; Abdullah et al., 2012). Another challenge is the availability and accessibility of LiDAR data. Due to the high initial cost and difficulty of handling and processing large amount of LiDAR data, it is difficult to obtained at the regional and country level. The scarcity of LiDAR data in developing countries are more severe due to economic constraints. However, LiDAR data for flood modelling and risk assessment studies continues to be sought out and improved upon.

2.3.2 Sea Level Rise

Global sea levels have varied greatly throughout the Earth's history, resulting from both geological and climatic changes. Geological records indicate that global sea levels have risen roughly 120 metres since the last glacial maximum which was around 20,000 years ago (IPCC, 2014). This rising trend has not been constant and there are a variety of factors that impact the rate of change. For example, sedimentary deposit records indicate that seas have historically risen rapidly during extreme warming events, with certain centuries witnessing one to four metre rises (IPCC, 2014). Geological records from the Mediterranean suggest that sea levels reached a relatively constant state around 6,000 years ago, with rises of only 0.1 to 0.2 mm/year over the last 3,000 years (IPCC, 2014). Within recent decades the rate of increase has accelerated rapidly and the primary contributing factor is the global rise in average air and ocean temperatures (IPCC, 2014).

Sea level projections under the five Shared Socioeconomic Pathways (SSPs) provide a range of possible future scenarios for global mean sea level (GMSL) rise based on varying levels of greenhouse gas emissions and socio-economic developments (Riahi et al., 2017). The latest report from the United Nation's Intergovernmental Panel on Climate Change (IPCC) predicts that by 2100 global mean sea levels will most likely rise will rise between 0.17 m (under SSP1-2.6) and 0.40 m (under SSP5-8.5) (NASA, n.d.). These are concerning SLR projections that pose a dangerous threat to low-lying coastal countries (Oppenheimer et al., 2019). Some researchers point out that the model used in IPCC's Special Report on the Ocean and Cryosphere in a Changing Climate may underestimate the likely upper level of sea level projections (Grinsted & Christensen, 2021). Bamber et al. (2019) state that a sea level rise more than 2.0 m may happen by 2100. Undoubtedly, increasing SLR will intensify coastal inundation, storm surge, erosion, and other coastal impacts (e.g., wetland loss, saltwater intrusion, damage to coral reefs, affect vegetation and beach erosion) which threaten vital infrastructure and services that support the economies of coastal areas (IPCC, 2014).

2.3.2.1 Measuring Sea Level Rise

Coastal zones are exposed to impacts of climate change which include sea-level rise and changes in the frequency, intensity and patterns of storm events. This results in increased exposure, vulnerability and susceptibility of populations and infrastructure to coastal hazards (IPCC, 2014).

Coastal inundation as a result of sea level rise and storm surge from extreme weather events is regarded as one of the most dangerous, harmful and destructive natural hazards (Douben, 2006). The IPCC AR5 estimates that the global population residing near the coast and exposed to the 1-in-100-year coastal inundation projections is set to increase from 270 million people in 2010 to 350 million people in 2050 (Jongman et al., 2012).

GIS techniques are widely used for understanding coastal inundation processes and assessing coastal hazards in scientific research, coastal management and spatial planning. To accurately map SLR, the ground surface and the water surface are needed. The ground surface refers to a DEM or DTM and serves as the base layer for mapping inundation. The water surface refers to the interface between water and air and represents the original sea level (Coastal Services Center, 2012). The water surface can be derived from existing water models, interpolated water surfaces, or single value water surfaces (Coastal Services Center, 2012). There are existing water models such as hydrodynamic and wave models developed from previous tide gauge observations during past extreme weather events. These models are available for many developed countries such as the SLOSH model in the United States. Other options are water surfaces interpolated from known data points (e.g., water level and tide gauges) or creating a single value water surface, which represents the water level for an entire study area. This single value can be obtained from atmospheric models, measurements from tide or water level gauges, or other empirical models (Coastal Services Center, 2012). With the single value of water surface level, the flooded or inundated zones can be identified following a simple Bathtub Method (sBTM). In a sBTM a grid cell is identified as inundated if its height is below the given sea level scenario and is hydrologically connected to the sea (Breili, Simpson, Klokkervold, & Ravndal, 2020; Gesch, 2009). It is widely used in coastal inundation mapping because of its simplicity and low computational cost. However, it is not the most accurate and incorrectly indicates low lying areas that are disconnected or remote from the coast as being flooded (Breili et al., 2020; Passeri et al., 2015). Although, it may not be as reliable for generating a flood mask in coastal storm-related inundation events, the sBTM can be suitable to flood assessments in low energy waterbodies such as wetlands (NOAA, 2012). Despite its weaknesses, the sBTM has been applied in both coastal and terrestrial analyses such as for SLR, storm surges and riverine flood assessments.

More recently, attempts have been made to refine the sBTM in order to improve its applicability to coastal flood scenarios. For instance, Li et al. (2014) developed a model in ESRI's ArcGIS Model Builder to determine inundation based on SLR. The Cost-Distance tool in the Spatial Analyst toolbox was used to instill the hydrological connectivity to the coast (Li et al., 2014). Building on this, Perini et al. further considered the slope of the beach over which the inundated water needed to travel (Perini et al., 2016). The input surface was a LiDAR derived 2 m resolution DTM while the output binary raster grid comprised of pathways indicating paths that either avoided or favoured inland water movement (Perini et al., 2016). Although the resulting model outputs were an improvement of the sBTM, a weakness is the assumption of a uniform beach slope value which may limit the size of the study site to which this approach can be applied. Another limitation is the exclusion of other physical processes relevant for flood modelling such as surface roughness and individual storm characteristics (Perini et al. 2016).

Apart from GIS based modelling, another method of determining coastal inundation is the use of Hydrodynamic models (HDm). These incorporate additional environmental parameters such as wind speed, direction and tides which can provide a more realistic projection of inundation hazards (Woodruff et al., 2017). HDm is commonly used to model storm surges generated by hurricanes (Balakrishnan Nair et al., 2013). However, there is a high learning curve for using HDm and it uses specialised software and high spec computers in order to run the simulations. This technology may not be a viable solution for standard risk reduction and coastal management environments.

GIS techniques are becoming more commonly used for coastal planning and risk assessments. There is a need for improved inundation modelling approaches that accurately captures the extent and severity of storm-related coastal flooding and is technologically accessible. The accelerating rate of SLR also compels researchers to generate accurate vulnerability or risk assessments and comprehensive adaptation plans (Cooper et al., 2013; Giardino et al., 2018). SLR vulnerability mapping is a type of hazard risk mapping utilizing GIS techniques to show assets at risk. Generating reliable SLR vulnerability maps can help identify sensitive areas, assess the expected damages and affected population, and improve planning for resilient infrastructure.

2.4 Methodology

The purpose of this study is to assess the vulnerability of buildings and roads to potential flooding and sea level rise. GIS techniques are useful for analyzing large amounts of data to identify the temporal and spatial vulnerabilities due to these disasters.

This study aims to answer the following research questions:
How can the influence of climate change on flooding be spatially represented? How can the impacts of a storm be quantified in terms of population, infrastructure, and services affected?
This study investigates this research question by:

1. Developing a flood model using a LiDAR derived digital elevation model
2. Mapping at risk areas according to four flood return periods and four sea level rise scenarios predicted by the Intergovernmental Panel of Climate Change

2.4.1 The Bluespot Model

A bluespot is a landscape depression where precipitation is trapped during heavy rainfalls and where the likelihood of flooding is relatively high. This study applied a bluespot model to map and analyze flood risk. A toolbox that models bluespots in ArcGIS Pro and developed by the Danish Road Directorate (2014) was applied. The data used for this analysis includes the DTM, building footprint and road dataset from City of Surrey. The next few sections describe the workflow of the bluespot model.

2.4.2 Preparing the data

LiDAR data was provided by the City of Surrey and the entire model consists of over 17 million points. In this study, a DTM generated from LiDAR ground points was used to represent bare terrain and assess the city's vulnerability to flooding and sea level rise. The DTM was then processed to remove elements such as bridges. Since bridges in the DEM are generally treated as part of elevated roads, they need to be removed to reflect the connectivity of the river/stream flowing beneath them. To verify this, a GIS dataset with information regarding location of bridges and culverts was used.

2.4.3 Identifying bluespots – Tool Outputs

Based on the DEM, the tool identifies all bluespots within the catchment (Balstrom, n.d.). It then traces the downstream flow of water from one bluespot to the next to prepare a layer outlining the stream network (Balstrom, n.d.). The volume in metres for each bluespot is also calculated and a pour point is assigned as the maximum capacity a bluespot can be filled before spilling over (Balstrom, n.d.). Therefore, each bluespot contains information about the maximum depth in metres, the capacity when filled to the pour point level, the local contributing watershed in m^2, and the fill up value in mm which indicates the amount of precipitation required to fill up a bluespot to its pour point level when assuming 100% surface runoff and no contributions from upstream spillovers (Balstrom, n.d.).

A series of uniform rain events are predefined to simulate the amount of water within the bluespots corresponding to a specific precipitation event. For the City of Surrey, rain event scenarios ranging from 20 to 220 mm in steps of 10 mm are considered, as these realistically reflect events occurring annually in the area versus those occurring only once in a thousand years (Weatherspark, n.d.).

2.4.4 Flood Scenarios

Return periods are common to describe the probability that natural disasters such as a flood will occur. A 1/10 year return period represents events that are relatively frequent, helping to design infrastructure and emergency responses for more regular occurrences. A 1/25- and 1/50-year return periods reflect less frequent but still significant events. These periods help in planning for moderate-risk infrastructure and are often used for urban drainage systems and flood defenses. A 1/100 year return period **r**epresents a rare but severe event, typically used for high-risk infrastructure and critical facilities like hospitals and power plants. The IPCC scenarios (SSPs and RCPs) provide projections of future climate conditions, including the likelihood and severity of extreme weather events such as floods. Under high-emission scenarios (e.g., SSP5-8.5), the frequency and intensity of extreme weather events, including heavy rainfall and storm surges, are expected to increase (IPCC, 2023). This means that what is currently a 1/100-year event could become more frequent, potentially shifting to a 1/50 or even a 1/25 year event.

Hence, understanding how these return periods might change under different climate scenarios is crucial for effective planning and adaptation.

Intensity-Duration-Frequency (IDF) curves are graphical tools used to describe the likelihood of a range of extreme rainfall events (Environment and Climate Change Canada, 2015). Duration refers to period of time of interest. Typical IDF curves include extreme precipitation durations ranging from 5 minutes to 24 hours (Environment and Climate Change Canada, 2015). Intensity refers to the average rainfall rate over the specific duration of interest, in units such as mm/h (Environment and Climate Change Canada, 2015). Frequency refers to a specified duration and intensity of an extreme event (Environment and Climate Change Canada, 2015). This is often described as a return period, which is defined as how often, on average, the event is expected to occur (Environment and Climate Change Canada, 2015). Frequency can also be thought of in terms of probability or likelihood (Environment and Climate Change Canada, 2015). For example, an event with a 1-in-20 year return period will occur on average once every 20 years, and therefore has a 1-in-20, or 5%, chance of occurring each year (Environment and Climate Change Canada, 2015). The IDF curves for the City of Surrey were obtained from the Government of Canada data portal and are based off of a high-emissions scenario (Environment and Climate Change Canada, 2015). To identify and assess building and road stocks that are vulnerable to flooding in Surrey, four return periods are selected: 1/10, 1/25, 1/50, and 1/100 return periods.

Table 1. Amount of precipitation for four different return periods in the City of Surrey

Return Period	Amount of Precipitation (mm)
1/10	191
1/25	214
1/50	232
1/100	249

2.4.5 Sea Level Rise Scenarios

According to IPCC, under a high emissions scenario 1m of SLR is expected by the end of the century, given the higher rates of ice melt and thermal expansion (IPCC, 2023). A 1m SLR scenario is commonly used because it represents a moderate level of sea level rise that could be reached by the end of the 21st century under intermediate to high emission scenarios. The 1.5m SLR scenario is used to account for higher levels of sea level rise that might occur if more significant contributions from ice sheets are realized. Further, a 2m SLR scenario represents an upper bound for sea level rise by 2100, useful for understanding extreme but plausible outcomes. A 2.5m sea level rise scenario represents an extreme but potentially plausible future condition that can occur by 2100 or later, especially if certain critical thresholds in ice sheet dynamics are crossed. This scenario helps to explore the upper bounds of possible sea level rise impacts and is particularly important for understanding the risks and planning necessary adaptation strategies for high-risk areas. Understanding different levels of sea level rise helps in assessing risks to coastal infrastructure, ecosystems, and human populations.

The bathtub model is the most common approach used by modelling areas that are inundated if its elevation is less than or equal to the projected sea level. The bathtub approach is general and reflects the impacts of other factors, such as flooding due to storm surges, in addition to SLR. However, inland areas that are lower than or equal to the projected sea level may unintentionally be mapped as inundated because they are not hydrologically connected to water bodies (Oswald and Treat, 2013). It is important for the DEM to be hydrologically corrected to remove areas such as bridges or culverts that may prevent the flow of water and also remove areas that show up to be inundated but not connected to a body of water.

In this research, the identification of inundated lands was conducted through many sequences using the ArcGIS application. First, the mean sea level (0.5 m) was derived from the mean elevation of classified water points near the shoreline. Mean sea level (MSL) refers to the average height of the sea's surface, measured over a long period, used as a standard in reckoning land elevation or sea depths. Second, a DTM was generated from classified ground points and hydrologically corrected. Third, inundation zones were derived from the DTM by setting the

elevation value to 1.0 m, 1.5 m, 2.0 m, and 2.5 m (mean sea level 0.5 m + sea level rise scenarios). Fourth, inland areas that were inundated and not directly connected to the water body were eliminated (Gesch, 2009). Finally, vector layers of inundated land were produced and overlaid with buildings and road network to assess the infrastructure that would be vulnerable to sea level rise. The LiDAR processing and sea level rise analysis were performed using ArcGIS and ArcGIS Pro.

2.5 Results

2.5.1 Assessment of Flooding Impacts

The following sections describe the results of this study. This study captures a total of 17,533 roads (2,312,729 metres) and 102,141 buildings in the City of Surrey. At a 1/10 year scenario, 46.21% of buildings and 38.13% of roads would be at risk to flooding. This is compared to a 1/100 scenario, where 46.93% of buildings and 38.24% of roads would be at risk to flooding.

Table 2. Quantity of buildings and roads impacted by flooding in Surrey

Return Period	Number of Buildings Impacted	Percentage of Buildings Impacted	Length of Roads Impacted (Metres)	Percentage of Roads Impacted
1/10	47,203	46.21	881,771.20	38.13
1/25	47,568	46.57	882,724.20	38.17
1/50	47,819	46.82	883,813.90	38.22
1/100	47,939	46.93	884,405.80	38.24

2.5.2 Assessment of Sea Level Rise Impacts1/10 f

At a 1m SLR scenario, 1.87% of buildings and 6.39% of roads would be at risk to flooding. At a 1.5m SLR scenario, 1.89% of buildings and 6.43% of roads would be at risk to flooding. At a 2m SLR scenario, 3.57% of buildings and 11.94% of roads would be at risk to flooding. At a 2.5m SLR scenario, 3.72% of buildings and 12.11% of roads would be at risk to flooding.

Table 3. Quantity of buildings and roads impacted by sea level rise in Surrey

SLR Scenario	Number of Buildings Impacted	Percentage of Buildings Impacted	Length of Roads Impacted (Metres)	Percentage of Roads Impacted
1m	1918	1.87	147949	6.39
1.5m	1940	1.89	148863	6.43
2m	3809	3.57	276152	11.94
2.5m	3646	3.72	280249	12.11

2.5.3 Temporal analysis of buildings and roads

Figure 2 shows the construction year of buildings at risk to flooding (City of Surrey, 2020). A greater quantity of buildings built after the 2000s are the most at risk to flooding, amounting to about 35.77% of buildings. Figure 3 shows the construction year of roads at risk to flooding (City of Surrey, 2022). Roads constructed in 1997 and 2014 are the most at risk to flooding, amounting to 18.58% in 1997 and 19.28% in 2014.

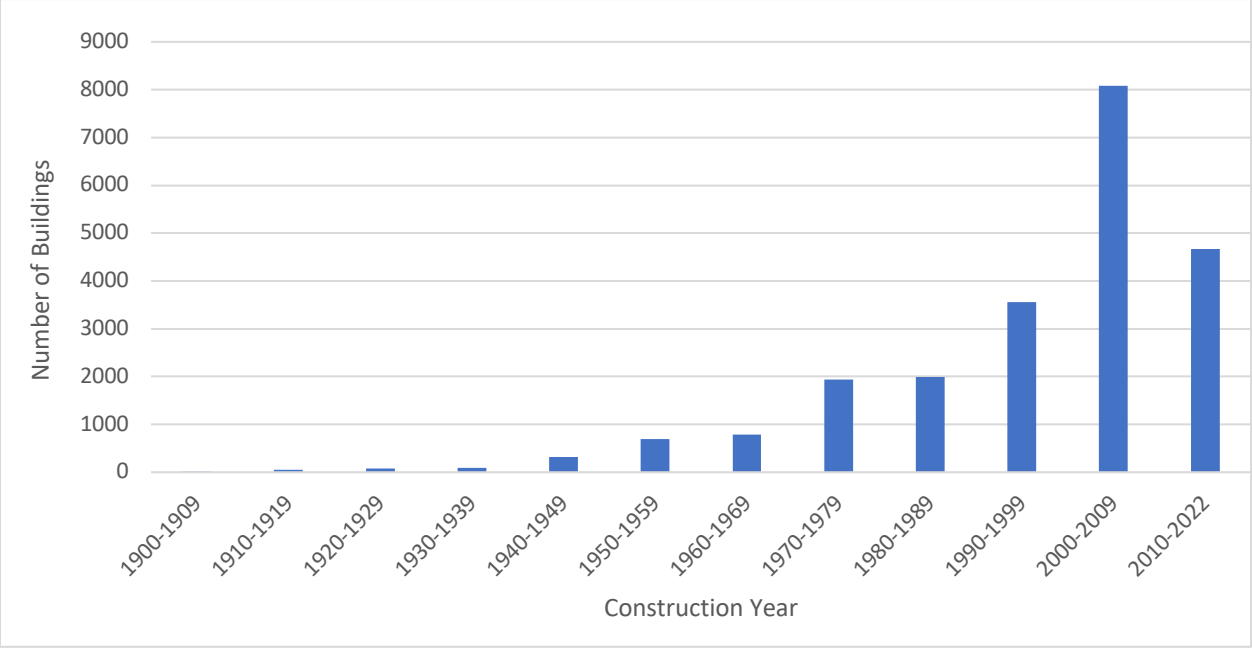


Figure 2. Number of buildings affected by flooding, categorized by construction year from 1900 to 2022



Figure 3. Number of roads affected by flooding, categorized by construction year from 1997 and 2017

2.5.1 Risk Maps of Critical Infrastructure

Through overlaying the depth-to-flood layer over infrastructure allows identification of critical infrastructure, which are the physical assets that support the basic functioning of communities and economies (ex.buildings and roads). within potential flood hazard areas. There were 3,636 roads (658,323 metres) and 25,091 buildings identified to be critical infrastructure at risk to flooding. This equates to about 24.56% of buildings and 28.47% of roads. could potentially be inundated by 0.25 metre or more during an extreme weather event. Surrey's floodplain located near the middle of Surrey is made up of mostly agricultural land. There are approximately 572 buildings in this area. Another area that is at high risk to flooding is a neighbourhood called South Westminster, located North of Whalley next to the Fraser River. There are approximately 584 buildings here.

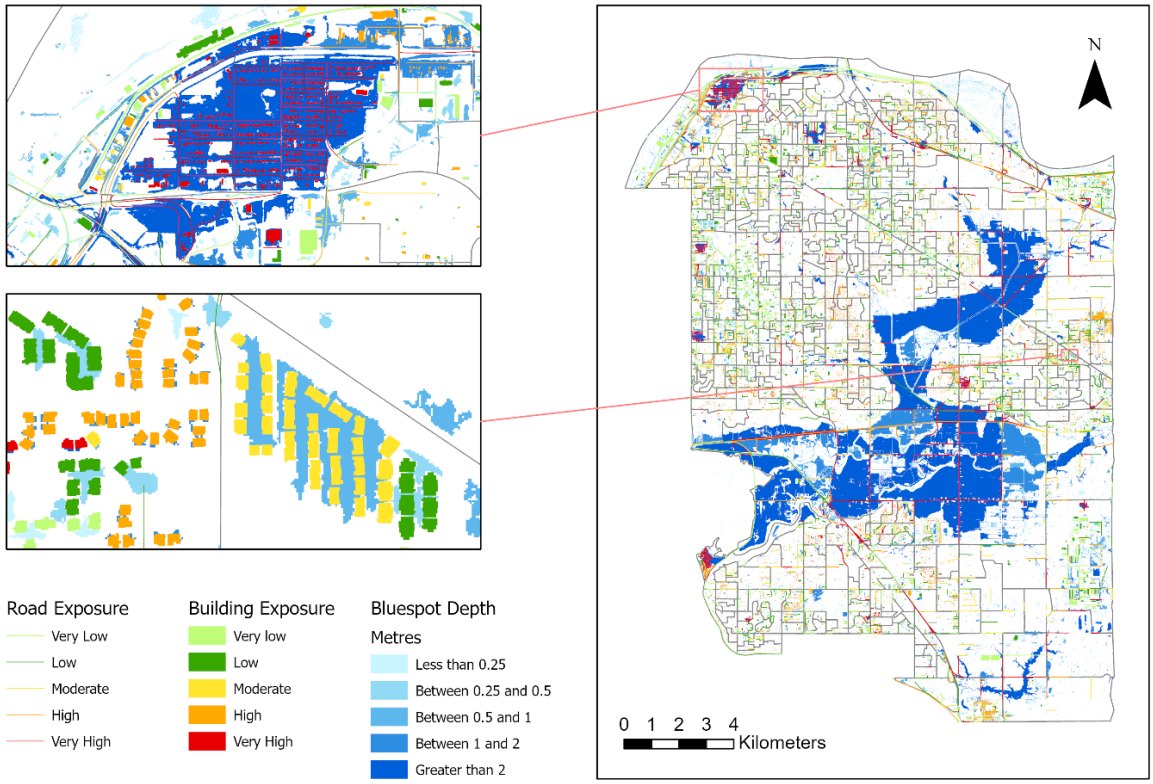


Figure 4. Map of buildings and roads exposed to flooding

Similar results are observed when the sea level scenarios are mapped. Most roads and buildings that are at high risk to sea level rise are in North Whalley near the Fraser River and in the low-lying agricultural fields in the middle of Surrey. Another area at risk is Northeast of the Fraser Heights neighbourhood. Although this are inhabited, it is a large greenspace home to different fauna and flora. It is likely that this natural habitat will be inundated in the future due to sea level rise.

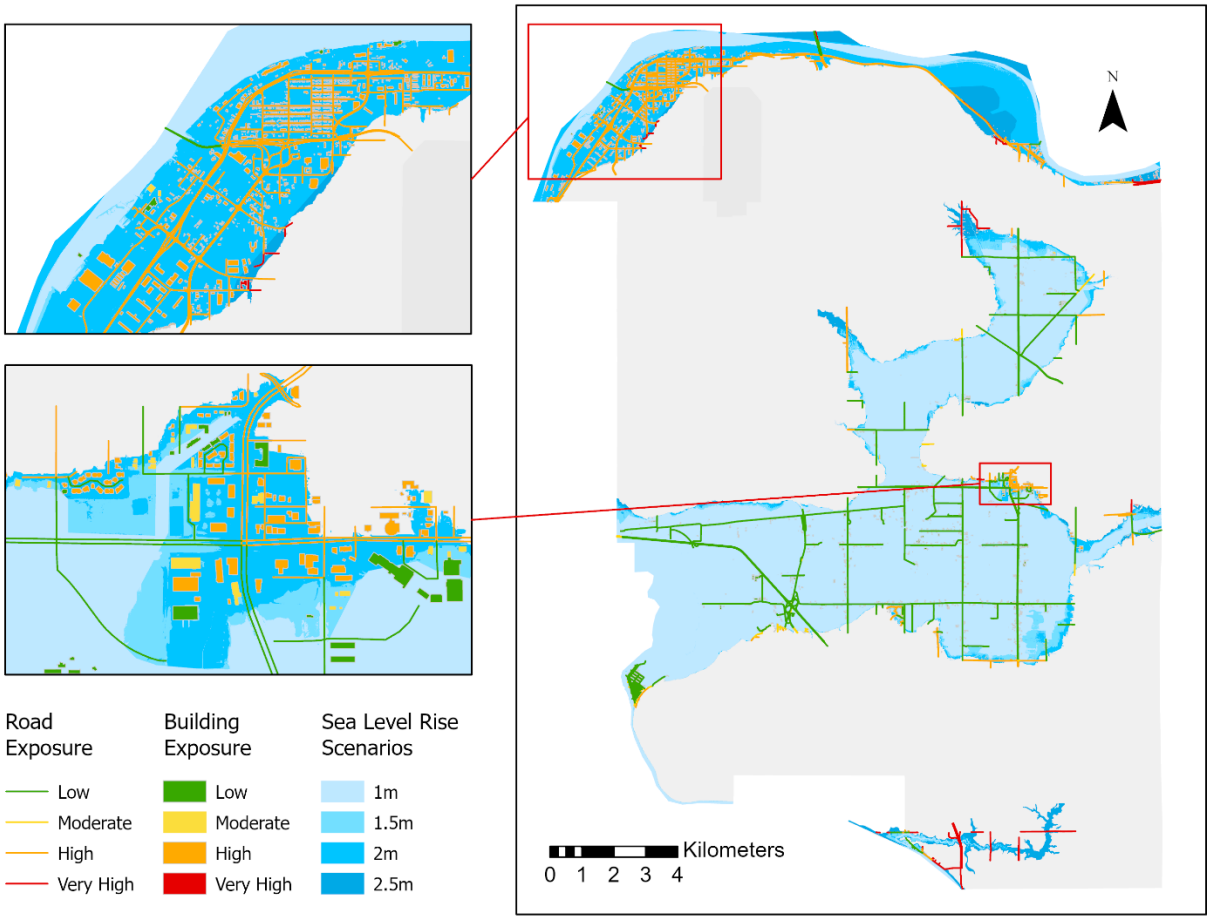


Figure 5. Map of buildings and roads exposed to sea level rise

The City of Surrey has dyking infrastructure in place to protect against flooding. However, as shown in Figure 6, many of these dykes are vulnerable to increasing sea level rise and flooding. The map shows the severity of dykes at risk color coded from red (vulnerable today) to green (dry). About 48.65% of dykes are considered to be vulnerable today and located in bluespots that are greater than 2 metres in depth. Whereas 47.77% of dykes are vulnerable by 2040, 29.85% of dykes are vulnerable by 2070, and less than 1% of dykes are not at risk.

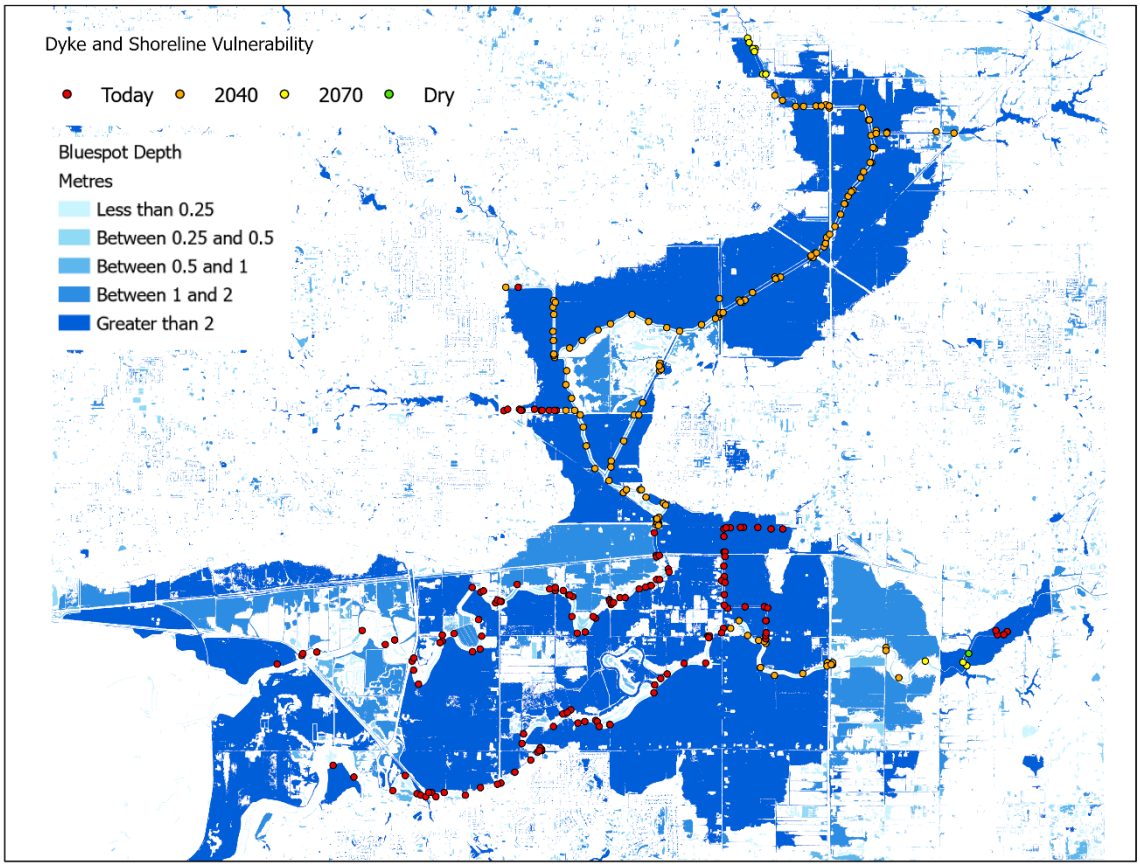


Figure 6. Map of dykes exposed to flooding

2.6 Discussion

This study maps vulnerable buildings and roads in different return periods and sea level rise scenarios in the City of Surrey. The results show that a 1/100 return period could affect nearly 12.59% of buildings and 27.17% of roads. Combined with a sea level rise of 1.0 m would affect most roads and buildings in Crescent Beach, Cloverdale, Colebrook, Mud Bay, Nico-Wynd and Semiahmoo First Nation. Figure 4 shows flood hazard exposure and Figure 5 shows sea level rise that could be expected today and in the future, if no improvements or changes are made. Flood depths and sea level rise of over one metre would flood the ground floor of most buildings and homes, lead to service and utility failures, require the evacuation of residents, and could carry vehicles off roadways (Public Safety Canada, 2022).

The City of Surrey has put in place protective measures against flooding through the implementation of dykes (City of Surrey, 2020). They have the largest dyking network in BC with three dyking districts in Mud Bay, Colebrook, and (City of Surrey, 2020). The results show that dykes put in place by the City of Surrey to limit flood damages will be vulnerable to increased flood hazards and become ineffective in limiting future flood damage. Sea level rise is projected to significantly increase dyke vulnerability and expose low-lying infrastructure along the shoreline to flooding (Lieske and Borneman, 2011). Figure 6 shows the dyking infrastructure that will be vulnerable to flooding today and in the future. According to Surrey's coastal flood adaptation strategy, Surrey's coastal floodplain is at risk to ground subsidence, estimated at an additional 2cm per decade and adding an extra 20cm to existing sea level rise projections by 2100 (City of Surrey, 2019).

Land subsidence is referred to as a gradual sinking of the Earth's surface and leads to increased extent of area at risk of flooding (Miguel et al., 2020). As land subsidence worsens, the impacts of flooding will spread from coastal areas towards the city center, where many residential, commercial, and institutional districts are located. Land subsidence combined with severe flooding can also result in an adverse slope in sewage systems and cause these systems to overflow and flood nearby buildings and roads (Hiroshi et al., 2017). Increased water levels as a result of a flooding event can lead to significant human and economic risks such as degradation of water quality and sanitary conditions, traffic jams, and electric blackouts (Hiroshi et al., 2017). Dykes can also cause large quantities of water to accumulate behind them and would require pumping stations to remove the water (Miguel et al., 2020). A study done in Jakarta assessed the impacts of future flooding on dyking infrastructure and highlight that "if land subsidence continues after 2030, the effectiveness of a 1-m high dyke will be nullified within 10 years of the dyke's completion" (Hiroshi et al., 2017). The study infers that by 2050, a 1 metre dyke would be overflowed, allowing water to rapidly propagate over land as if there was no coastal protection (Hiroshi et al., 2017). A 3-m high dyke will provide protection for a longer period, but its effectiveness may only hold up 10 or 15 years after if the ground beneath continues to subside and will likely end up being totally submerged before 2050 (Miguel et al., 2020).

To reduce potential damage and losses of future floods, flood susceptibility maps are a practical way to identify the hazardous areas in which early warning, evacuation, and mitigation plans. The availability of remote sensing data enhances understanding and modeling of floods and provide fast and accurate analysis, visualization, and information extraction of data that are essential in natural disaster management and urban planning (Lopez et al., 2020). This study highlights the importance of hydrologically correcting a DEM. In this study a GIS-based method was applied for DEM correction. Xing et al. (2022) noted that on DEMS bridges usually cut off the flow of water and forms ponds or reservoirs upstream, diverting the flows parallel to the edge of the bridges. In real life, water flows under these structures and the blockage effect may lead to inaccurate flood simulation which underestimates flood risk in the downstream areas (Xing et al., 2022). Unlike buildings, bridges especially those over roads cannot be directly derived from digital maps and a methodology must be developed to identify the locations of bridges and correct the DEM to ensure intrinsic flow connectivity, and more accurate flood simulations results.

This study highlights the importance of combining high spatial information from LiDAR data with flood simulation model to generate informative maps showing the exposure and vulnerability of buildings to flooding. The results of this study shows the spatial distribution of buildings exposed to low, medium and high hazard levels of flooding caused by extreme rainfall events with return periods of 25, 50 and 100 years. The information generated from the analysis can be very useful in flood risk management and disaster preparedness. Measures to improve preparedness can include changes in land-use planning, implementation of specific flood-proofing measures, and creation of emergency response plans. Flood hazard assessments can be further expanded to assess specific risks, which take into consideration the socioeconomic characteristics, such as the population, property, and environment at risk during occurrence of flood in a specific area of the exposed areas.

2.7 Limitations

The flood model developed for this study focused mainly on the influence of precipitation to potential flooding in the City of Surrey. However, there are other physical factors that impact

flooding and should be considered when developing a flood model. For instance, the type of soil has a significant impact on the rate of precipitated water infiltration and the capacity of an area to store water and is one of the critical factors in defining flood-prone areas (Hagos et al., 2022). The ability of various soil textures to absorb water varies; sandy soils are saturated at a higher rate than finer grained soils due to the greater pore space between the soil particles (Wondim 2016). Infiltration has a significant impact on the availability and quantity of surface runoff produced by the rainfall-runoff process (Morgan, 1995). Another factor is land use land cover (LULC) which refers to the type of soil deposits and the distribution of built-up areas, such as cropland, grassland, shrubland and forestland within a given region. The LULC of a watershed play an important role in flood water movement by impeding, delaying or accelerating surface flow (Hagos et al., 2022). As cities expand in size, impervious cover increases while forest cover decreases, contributing to an increase in run-off (Tucci, 2007; Fura, 2013; Blistanova et al., 2016; Wondim, 2016; Gazi et al., 2019; Arya & Singh, 2021). It is important to include these factors that can influence the rate of floods for a more accurate flood model.

2.8 References

Abou Samra, R. M., El-Gammal, M., Al-Mutairi, N., Alsahli, M. M., & Ibrahim, M. S. (2021). GIS-based approach to estimate sea level rise impacts on Damietta coast, Egypt. *Arabian Journal of Geosciences*, *14*(6). https://doi.org/10.1007/s12517-021-06810-3

Ahmad D., Afzal M. Household vulnerability and resilience in flood hazards from disaster-prone and pitfalls for global coupled hydrologic-hydraulic modeling of floods. *Water Resour. Res.* 2019;**55**:5277–5300.

areas of Punjab, Pakistan. *Nat. Hazards.* 2019;**99**:337–354. doi: 10.1007/s11069-019-03743-9.

Arya AK, Singh AP (2021) Multi criteria analysis for flood hazard mapping using GIS techniques: a case study of Ghaghara River basin in Uttar Pradesh, India. Arab J Geosci 14(8):1–12

Berchum, E. C., Mobley, W., Jonkman, S. N., Timmermans, J. S., Kwakkel, J. H., & Brody, S. D. (2018). Evaluation of flood risk reduction strategies through combinations of interventions. *Journal of Flood Risk Management*, *12*(S2). https://doi.org/10.1111/jfr3.12506

Blastrom, T. (n.d.). *Model bluespots to map flood risk*. Learn ArcGIS. Retrieved October 20, 2022, from https://learn.arcgis.com/en/projects/model-bluespots-to-map-flood-risk/

Blistanova M, Zeleňáková M, Blistan P, Ferencz V (2016) Assessment of flood vulnerability in Bodva river basin Slovakia. Acta Montanistica Slovakia 21(1):19–28

Cenci L., Pulvirenti L., Boni G., Chini M., Matgen P., Gabellani S., Squicciarino G., Pierdicca N. An evaluation of the potential of Sentinel 1 for improving flash flood predictions via soil moisture–data assimilation. *Adv. Geosci.* 2017;**44**:89–100.

City of Surrey. (2020). *Buildings* [Data set]. City of Surrey. https://data.surrey.ca/dataset/buildings

City of Surrey. (2022). *Road Centrelines* [Data set]. City of Surrey. https://data.surrey.ca/dataset/buildings

City of Surrey. (2022). *Raw LIDAR Data 2022* [Data set]. City of Surrey. https://data.surrey.ca/dataset/buildings

City of Surrey. (2019, November). *Coastal flood adaptation strategy*. City of Surrey. Retrieved October 20, 2022, from https://www.surrey.ca/services-payments/water-drainage-sewer/flood-control/coastal-flood-adaptation-strategy

City of Surrey. (2020, November 10). *Dyking & drainage on farmlands*. City of Surrey. Retrieved October 20, 2022, from https://www.surrey.ca/services-payments/water-drainage-sewer/dyking-drainage-on-farmlands

Clement, M. A., Kilsby, C. G., & Moore, P. (2017). Multi-temporal synthetic aperture radar flood mapping using change detection. *Journal of Flood Risk Management*, *11*(2), 152–168. https://doi.org/10.1111/jfr3.12303

Combining Landsat observations with hydrological modelling for improved surface water monitoring of small lakes. *J. Hydrol.* 2018;**566**:109–121.

Environment and Climate Change Canada. (2015, January 28). Short-duration Rainfall Intensity-Duration-Frequency. Retrieved October 20, 2022, from https://open.canada.ca/data/en/dataset/15aa455c-9f9f-4405-8eee-4445d02fd35c.

Environment and Climate Change Canada. (2022, October 20). *Total precipitation - monthly data for Vancouver*. Amateur Weather Statistics for Vancouver, British Columbia. Retrieved October 20, 2022, from https://vancouver.weatherstats.ca/charts/precipitation-monthly.html

Environment and Climate Change. (2013, July 19). *Government of Canada*. Canada.ca. Retrieved October 20, 2022, from https://www.canada.ca/en/environment-climate-change/services/water-overview/quantity/reducing-flood-damage.html

Fura GD (2013) Analyzing and modeling urban land cover change for run-off modeling in Kampala, Uganda. Thesis of master of science. University of Twente, Enschede, The Netherlands

Gazi Y, Islam A, Hossai S (2019) Flood-hazard mapping in a regional scale-way forward to the future hazard Atlas in Bangladesh. Malaysian J Geosci 3(1):01–11

Grimaldi S., Schumann G.P., Shokri A., Walker J.P., Pauwels VR N. Challenges, opportunities, LiDAR-derived channel geometries. *J. Hydrol. Eng.* 2010;**15**:97–106.

Hamidi, A. R., Jing, L., Shahab, M., Azam, K., Atiq Ur Rehman Tariq, M., & Ng, A. W. (2022). Flood exposure and social vulnerability analysis in rural areas of developing countries: An empirical study of Charsadda District, Pakistan. *Water*, *14*(7), 1176. https://doi.org/10.3390/w14071176

IPCC, 2023: Summary for Policymakers. In: Climate Change 2023: Synthesis Report. Contribution of Working Groups I, II and III to the Sixth Assessment Report of the Intergovernmental Panel on Climate Change [Core Writing Team, H. Lee and J. Romero (eds.)]. IPCC, Geneva, Switzerland, pp. 1-34, doi: 10.59327/IPCC/AR6-9789291691647.001

Janizadeh S., Vafakhah M., Kapelan Z., Dinan N.M. Novel Bayesian Additive Regression Tree Methodology for Flood Susceptibility Modeling. *Water Resour. Manag.* 2021;**35**:4621–4646.

Kalantar B., Ueda N., Saeidi V., Janizadeh S., Shabani F., Ahmadi K., Shabani F. Deep Neural Network Utilizing Remote Sensing Datasets for Flood Hazard Susceptibility Mapping in Brisbane, Australia. *Remote Sens.* 2021;**13**:2638. doi: 10.3390/rs13132638.

Klemas, V. (2015). Remote sensing of floods and flood-prone areas: An overview. *Journal of Coastal Research*, *314*, 1005–1013. https://doi.org/10.2112/jcoastres-d-14-00160.1

Lamichhane N., Sharma S. Development of Flood Warning System and Flood Inundation Mapping Using Field Survey and LiDAR Data for the Grand River near the City of Painesville, Ohio. *Hydrology.* 2017;**4**:24. doi: 10.3390/hydrology4020024.

Lieske, D., & Bornemann, J. (2011, October). *Coastal Dykelands in the Tantramar Area : Impacts of Climate Change on Dyke Erosion and Flood Risk*. Atlantic Climate Adaptation Solutions Association. Retrieved October 20, 2022, from https://arcgis.mta.ca/docs/CoastalDykelandsinTantramar-ImpactsofClimateChange.pdf

Makinano-Santillan M., Santillan J.R. Effective Flood Forecasting and Early Warning through Application of Lidar and Related Geospatial Technologies; Proceedings of the 37th Asian Conference on Remote Sensing; Colombo, Sri Lanka. 17–21 October 2016.

Ministry of Transportation and Infrastructure. (2022, August 31). *2021 B.C. Highway Flood Recovery Projects*. Province of British Columbia. Retrieved October 20, 2022, from https://www2.gov.bc.ca/gov/content/transportation-projects/bc-highway-flood-recovery

Morgan RP (1995) Soil erosion and conservation. Longman, Harlow, p 198

Munawar, H. S., Hammad, A. W., & Waller, S. T. (2022). Remote Sensing Methods for flood prediction: A Review. *Sensors*, *22*(3), 960. https://doi.org/10.3390/s22030960

NASA. (n.d.). IPCC AR6 Sea Level Projection Tool. NASA Sea Level Change Portal. Retrieved July 22, 2024, from https://sealevel.nasa.gov/ipcc-ar6-sea-level-projection-tool?psmsl_id=1245&data_layer=scenario

Ogilvie A., Belaud G., Massuel S., Mulligan M., Le Goulven P., Malaterre P.-O., Calvez R.

Pinton, D., Canestrelli, A., Wilkinson, B., Ifju, P., & Ortega, A. (2021). Estimating ground elevation and vegetation characteristics in coastal salt marshes using UAV-based LIDAR and Digital Aerial Photogrammetry. *Remote Sensing*, *13*(22), 4506. https://doi.org/10.3390/rs13224506

Population Estimates & Projections. City of Surrey. (2022, September 22). Retrieved October 20, 2022, from https://www.surrey.ca/business-economy/business-data/population-estimates-projections

Public Safety Canada. (2022, August 1). *Adapting to rising flood risk - an analysis of insurance solutions for Canada*. Adapting to Rising Flood Risk - An Analysis of Insurance Solutions for Canada. Retrieved October 20, 2022, from https://www.publicsafety.gc.ca/cnt/rsrcs/pblctns/dptng-rsng-fld-rsk-2022/index-en.aspx#s1.1

Public Safety Canada. (2022, May 31). *Floods*. Public Safety Canada. Retrieved October 20, 2022, from https://www.getprepared.gc.ca/cnt/hzd/flds-en.aspx#a1

Riahi, K., van Vuuren, D. P., Kriegler, E., Edmonds, J., O'Neill, B. C., Fujimori, S., Bauer, N., Calvin, K., Dellink, R., Fricko, O., Lutz, W., Popp, A., Crespo Cuaresma, J., KC, S., Leimbach, M., Jiang, L., Kram, T., Rao, S., Emmerling, J., Ebi, K., Hasegawa, T., Havlik, P., Humpenöder, F., Da Silva, L. A., Smith, S., Stehfest, E., Bosetti, V., Eom, J., Gernaat, D., Masui, T., Rogelj, J., Strefler, J., Drouet, L., Krey, V., Luderer, G., Harmsen, M., Takahashi, K., Baumstark, L., Doelman, J. C., Kainuma, M., Klimont, Z., Marangoni, G., Lotze-Campen, H., Obersteiner, M., Tabeau, A., & Tavoni, M. (2017). The Shared Socioeconomic Pathways and their energy, land use, and greenhouse gas emissions implications: An overview. *Global Environmental Change, 42*, 153-168. https://doi.org/10.1016/j.gloenvcha.2016.05.009

Sakamoto, T., Van Nguyen, N., Kotera, A., Ohno, H., Ishitsuka, N., & Yokozawa, M. (2007). Detecting temporal changes in the extent of annual flooding within the Cambodia and the Vietnamese Mekong Delta from Modis Time-series imagery. *Remote Sensing of Environment*, *109*(3), 295–313. https://doi.org/10.1016/j.rse.2007.01.011

Sandink, D. *Urban Flooding in Canada*; Institute for Catastrophic Loss Reduction: London, ON, Canada, 2013; Volume 52, pp. 1–94

Schumann, G. J.-P., Neal, J. C., Mason, D. C., & Bates, P. D. (2011). The accuracy of sequential aerial photography and SAR data for observing urban flood dynamics, a case study of the UK summer 2007 floods. *Remote Sensing of Environment*, *115*(10), 2536–2546. https://doi.org/10.1016/j.rse.2011.04.039

Shahabi H., Shirzadi A., Ghaderi K., Omidvar E., Al-Ansari N., Clague J.J., Geertsema M., Khosravi K., Amini A., Bahrami S., et al. Flood Detection and Susceptibility Mapping Using Sentinel-1 Remote Sensing Data and a Machine Learning Approach: Hybrid Intelligence of Bagging Ensemble Based on K-Nearest Neighbor Classifier. *Remote Sens.* 2020;**12**:266. doi: 10.3390/rs12020266.

Shatnawi F.M., Goodall J.L. Comparison of flood top width predictions using surveyed and

Slepian, K., News, & Video. (2021, November 18). *B.C. declares state of emergency amid devastating floods, landslides - surrey now*. Leader. Retrieved October 20, 2022, from https://www.surreynowleader.com/news/breaking-b-c-declares-state-of-emergency-amid-devastating-floods-landslides/

Supporting information: Estimating discharge in low-order rivers with high-resolution aerial imagery. (n.d.). *HydroShare Resources*. https://doi.org/10.4211/hs.9badb941303d4813b3c398cdab038368

United Nations. (n.d.). *The 17 goals | sustainable development*. United Nations. Retrieved October 20, 2022, from https://sdgs.un.org/goals

Vu, H. T., Trinh, V. C., Tran, D. D., Oberle, P., Hinz, S., & Nestmann, F. (2021). Evaluating the impacts of rice-based protection dykes on floodwater dynamics in the Vietnamese mekong delta using geographical impact factor (GIF). *Water*, *13*(9), 1144. https://doi.org/10.3390/w13091144

Ward RC, Robinson M (1990) Principles of hydrology. McGraw-Hill, London, p 365

Weatherspark. (n.d.). *Weatherspark.com*. Surrey Climate, Weather By Month, Average Temperature (Canada) - Weather Spark. Retrieved October 20, 2022, from https://weatherspark.com/y/1005/Average-Weather-in-Surrey-Canada-Year-Round

Wieland, M., & Martinis, S. (2019). A modular processing chain for automated flood monitoring from multi-spectral satellite data. *Remote Sensing*, *11*(19), 2330. https://doi.org/10.3390/rs11192330

Wondim YK (2016) Flood hazard and risk assessment using GIS and remote sensing in lower Awash sub-basin Ethiopia. J Environ Earth Sci 6(9):69–86

Yang, H., Kong, J., Hu, H., Du, Y., Gao, M., & Chen, F. (2022). A review of remote sensing for Water Quality Retrieval: Progress and challenges. *Remote Sensing*, *14*(8), 1770.

Hagos, Y. G., Andualem, T. G., Yibeltal, M., & Mengie, M. A. (2022). Flood hazard assessment and mapping using GIS integrated with multi-criteria decision analysis in Upper Awash River basin, Ethiopia. *Applied Water Science*, *12*(7). https://doi.org/10.1007/s13201-022-01674-8

Zhang Q., Gu X., Singh V.P., Xiao M. Flood frequency analysis with consideration of hydrological alterations: Changing properties, causes and implications. *J. Hydrol.* 2014;**519**:803–813. doi: 10.1016/j.jhydrol.2014.08.011.

3.0 Connecting Manuscript 1 and 2

The previous manuscript (Chapter 2) focused on the implications of flooding and sea level rise on infrastructure such as buildings and roads. It is also important to evaluate the specific materials contained within infrastructure that would be impacted. The second manuscript explores this through conducting a material stock analysis of the material buildup in buildings and roads for the City of Surrey. The methodology combines flood assessment with material stock analysis, offering a unique perspective on how material stocks are distributed and how they might be impacted by flood risks. This approach enhances the understanding of material resources within urban environments while also integrates critical flood risk considerations, thus advancing the field of urban resilience and infrastructure management.

4.0 Accounting for building and road material stocks for the City of Surrey, British Columbia

4.1 Introduction

4.1.1 Socioeconomic Metabolism

The idea of social metabolism came about in the 1990s and has since then become an important part of sustainability science (Haberl, Wiedenhofer, Erb, Görg, & Krausmann, 2017). It can be defined as the way in which societies maintain the exchange of materials and energy with nature (Padovan, 2000). The operational model views society as capable of regulating, maintaining, and reproducing itself through organizing materials and energy flows from its environment into socioeconomic systems (Pauliuk & Hertwich, 2015). The material components of a society are comprised of biophysical stocks such as human population, domesticated livestock, buildings, roads, and any products that remain in the system for longer than a year (Arora et al., 2019; Gontia et al., 2018; Miatto, Schandl, Wiedenhofer, Krausmann, & Tanikawa, 2017). To maintain a certain level of biophysical stocks for proper functioning of the system, biophysical stocks need to be expanded or reproduced through constant flows of material and energy resources (Gordon, Bertram, & Graedel, 2006). The system must have an input process in which resources and services are extracted from nature and an output process in which wastes and emissions are disposed back to nature (Fishman et al., 2014). The study of social metabolism is important for understanding the relationships and flow of interactions between society and nature (Pauliuk & Hertwich, 2015).

The diagram in Figure 7 demonstrates the components and relationships that define socio-economic metabolism. The framework includes inputs that flow into the socio-economic system which then become in-use material stocks (MS) (Fishman, 2016; Gordon, Bertram, & Graedel, 2006; Wiedenhofer et al., 2015). These in-use material stocks such as buildings and roads support the system's operation by offering large numbers of services including transportation, recreation, and housing. Outputs flow out as waste emissions or exports to external socioeconomic systems. (Fishman, 2016; Gordon, Bertram, & Graedel, 2006; Wiedenhofer et al., 2015). The increase of aging buildings and facilities, the scarcity of data, and the intensive

investment for rapid infrastructure development pose significant challenges for sustainable development (Ozawa, 2008; Yashiro, 2008). Improving the management of in-use material stocks and developing are detailed and accurate material stock databases are highly important for a country's sustainable development plans.

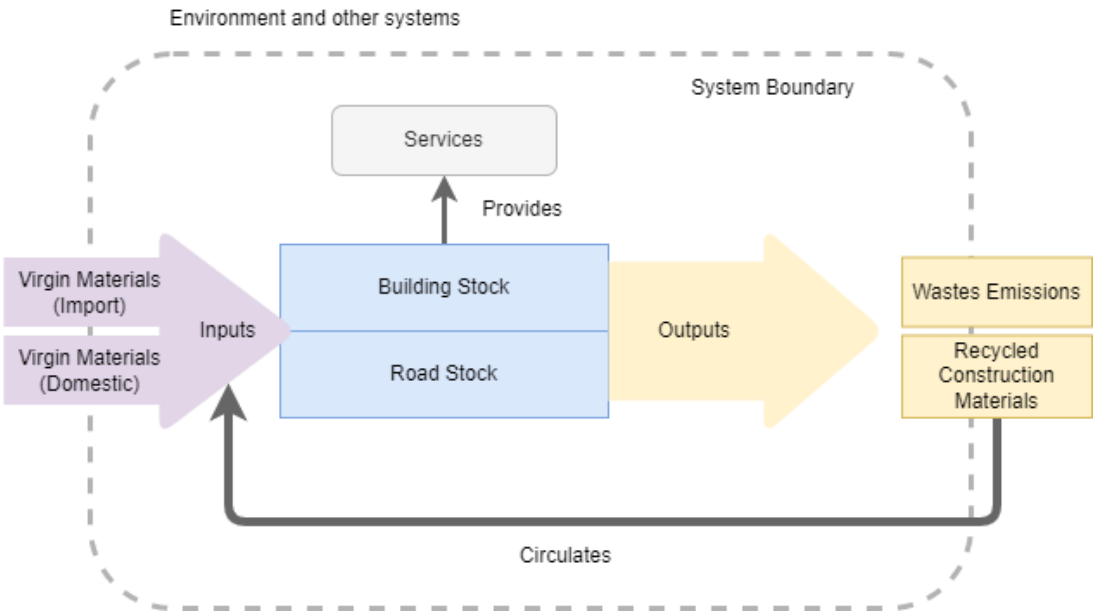


Figure 7: Socio-economic metabolism conceptual diagram (modified from De Kroon, 2020; Krausmann, 2018; Wiedenhofer et al., 2015).

4.1.2 Top-down approach

The top-down approach refers to the change in stock as a result of the difference between inflows and outflows of a material over time (NAS; Augiseau & Barles, 2017; Kavgic et al., 2010). This approach is effective in capturing stock dynamics over a long period of time (Augiseau & Barles, 2017). Top-down approaches are usually divided into flow-driven accounting and demand-driven modeling (Fishman, 2016; Kavgic et al., 2010). Flow-driven approaches use historical material inputs and output data to measure annual net additions to stock (NAS; Fishman, 2014; Symmes, 2018). This approach allows for simulation of future material cycles and demand through looking at historical patterns of built environment stocks (Muller et al., 2006). For instance, Pauliuk et al. (2015) investigated the demand for steel production through conducting a material flow analysis of the entire steel cycle from production to waste.

Similar studies modelled past and future stocks and flows of specific materials (Zeltner, 1999; Kapure et al., 2008). The outflows from stock are modeled using the life-cycle assessment, which divides in-use material stocks by characteristics such as buildings and infrastructures, transportation, or machinery (Y. Zhang, 2018).

Rather than using historical inflow data, demand-driven modelling looks at socioeconomic indicators such as population or income to model demand over time (Fishman, 2016). Muller (2006) determined that stock of in-use services were one of the drivers for material flows. It is assumed that in-use stocks reflect better quality of life which influences demand for stocks. For instance, Bergsdal et al. (2007) investigated the dynamics of the Norwegian dwelling stock and its influence on corresponding stocks and flows of building materials. Projections of waste generation and demand in materials can be made by linking a materials' life cycle to the population and lifestyle (Hu et al., 2010; Pauliuk et al., 2013).

Top-down approaches are often limited to accounting for national material stocks where historical data is available (Fishman, 2016). Historical data can be difficult to obtain since there is uncertainty regarding data quality and reliability when dealing with different sources (Fishman, 2016). In addition, modelling the accumulation of stock depends on knowing the average lifetime, but there are few empirical data which introduces further uncertainty (Lanau et al., 2019).

4.1.3 Bottom-up approach

The bottom-up approach is creating an inventory of end-use objects in order to account for in-use material stocks (Kavgic et al., 2010; Tanikawa, Fishman, Okuoka, & Sugimoto, 2015). This approach is often referred to as "snapshots" of material stocks in a defined area at a specific point in time, also known as "static analysis" (Fishman, 2015, pg 779). The materials contained in end-use objects are calculated using material intensity coefficients, which are the amount of materials in each stock unit (Tanikawa et al., 2015). A study by calculated material stocks for buildings in Vienna by characterizing different building types with material intensity characteristics (Kleeman et al., 2016). It also combined the results with information about

demolition activity to quantify the amount of wastes and contribute information on materials that could be recycled.

Geographic Information Systems (GIS) has been used to estimate, map the spatial distribution of, and compare material stocks at different scales and periods of time s (Gontia et al., 2018; Ortlepp et al., 2016). A GIS model was used to store information about different building types, classify building stock, and map the spatial accumulation of materials in a Peruvian city (Mesta et al., 2019). Incorporating GIS methods can be applied to account for materials in other infrastructure, roads or railways (Guo et al., 2014; Han & Xiang, 2013, Tanikawa et al., 2015; Miatto et al., 2017). Ngyuen, Fishman, and Tanikawa (2019) estimated the material stocks for roads in Vietnam and highlighted the challenges of such research in a developing country.

4.2 Methodology

The purpose of this study was to assess the vulnerability of building and material stocks to potential flooding and sea level rise in the City of Surrey. A GIS-based bottom-up approach to model in-use building and road material stocks was applied. The results of the flooding and sea level rise analysis were combined with the material stocks accounts to estimate the exposure and quantify the impact.

This study aims to answer the following research questions:

How can the influence of climate change on flooding be spatially represented? How can the impacts of a storm be quantified in terms of population, infrastructure, and services affected?

This study investigates this research question by:

1. Developing a flood model using a LiDAR derived digital elevation model
2. Mapping at risk areas according to four flood return periods and four sea level rise scenarios predicted by the Intergovernmental Panel of Climate Change

4.2.1 Data Collection and Creating a Geodatabase

In order to conduct a spatial analysis of building stocks, building footprints and spatial data were required. A geodatabase was created for both study areas and data was imported into respective geodatabases for ease of use and organization. Metadata for the City of Surrey and all of the spatial information collected along with their sources are provided in Appendix B. Utilizing spatial information is a beneficial method of identifying the location of geographic phenomena. Spatial methodologies can assist cities and small island countries in examining relationships and making predications about historical data and the current state of affairs (Sugimoto et al., 2015).

4.2.2 System Boundary and Data Sources

System boundaries of a socioeconomic system are established to define what is inside or outside a system. For a city, the geographic boundary of the municipality is considered as the system boundary and anything inside the municipality is considered domestic. Materials that flow into the city are imports, while materials that leave the city are exports. All materials stocked within the system and being used by humans during a given time period are considered to be in-use material stocks (Gerst & Graedel, 2008; Krausmann, 2018; Symmes et al., 2019; Wiedenhofer et al., 2015). In this research, the analysis focuses on a subset of in-use material stocks: building stocks and road stocks. The types of materials for buildings include brick, concrete, timber, aggregate, and steel; materials for roads include aggregate, rock, and asphalt.

Some materials were not included in the overall calculation of materials stocks for the following reasons:

1. Other materials in modern-day buildings (e.g. glass, plastics, ceramics, aluminum, etc): These materials represent a small share of the total material stocks and also have higher variability between buildings, making it more difficult to find a typical representative value when calculating the material intensity
2. Smaller durable goods (e.g. furniture): These materials are highly variable in quality and quantity and have different life cycles compared to buildings

3. Sheds, shacks, and temporary structures: The building footprint data consists of many small features such as sheds and recreational vehicles but differentiating between these was not possible. Since they are a small representative, these structures were removed from the dataset.

4.2.3 Material Intensities

Material intensities (MI) are site specific and represent different construction styles and building codes. Different studies have specific material intensity typologies for the determined study area such as Italy (Miatto et al., 2019), Vienna (Kleeman et al., 2016), Grenada (Symmes et al., 2019), Japan (Tanikawa et al., 2015). Since building codes can change over time and building styles are dependent on the design of developers and engineers, it can be difficult to calculate material intensities. For instance, Kleeman et al. (2016) analyzed the material composition of buildings from different time periods and compared with other studies to derive the material intensity typologies. Similarly, Mesta et al. (2019) categorized building types by year of construction and calculated the material intensity by looking at changes in construction type and popular materials used during those years. These studies were limited to looking at buildings on a local scale rather than a city-wide building scale.

More recently, Symmes (2018) developed a methodology for assigning material intensity typologies to a larger scale, specifically Caribbean islands. The process required a combination of fieldwork and consulting building construction codes of practice. This methodology was further applied to a city scale (De Kroon, 2020), which will be adopted for this research in looking at Surrey, British Columbia. For this study, material intensities were generated for five main construction materials which are aggregate, wood, concrete, brick and steel. These were generated based on main structural design components for building typologies found from the National Building Code of Canada, BC Building Code, and various city construction guidelines.

4.3 Assigning Building Occupancy Classes

Buildings were classified into occupancy classes to describe specific use-types (e.g. residential, commercial, industrial). Each occupancy class share similar material compositions

(e.g. concrete, wood, brick). The building footprints dataset for Surrey already contained attribute information on occupancy classes available. These were not all organized or were missing information. The data was grouped into similar classes and recoded to ensure that all the buildings were assigned to a single occupancy class as show in Table _.

4.3.1 Physical Size of Buildings

The calculation of material stocks is based on the size of a building that is collected within a GIS environment. Georeferenced building footprints provide length and width dimensions that allow for total building area to be calculated. Height information is necessary to calculate the gross volume (GV) of a building. This information is provided in the building footprints dataset provided by the City of Surrey. Calculating GV is a more precise representation of the mass of materials present in a building. An example of a subset of calculations for deriving material intensity are shown in Appendix B and adopted from De Kroon (2020). These calculations are completed for each building and building typology class. The amount of material intensity per cubic metre is averaged to determine a single material intensity value for each category.

4.3.2 Material Intensities for Buildings

Table 4. Material Intensity Calculation break down of materials and material intensity classes in kg/m3

	Aggregate	**Concrete**	**Timber**	**Steel**	**Masonry (Brick)**
Foundation with Reinforced Concrete					
Foundation - Strip Footings	-	6.83	-	-	-
Foundation - Ground Slab	47.93	22.19	-	0.80	-
Floors	-	-	0.37	-	-
Walls (2 types: red (brick exterior), vinyl (nothing added))	-	26.64 (basement wall)	0.76	3.58	
Roof- Frame	-	-	0.48	-	-
Roof – Covering	-	-	5.72	-	-

Total a. (brick exterior)	47.93	55.66	7.33	4.38	
Total b. (vinyl exterior)	47.93	55.66	7.33	4.38	-
Concrete Structure 1a (Under 4 storeys, brick exterior)					
Foundation - Footing	-	13.42	-	-	-
Foundation - Ground Slab	66.54	33.27	-	0.36	-
Floors	-	-	0.46	-	-
Walls (Other)	-	63.41	0.81	-	-
Walls (Brick exterior)	-	-	-	-	33.89
Roof	-	72.03	-	0.23	-
Total	66.54	182.13	1.27	0.59	33.89
Concrete Structure 1b (Low Rise Apartments)					
Foundation - Footing	-	2.28	-	-	-
Foundation - Ground Slab	34.24	17.12	-	0.61	-
Floors	-	-	0.24	-	-
Walls (Other)	-	10.30	0.44	-	-
Walls (Brick exterior)	-	-	-	-	
Roof	-	37.07	-	0.38	-
Total	34.24	66.77	0.68	0.99	
Concrete Structure 2 – Steel Reinforced (High Rise Apartments)					
Foundation – Raft Slab	-	1.22	-	0.01	-
Floors	-	64.22	-	4.14	-
Walls	-	3.92	-	0.25	-
Roof	-	7.93	-	0.08	-
Total		77.29	-	4.48	-
Steel Structure – Steel Walls					
Foundation – Pad Footing	-	11.87	-	-	-
Foundation – Ground Slab (Floor)	-	47.24	-	34.24	-
Walls – Structure and Steel Walls	-	-	-	6.53	-
Roof - Frame		-	-	0.56	-

Roof - Covering				0.63	
Total		59.11		41.96	
Steel Structure – Precast					
Foundation – Pad Footing	-	8.28	-	-	-
Foundation – Ground Slab (Floor)	-	43.23	-	31.33	-
Walls – Structure	-	-	-	5.94	-
Walls - Precast	-	63.41	-	23.23	-
Roof - Frame	-	-	-	0.52	-
Roof - Covering	-	-	-	0.58	
Total		75.92		61.6	

The material intensity values used for the final calculations of material stock are shown in Table 5. These values were the total of each building typology and material intensity class. These values are mapped back to each building footprint in ArcGIS Pro.

Table 5. Final material intensities summarized within each building occupancy class (kg/m3)

	Aggregate	**Concrete**	**Timber**	**Steel**	**Masonry (Brick)**
Foundation with reinforced concrete					
Total a. (brick exterior)	47.93	55.66	7.33	4.38	26.72
Total a. (vinyl exterior)	47.93	55.66	7.33	4.38	-
Concrete Structure 1a					
Total	66.54	182.13	1.27	0.59	33.89
Concrete Structure 1b					
Total	34.24	66.77	0.68	0.99	-
Concrete Structure – Steel Reinforced					
Total	-	77.29	-	4.48	-
Steel Structure – Steel Walls					

Total	-	59.11	-	41.96	-
Steel Structure - Precast					
Total	-	75.92	-	61.6	-

4.3.3 Building Material Stocks

Material stocks are calculated as a function of the total gross volume of buildings as kilograms per cubic metre. The total material stock mass was calculated based on the following equation:

$$MS_i = \sum_{OC} MI_{i,OC} \times GV_{OC}$$

MS = Material stock
i = material intensity for individual material class (concrete, timber, steel or aggregate) MI = material intensity
oc= occupancy class
GV = gross volume

4.4 Assigning Road Classes

A bottom-up methodology is applied to estimate the material stocks contained in roads. The road network in Surrey was first categorised into different road types and assigned specific road widths and material intensities. The quantity of road stocks were calculated using the material intensities and gross area of roads. GIS techniques were used to approximate road length measurements, analyze the spatial distribution of road stocks, and improve the current transportation geodatabase for Surrey.

The City of Surrey classified roads into five classes according to their functions: local, collector, arterial, provincial highways, and gravel roads. Surrey's road classes were derived from the province's available road design guidelines. Highways and arterials consist of roads of national importance and have highest mobility and limited access to property. Collectors and local roads are comprised of roads of regional importance and local importance and have higher accessibility and lower mobility. Gravel roads are often private or temporary roads and are not

considered in this study since many are unpaved, not developed, or maintained by the government, or challenging to estimate accurately.

To quantify and map the in-use road material stocks in Surrey, road network GIS data from Surrey's open data portal were used to classify the road network, calculate the road surface area, estimate the road material stocks, and map the spatial distribution of stocks. Road network data from Surrey's open data portal had an initial road classification that can be used to define the road hierarchy.

4.4.1 Road Pavement Structures

Different functional road classes can have different pavement structures which result in different material intensities. The second step in road classification was to further classify functional road classes into different road types based on pavement structures. The City of Surrey's Pavement Structure Design Guidelines (2015) outlines road design standards. According to the design guidelines, road pavement structures are made up of four main layers of surface course, base course, subbase course, and subgrade course. The thicknesses and materials of these layers affect the strength and quality of the pavement. The surface course is the layer that is immediately in contact with traffic loads. It prevents the entry of surface water into underlying layers. This layer is usually constructed from hot mix asphalt (HMA). The layer immediately beneath is called the base course. It provides a uniform and stable support for the surface course. It distributes stresses transmitted from traffic evenly onto the layers below. It is usually composed of crushed aggregate or HMA. The next layer is called the subbase course which improves the load distribution of the base course and enables free drainage of water entering the pavement. It is usually composed of rock or soil aggregates. Below this is the subgrade which is compacted natural soil and acts as the foundation for the layers above.

4.4.2 Physical Size of Road

Surrey's road dataset contains 13, 353 lines with detailed information regarding the location of roads, road types, and length. The physical size of roads and calculating surface area involves considering the road width and road length. The width of road segments for Surrey's

road network were estimated based on regional pavement design manuals and assigned for each road type in the classification system. The length of the roads was measured physically based on GIS datasets. The total surface area of roads was then calculated by multiplying the length by the width.

4.4.3 Material Intensities for Roads

Each road type is assumed to share the same pavement structure and have the same material intensity. Pavement structures of roads were derived from consulting local and regional pavement design manuals (BC Ministry of Transportation and Infrastructure, 2015 and City of Surrey, 2020). Each pavement structure consists of three pavement layers (I.e., subbase, base, and surface layers), and each pavement layer is composed of one main type of material (e.g., aggregate, asphalt, soil, rock). The typical road cross-section profiles for each road type pavement structure have different road widths, thickness of each layer, and materials that compose the paving layer.

Table 6. Material Intensity Calculation break down of materials and material intensity classes in kg/m^3

Road Type	**Material Intensity**		
	Asphalt	Aggregate	Soil
Lane			
Surface	232		
Base		252	
Subbase			320
Total	**232**	**252**	**320**
Local			
Surface	232		
Base		252	
Subbase			320
Total	**232**	**252**	**320**
Collector			

Surface	302		
Base		252	
Subbase			480
Total	**302**	**252**	**480**
Arterial			
Surface	348		
Base		252	
Subbase			480
Total	**348**	**250**	**480**

4.4.5 Road Material Stocks

After importing the GIS file into the spreadsheet and sorting the roads, MIs are added for each group. Using the length and width of the roads, the total surface area of each road was calculated. With the area of roads and material intensities established, the materials stocked in roads was calculated based on the following equation:

$$MS_{roads,\,y} = \sum_{i=1}^{m} \sum_{j=1}^{n} MI_i \,.\, V_j$$

Where, m is the total number of road categories,
n is the total number of roads in each category,
i represents each road category,
j represents each road in each category,
y represents the year when the material stocks are calculated,
V is the volume of the road in units of cubic metres,
MI is the Material Intensity Factor in units of kg per square meter,
and MS is the total materials used in the road and sidewalk stocks in units of kg.

4.5 Results

4.5.1 Material Stock (MS) in buildings

The total so in buildings and roads are measured using the material intensities of different building typologies and their physical attributes. Following this, the spatial distribution of these stocks are shown on city scale maps. As well, the quality and quantity of material stocks impacted by the flood scenarios modeled in the first manuscript are described and mapped.

4.5.1.1 Material Stock (MS) by Material Category

The total material stocks in buildings in 2020 was calculated to be 66,842,923 kilotonnes or 111.47 tonnes per capita given that year's population. As seen in Figure 8 below, concrete accounted for the largest share of MS at 54% or 61.85 t/capital. Aggregate was the second largest class with 26% of total materials and equivalent to 30.12 t/capita. Steel was the third largest class with 9% of total materials, equivalent to 10.1 t/capita. Next was brick with 8% of total materials, equivalent to 9.22 t/capita. Timber had the lowest amount of stock with 3%, equivalent to 3.86 t/capita.

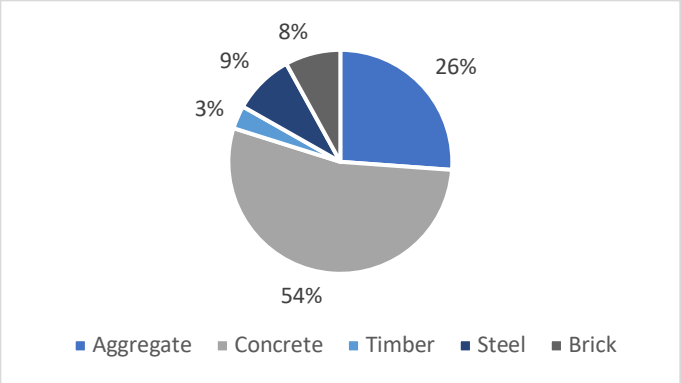


Figure 8. Percentage of building material stocks by material type

Table 7 presents a detailed breakdown of the material stocks used in buildings and roads, categorized by material type. The table includes two key metrics for each material type. The total material in weight (kt/m³) shows the total quantity of each material type, and provides an

understanding of the absolute volume and mass of materials present in the infrastructure. The material in kt/capita column presents the per capita amount of each material type, measured in kilotonnes per person. It offers a perspective on how much of each material is available per resident, helping to gauge the material intensity of the built environment in relation to the population.

Table 7. Building material stocks by material type

Material	Total material in weight (kt/m^3)	Material in kt/capita
Aggregate	17480149	30.75
Concrete	35898663	63.16
Timber	2241391	3.94
Steel	5867181	10.32
Brick	5355540	9.42

4.5.1.2 Stock by building use-type

The total MS is largely dominated by residential buildings, accounting for 59% of MS, equivalent to 40,733,203 kilotonnes or 70.19 t/capita. Other categories were much smaller, institutional buildings at 14.71%, commercial at 5.30%, industrial at 3.55%, government at 2.45% and agricultural at 2.30%. The distribution of other building use-types are shown in Table 8. Measuring material stocks by use-types (such as residential, commercial, industrial, and infrastructure services) provides a detailed view of where and how materials are utilized within different sectors. It helps in understanding sector-specific material demands and consumption patterns.

Table 8. Breakdown of material stock per capita in building use-types by material category

Use-Type	Aggregate	Concrete	Timber	Steel	Brick
Agricultural	0	1659.38	0	1177.93	0
Commercial	0	6226.15	0	361.88	0
Educational	4092.16	11200.86	78.10	36.28	2084.21

Government	704.17	1933.09	13.44	6.57	358.65
Industrial	0	904.29	0	641.92	0
Non Residential	1.19	1932.39	0.02	1293.84	0.61
Recreational	481.22	1904.85	9.18	38.33	0
Religious	398.55	1548.38	7.61	30.05	3.88
Residential	25079.89	29664.60	3835.47	2341.57	6975.92
Storage	0.30	6192.08	0.05	4395.31	0.16

Furthermore, Table 9 shows the distribution of material stocks per capita in building-use types by material stocks category. Assessing material stocks per capita helps in understanding how resources are distributed among the population. It provides insights into resource availability and usage efficiency, highlighting potential inequalities or surpluses in material distribution.

Table 9. Percentage of breakdown of material stock per capita in building use-types by material category

Use-Type	Aggregate	Concrete	Timber	Steel	Brick
Agricultural	0	2.63	0	11.41	0
Commercial	0	9.86	0	3.51	0
Educational	13.30	17.73	1.98	0.35	22.12
Government	2.29	3.06	0.34	0.06	3.81
Industrial	0	1.43	0.00	6.22	0
Non Residential	0.004	3.06	0.00	12.53	0.01
Recreational	1.56	3.02	0.23	0.37	0
Religious	1.30	2.45	0.19	0.29	0.04
Residential	81.54	46.96	97.25	22.68	74.03
Storage	0.001	9.80	0.001	42.58	0.002

4.5.1.3 Spatial Distribution of Building and Road Material Stocks

Addressing the first objective of this research, the spatial distribution of material stock for the entire city of Surrey is presented in two maps. Figure 9 shows the building stock distribution

by community. The largest proportion of building stocks are located in Newton at 26%, followed closely by South Surrey at 24%. These are the two largest communities by land area.

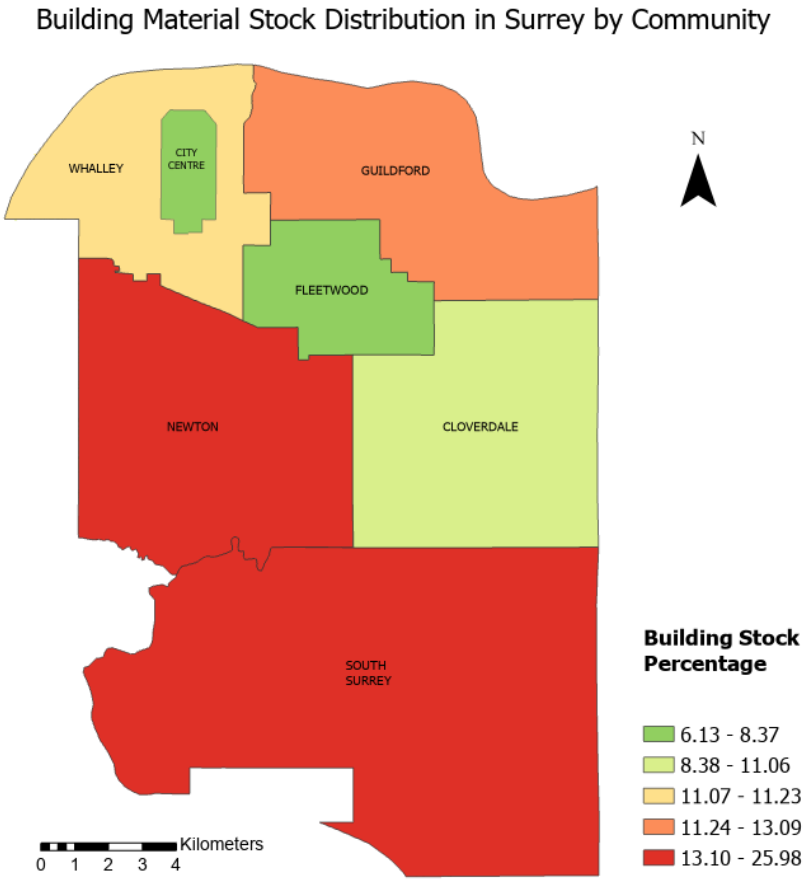


Figure 9. Map of building material stock distribution by community in Surrey

Figure 10 shows the building stock distribution by census dissemination area. Dissemination areas are the smallest geographic areas for which all census data are disseminated. Calculating and visualizing material stocks at the DA level enable comparison of material stock data with census statistics about the population in Surrey. The largest stock concentrations are found in industrial and manufacturing sectors. These areas are usually further away from the city centre since these buildings take up a large area of land and have a high volume. Residential buildings are often clustered together and have a lower concentration of stock since they have a smaller volume and are more uniform.

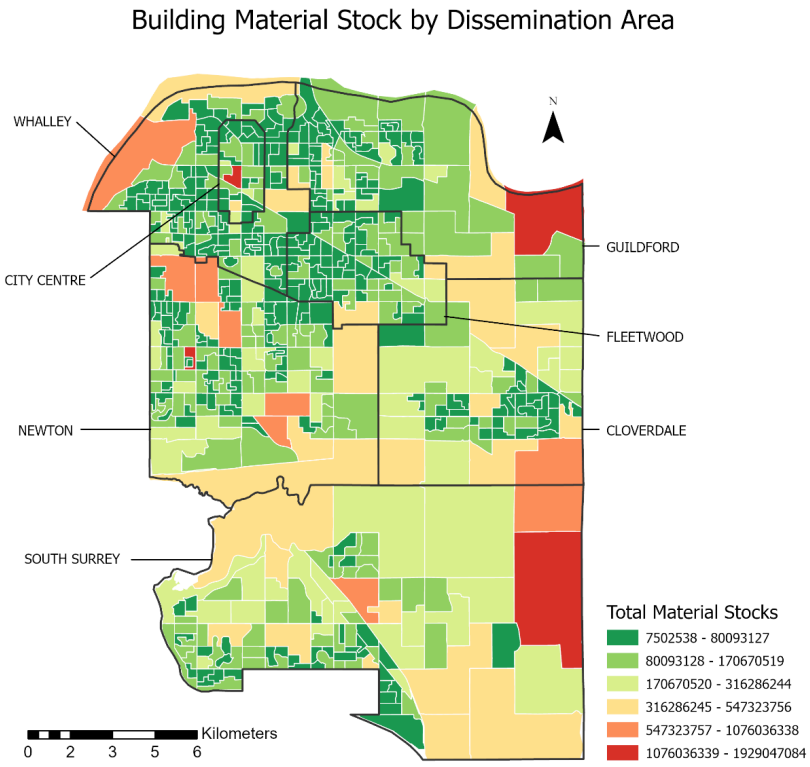
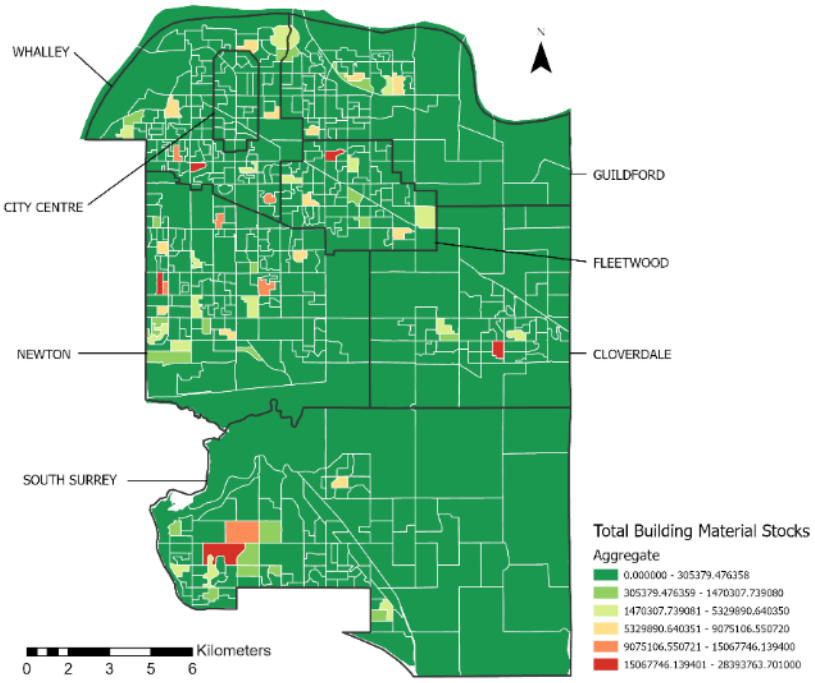
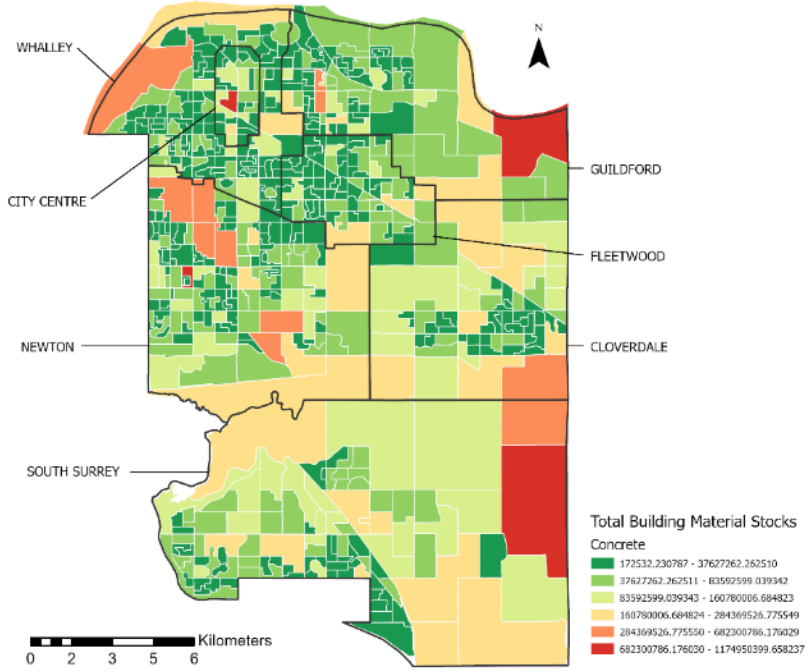
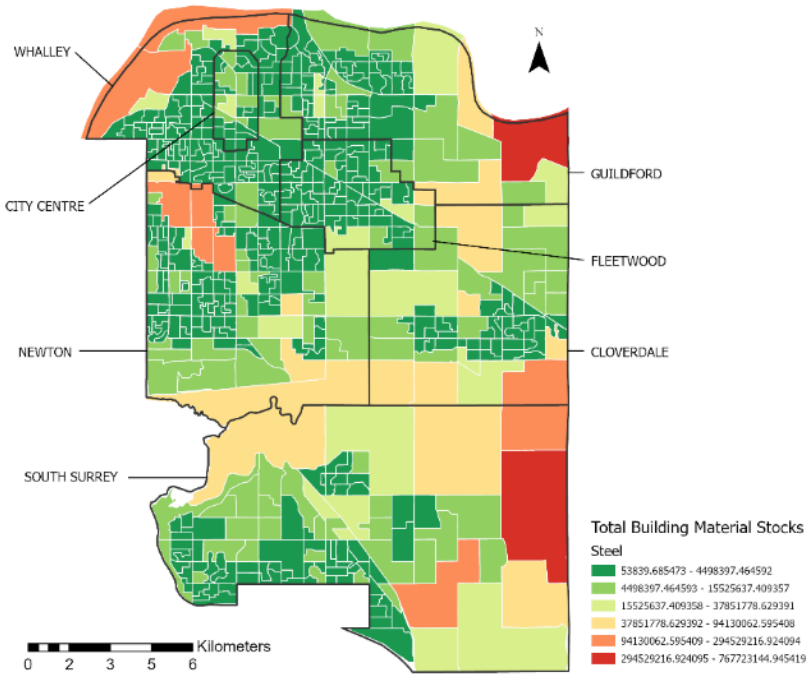


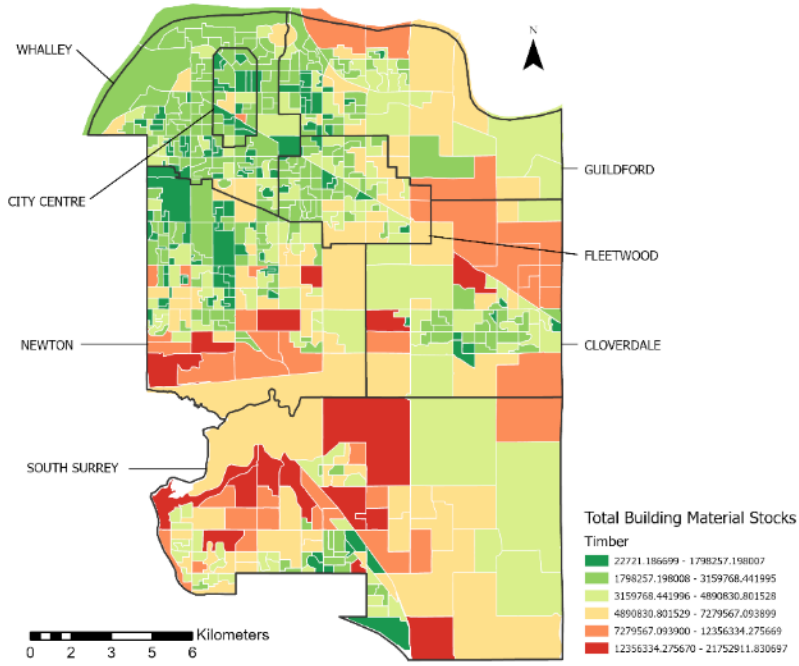
Figure 10. Map of building material stock distribution by dissemination area in Surrey

Figure 11 shows the building stock density by different material categories at the DA level. Concrete stocks make up the largest proportion of building stocks compared to other materials. Concrete stocks tend to cluster in surrounding suburban areas where most building use types are industrial and manufacturing. Steel stocks have a similar spatial distribution where large concentrations are found in industrial and manufacturing sectors. Timber stocks tend to cluster in large residential communities with single- or two-family homes and townhouse complexes. Aggregate and brick account for lower concentrations of stock since they are primarily used for foundation and exterior of residential buildings.


WHALLEY
CITY CENTRE
NEWTON
SOUTH SURREY
GUILDFORD
FLEETWOOD
CLOVERDALE
N
Kilometers
0 2 3 5 6
Total Building Material Stocks
Aggregate
0.000000 - 305379.476358
305379.476359 - 1470307.739080
1470307.739081 - 5329890.640350
5329890.640351 - 9075106.550720
9075106.550721 - 15067746.139400
15067746.139401 - 28393763.701000


WHALLEY
CITY CENTRE
NEWTON
SOUTH SURREY
GUILDFORD
FLEETWOOD
CLOVERDALE
N
Kilometers
0 2 3 5 6
Total Building Material Stocks
Concrete
172532.230787 - 37627262.262510
37627262.262511 - 83592599.039342
83592599.039343 - 160780006.684823
160780006.684824 - 284369526.775549
284369526.775550 - 682300786.176029
682300786.176030 - 1174950399.658237


WHALLEY
CITY CENTRE
NEWTON
SOUTH SURREY
GUILDFORD
FLEETWOOD
CLOVERDALE
N
Kilometers
0 2 3 5 6
Total Building Material Stocks
Steel
53839.685473 - 4498397.464592
4498397.464593 - 15525637.409357
15525637.409358 - 37851778.629391
37851778.629392 - 94130062.595408
94130062.595409 - 294529216.924094
294529216.924095 - 767723144.945419


WHALLEY
CITY CENTRE
NEWTON
SOUTH SURREY
GUILDFORD
FLEETWOOD
CLOVERDALE
N
Kilometers
0 2 3 5 6
Total Building Material Stocks
Timber
22721.186699 - 1798257.198007
1798257.198008 - 3159768.441995
3159768.441996 - 4890830.801528
4890830.801529 - 7279567.093899
7279567.093900 - 12356334.275669
12356334.275670 - 21752911.830697

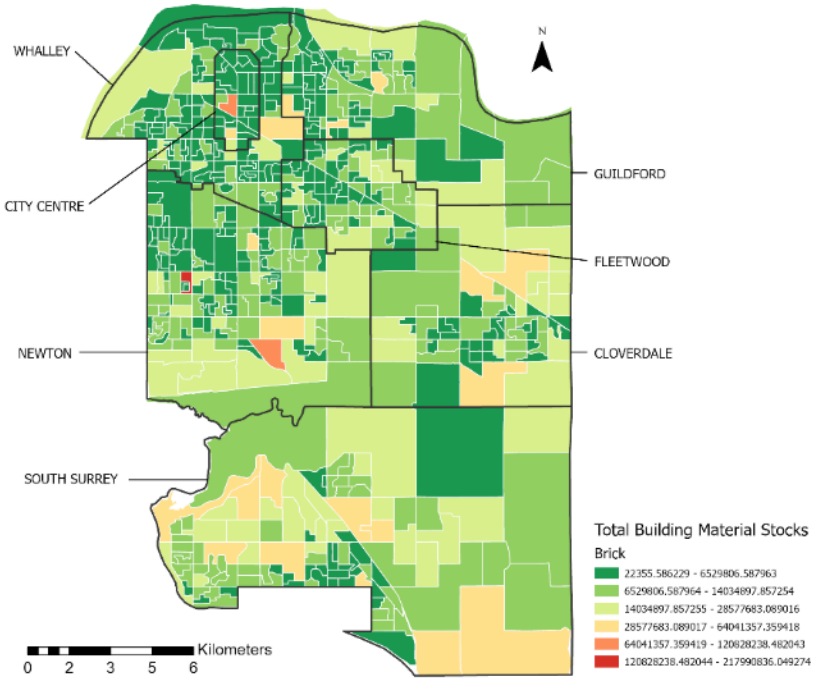


Figure 11. Road material sock distribution (break down of five materials) by dissemination area in Surrey

4.5.2 Material Stocks in Roads

The results of this study indicate that 682,185,04.40 kilotons of materials were contained in roads, equaling 113.77 kilotons per capita. The quantity of materials used in road stocks are shown in Table10 individually. The quantity of soil is the highest, totalling 9.81 kilotons per capita and accounts for 42% of the road stocks. This is followed by asphalt at 30%, then aggregate at 28%. The amounts of each material correspond to the thickness of each layer, where the thickest layer is the subbase course, accounting for the largest portion of road stock.

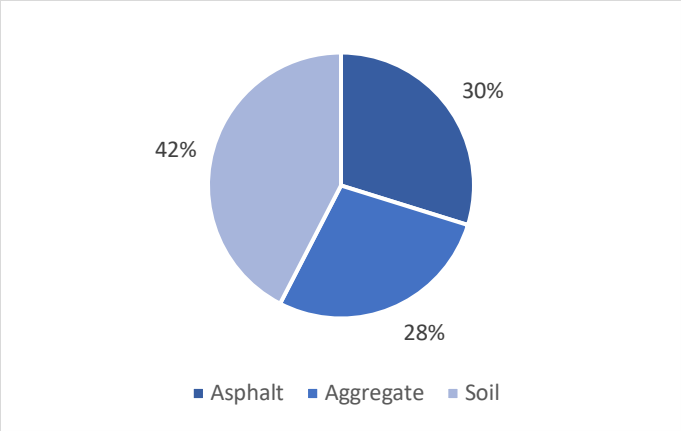


Figure 12. Percentage of road material stocks by material type

Table 10. Road Material stocks by Material type

Material	Total material in weight	Material in kt/capita
Asphalt	3916403	6.89
Aggregate	3649638	6.42
Soil	5574581	9.81

4.5.2.1 Spatial Distributions of Road Stocks

Two maps illustrate the spatial distribution of road stocks in the City of Surrey. Figure 13 shows the road stock distribution by community. The largest proportion of road stocks are located in South Surrey at 24%, followed by Newton at 20%. These are the two largest communities by land area.

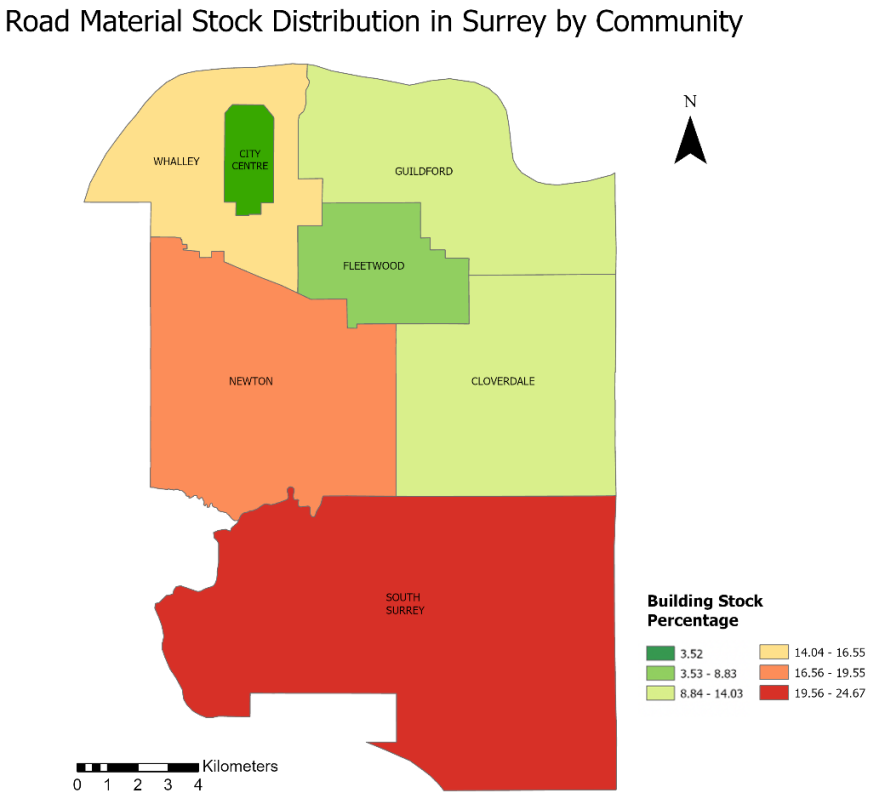


Figure 13. Map of road material stock distribution by community in Surrey

Figure 14 shows the road stock distribution by census dissemination area. The largest stock concentrations are found in areas with highways or arterial roads. Roads stocks also cluster around connecting roads between communities such as between South Surrey and Newton.

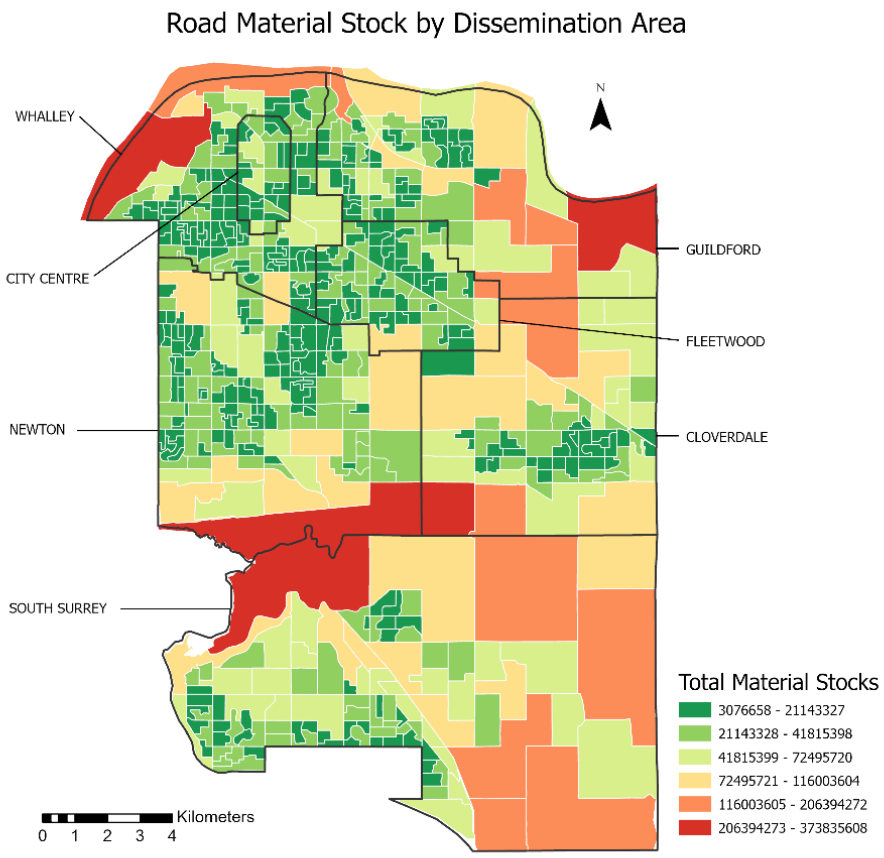
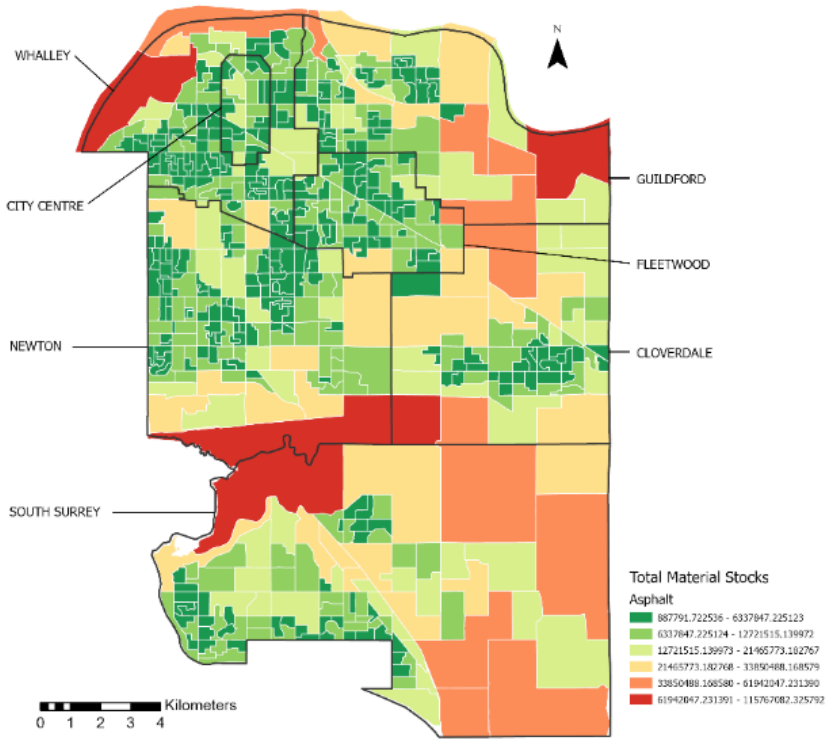
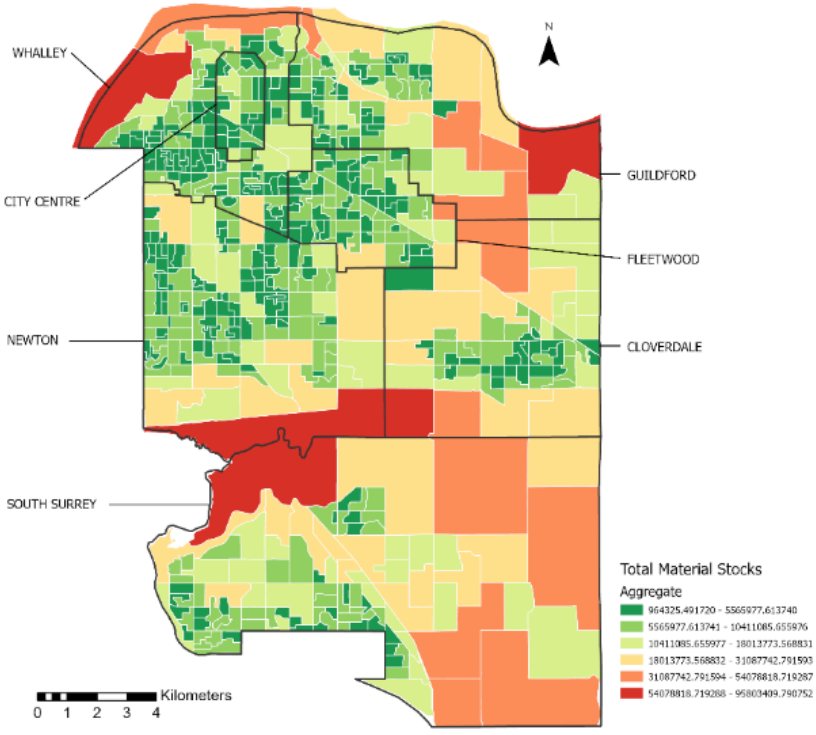


Figure 14. Map of road material stock distribution by dissemination area in Surrey

The distribution of road stock by material is similar since there is minimal difference between the thickness of each layer.


WHALLEY
CITY CENTRE
NEWTON
SOUTH SURREY
GUILDFORD
FLEETWOOD
CLOVERDALE
N
Kilometers
0 1 2 3 4
Total Material Stocks
Asphalt
887791.722536 - 6337847.225123
6337847.225124 - 12721515.139972
12721515.139973 - 21465773.182767
21465773.182768 - 33850488.168579
33850488.168580 - 61942047.231390
61942047.231391 - 115767082.325792


WHALLEY
CITY CENTRE
NEWTON
SOUTH SURREY
GUILDFORD
FLEETWOOD
CLOVERDALE
N
Kilometers
0 1 2 3 4
Total Material Stocks
Aggregate
964325.491720 - 5565977.613740
5565977.613741 - 10411085.655976
10411085.655977 - 18013773.568831
18013773.568832 - 31087742.791593
31087742.791594 - 54078818.719287
54078818.719288 - 95803409.790752

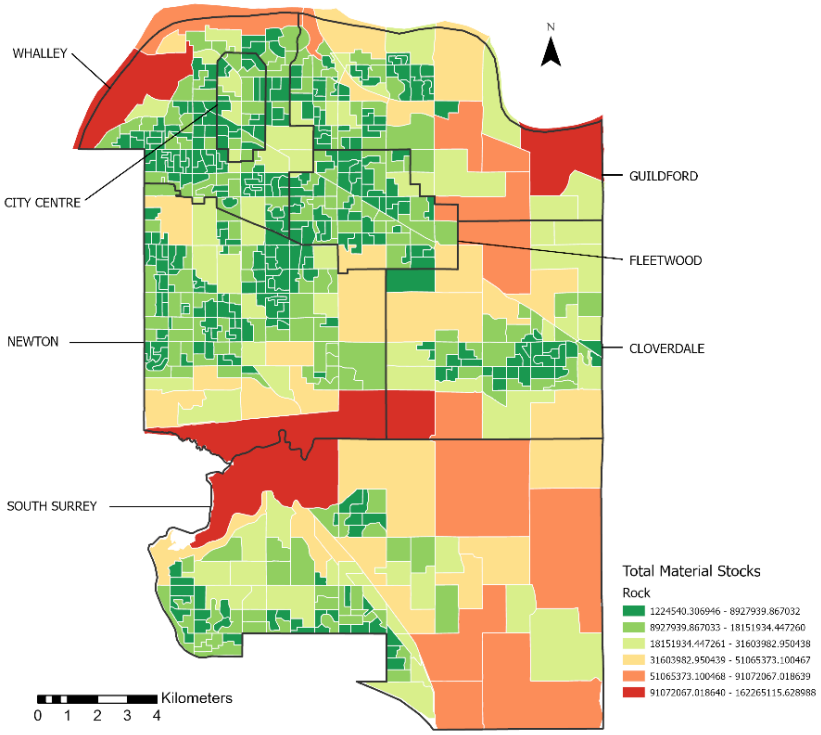


Figure 15. Road material sock distribution (break down of five materials) by dissemination area in Surrey

4.5.3 Temporal Changes of Material Stock

4.5.3.1 Buildings

Figure 16 shows the gradual increase trend of the in-use MSs between 1900 and 2022. The growth of accumulated MSs has accelerated since 1970, attributed to a large number of new residential and educational use buildings built after 1970. In Surrey, approximately 91% of all material flows have been added to stocks since 1970. As for the compositions, aggregate and concrete are the largest materials in each period, which account 30%-40% of MSs, respectively.

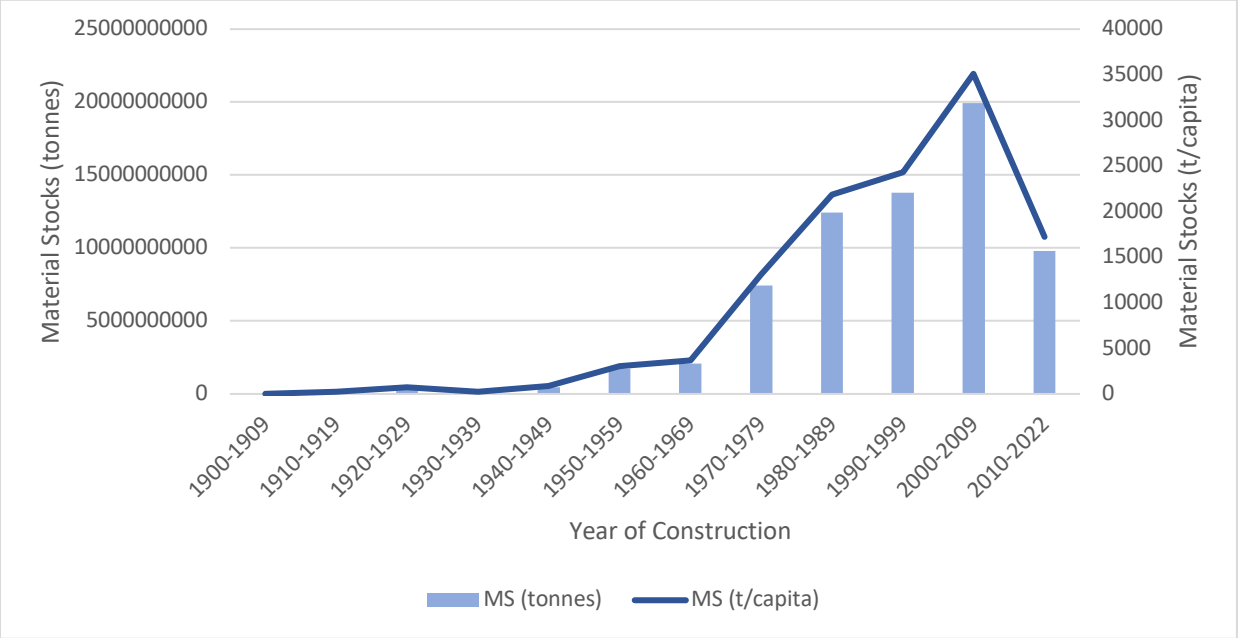


Figure 16. Temporal change in material stocks in buildings between 1900 and 2022

According to Figure 17, a majority of buildings were constructed between 2000 and 2009. The population grew by 10% between 2000 and 2009. As population increases, demand for buildings increases. Another period that experienced rapid increase in population was in the late 1900s. Population and demand is expected to continue increasing in the future.

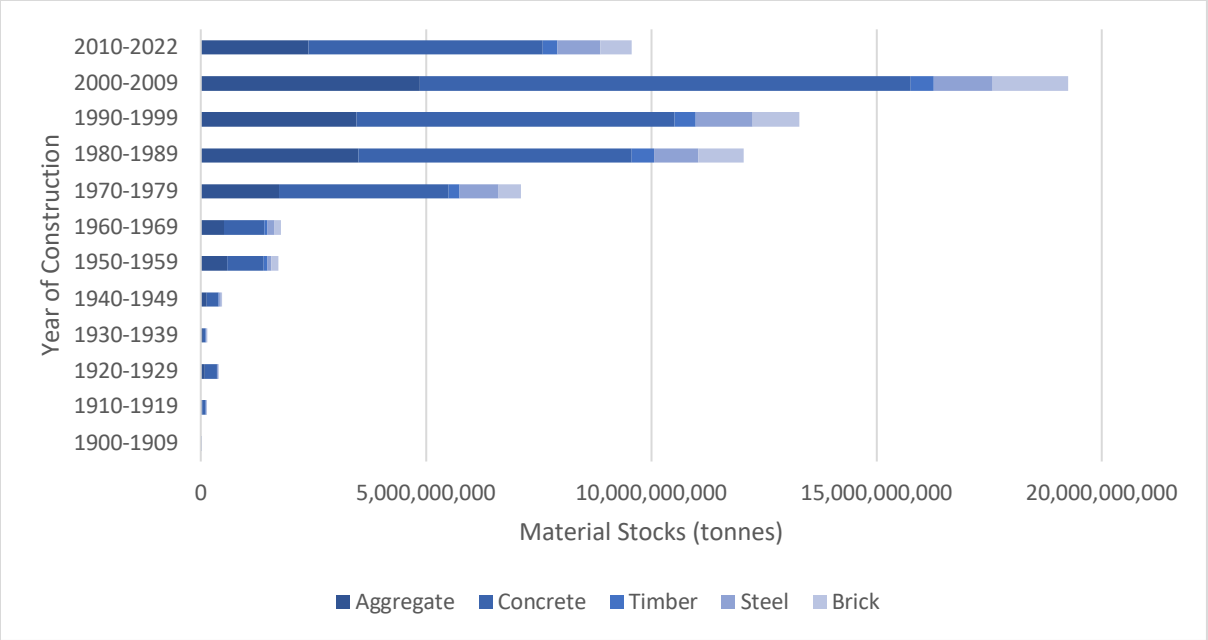


Figure 17. Temporal change in material breakdown in buildings between 1900 and 2022

Concrete remains the highest amount of material used in buildings between 1900 to 2022. Following 1980, the use of brick in buildings continued to increase. However, between 2010 and 2022, the use of steel exceeded the amount of brick used in construction.

4.5.3.2 Roads

Figure 18 shows the gradual increase trend of the in-use MSs between 1900 and 2022. The growth of accumulated MSs has accelerated since 1970, attributed to a large number of new residential and educational use buildings built after 1970. In Surrey, approximately 91% of all material flows have been added to stocks since 1970. As for the compositions, aggregate and concrete are the largest materials in each period, which account 30%-40% of MSs, respectively.

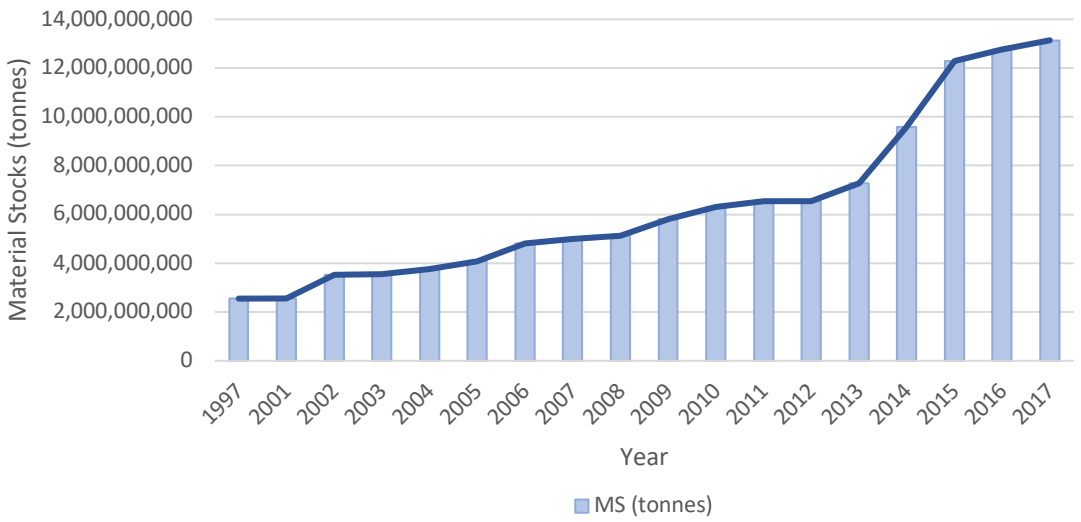


Figure 18. Temporal change in material stocks in roads between 1900 and 2022

According to figure 19, there is a steady increase in road material stocks due to the construction of new roads and maintenance or repair of roads. There was a rapid increase in the construction and repair of roads between 2013 and 2015, before reaching a plateau after.

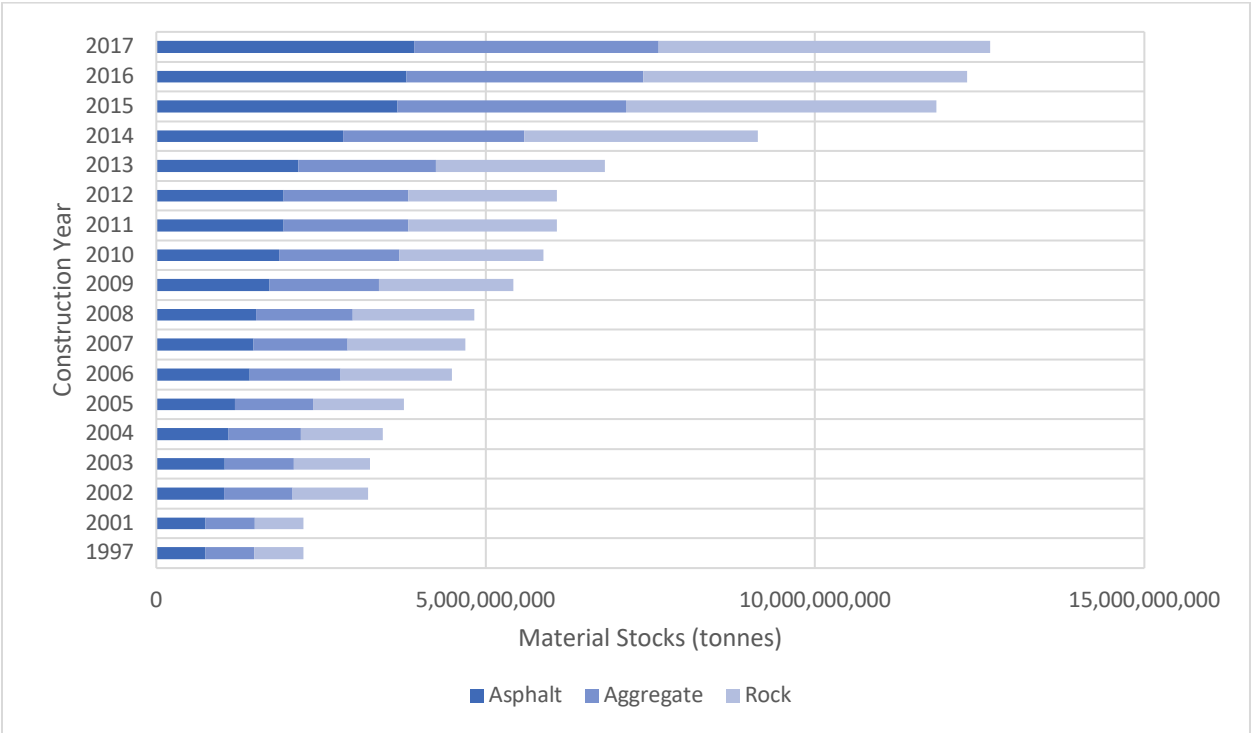
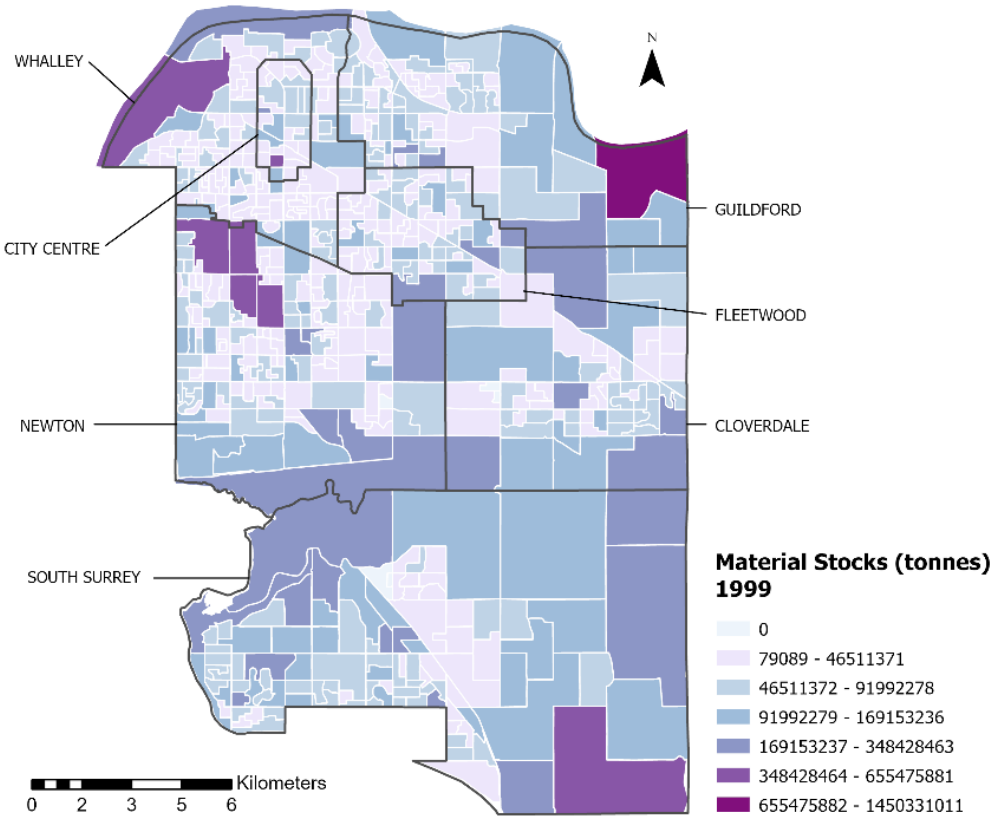


Figure 19. Temporal change in material breakdown in roads between 1900 and 2022

4.5.4 Spatiotemporal analysis of material stocks

4.5.4.1 Buildings

Figure 20 depicts the spatial distribution of initial building MS in Surrey in 1999 and 2022. The deeper color indicates the higher accumulation of buildings' MSs located in areas with a cluster of industrial or manufacturing building types. The lighter colour demonstrates the area with a lower material quantity with a lower population and housing density. The spatial pattern of initial MSs has changed over this period. The MSs accumulated in the urban area and sprawl to the rural area during this period. From 1960 to 1989, the MSs have increased along with the increasing number of newly built housing, especially in South Surrey, where the floor area of housing built during this period accounts for about 59% of total housing stocks. The MSs have increased significantly from 1999 to 2022, particularly in areas where commercial and residential spaces were built during this period.



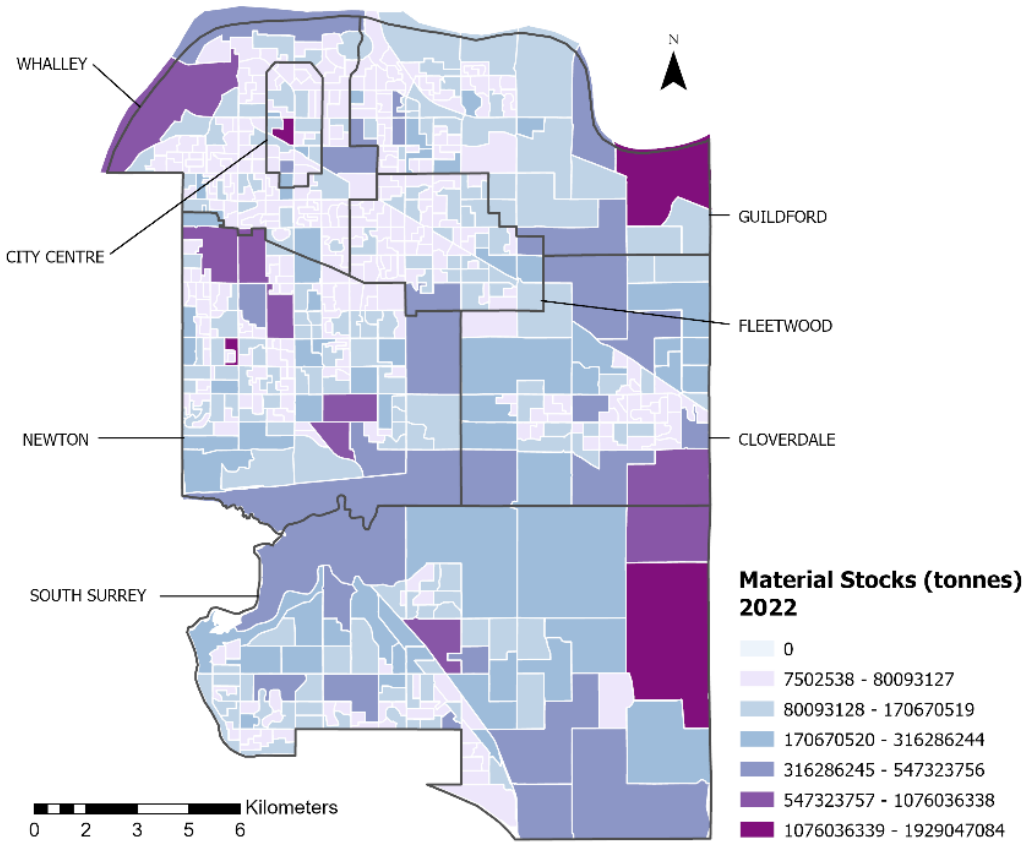
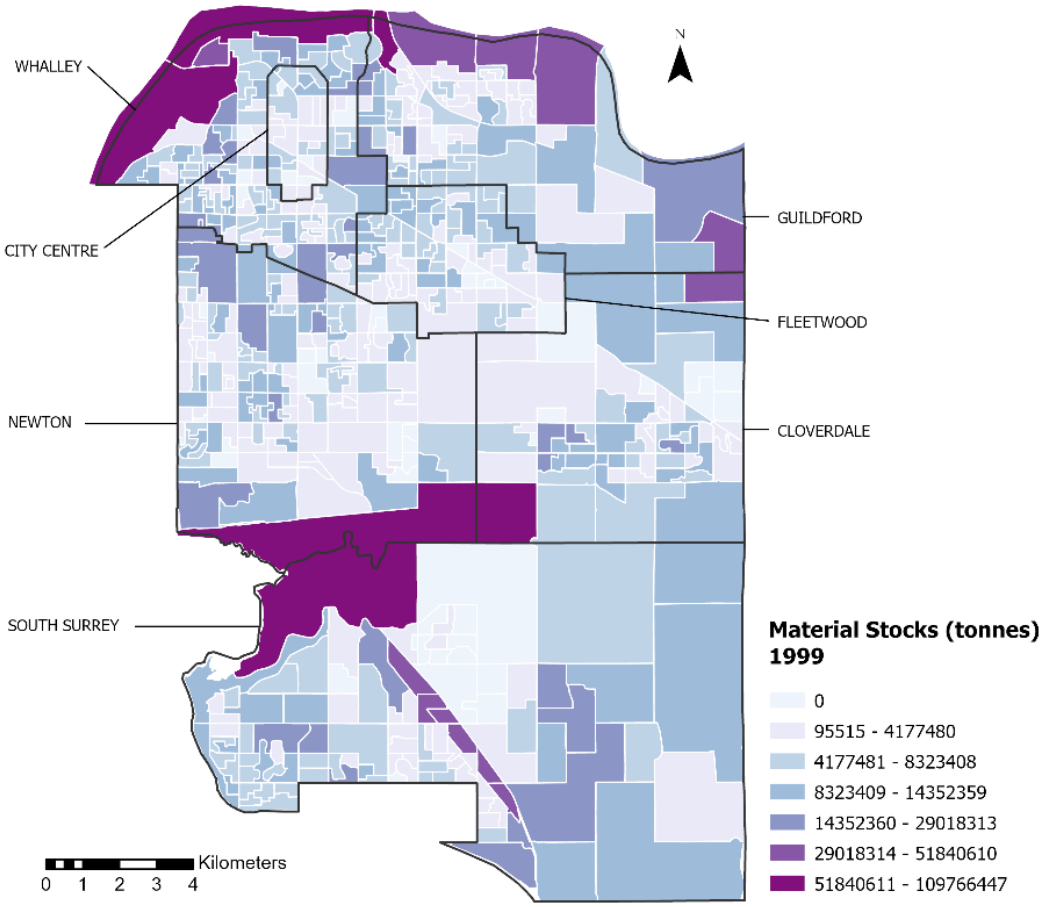


Figure 20. Spatial distribution in material stocks in buildings in 1999 and 202

4.5.4.2 Roads

Figure 20 depicts the spatial distribution of initial building MS in Surrey in 1999 and 2017. The deeper color indicates the higher accumulation of road MS, associated with areas where there is a larger concentration of arterial or collector roads. The lighter colour demonstrates the area with a lower material quantity such as a greater concentration of local roads. In 1999, a majority of MS clustered near bodies of water since early settlements were located there. Overtime, settlement has expanded further inward and it can be seen that roads are being developed away from the waterfront to service those new communities.



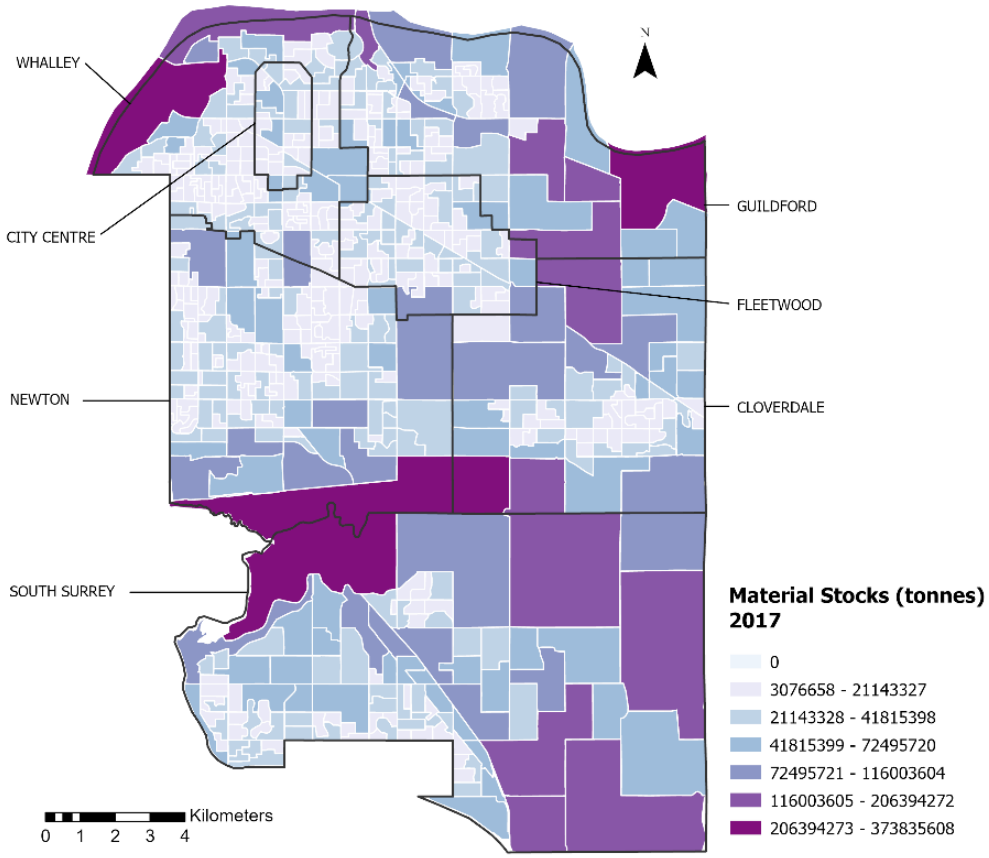


Figure 20. Spatial distribution in material stocks in roads in 1999 and 2017

At a 1/10 return period, the total amount of building material stocks impacted is 87,039.20 kt compared to 87,574.74 kt at a 1/100 scenario. This equates to an extra 535.53 kt that would be lost during a 1/100 scenario. For each return period, concrete appears to have the highest quantity impacted to flooding, whereas timber has the lowest quantity impacted.

Table 11. Quantity of building material stocks impacted by flooding in kilotonnes

Return Period	Aggregate	Concrete	Timber	Steel	Brick
1/10	17,328.37	49,089.70	1,978.55	12,587.95	6,054.63
1/25	17,413.40	49,193.70	1,991.49	12,597.99	6,078.26
1/50	17,483.72	49,294.20	2,002.08	12,617.86	6,098.16
1/100	17,511.18	49,328.37	2,006.24	12,620.99	6,107.97

As for roads, a 1/10 return period had an estimate of 8,209.83 kt impacted compared to 8,232.09 kt at a 1/100 return period. This equates to an extra 22.27 kt that would be lost during a 1/100 scenario. For each return period, rock appears to have the highest quantity impacted to flooding, whereas aggregate has the lowest quantity impacted.

Table 12. Quantity of road material stocks impacted by flooding in kilotonnes

Return Period	Aggregate	Rock	Asphalt
1/10	2,310.90	3,461.85	2,437.08
1/25	2,312.94	3,464.95	2,439.32
1/50	2,315.24	3,469.17	2,442.06
1/100	2,316.67	3,471.72	2,443.71

At a 1 metre rise in sea level, the total amount of building material stocks impacted is 1,192,606.43 kt compared to 3,445,953.29 kt at a 2.5 metre sea level rise scenario. This equates to an extra 2,253,346.86 kt that would be lost during a 2.5 metre sea level rise scenario. For each return period, concrete appears to have the highest quantity impacted to flooding, whereas timber has the lowest quantity impacted.

Table 13. Quantity of building material stocks impacted by sea level rise in kilotonnes

Sea Level Rise	Aggregate	Concrete	Timber	Steel	Brick
1	276.07	1,100.49	40.34	555.70	83.48
1.5	342.78	1,202.35	49.59	561.50	107.71
2	536.20	1,202.35	49.59	1,765.29	212.63
2.5	536.20	3,355.35	71.42	1,765.29	212.63

As for roads, a 1 metre sea level rise scenario had an estimate of 905,479.07 kt impacted compared to 1,695,985.52 kt at a 2.5 metre sea level rise scenario. This equates to an extra 790,506.45 kt that would be lost during a 2.5 metre sea level rise scenario. For each return period, rock appears to have the highest quantity impacted to flooding, whereas aggregate has the lowest quantity impacted.

Table 14. Quantity of road material stocks impacted by sea level rise in kilotonnes

Sea Level Rise	Aggregate	Rock	Asphalt
1	394.62	687.28	479.17
1.5	426.85	741.87	516.58
2	732.40	1,249.62	877.04
2.5	746.77	1,279.12	898.02

4.6 Discussion

The following section discusses the results from the material stock analysis and the impacts of flooding and sea level rise to material stocks in Surrey. The limitation and future direction of work are discussed.

4.6.1 Building and road material stocks in the City of Surrey

The total material stocks in buildings for the City of Surrey is estimated to be 111 t/cap in 2020. In comparison to other case studies around the world, Surrey seems to have a similar range of construction material per capita. For instance, Japan estimated a 110 t/cap of material consumption, which is slightly lower than Surrey's in both buildings and roads. Other studies

include Vienna at 210t/cap in 2013 a (Kleemann et al. 2016) and Padua at 209 t/cap in 2007 (Alessio et al., 2019). The range of per capita material consumption is different in each urban area and it is related to multiple reasons. Construction norms and regulations, climate, topography, common engineering practices, and available construction materials in the area are some of the factors that affect the material use rate in cities (Fishman et al., 2014). It is difficult to compare the results of different cities since each study has included different types of stocks and construction materials in their analysis. An accurate comparison is only possible if the conditions are similar in the compared areas.

The total material stocks in roads for the city of Surrey is estimated to be 113t/cap. p. Comparing the MSA results in the road and sidewalk stocks is difficult since most city level MSA studies have not included roads in their analysis. However, at the country level, the study conducted by Miatto et al. (2017) shows the material stocks in roads in USA in 2015 was estimated to be 15.1 Gt which translates into a per capita consumption rate of 41 t/cap (Miatto et al., 2017). A similar study conducted in the road networks of Vietnam indicates 30 t/cap consumption rate in 2012 (Nguyen et al., 2018). Since Vietnam is a developing country it is predicted that the consumption rate will increase as more construction activities take place in the country, whereas in USA it was mentioned that the quantity of materials in road stocks have been almost consistent in the past decade and therefore, the consumption rate is decreasing (Miatto et al., 2017; Nguyen et al., 2018).

In Surrey, the total length of roads was estimated to be 6369 kilometers, which averaged to be 2,063 tonne per kilometer. Compared to the United States, in 2015, the average material stocks per kilometer was estimated to be 2, 268 tonnes (Miatto et al., 2017). In Vietnam, Ngyuen et. al (2019) estimated 12,258 tonnes per kilometer of material stock in 2012. The average material stock per kilometer in Surrey is closer to the United States than Vietnam. The road pavement structure in Vietnam was divided into a surface layer (80 to 140 mm) and a base layer (300 mm; Nguyen et al., 2019). In comparison, in Surrey, the road pavement structure is divided into a surface course, base course, subbase course, and subgrade course. In addition, the materials analyzed by Nguyen et al. (2019) and Miatto et al. (2017) broke down the road surface

materials into gravel, sand, cement, and bitumen (i.e., asphalt) categories. Rather for Surrey, the road surface materials were broken down into soil, aggregate, and asphalt.

4.6.2 Temporal and spatial distribution of building and road material stocks

The time series shows a steady growth in building MS between 1900 and 1940, followed by an increase between 1940 and 1960, and rapid growth between 1960 and 2009. World War II (1939–1945) and its aftermath saw a rapid growth of population and development in Surrey (City of Surrey, 2022). Prior to 1945, most building use types were agricultural or residential, but after 1945 there was a sudden increase in industrial buildings. The wartime industrial demands resulted in shortages of steel and other building materials, leading to the adoption of new materials, such as aluminum and reinforced concrete (Van de Voorde, 2015). By the end of World War II, concrete was adopted as a common building material across the globe (Van de Voorde, 2015). In 1937, the opening of the Pattullo Bridge and the completion of King George Highway in 1940 also improved access to the main district (Bauerfind, 2019). Along with housing shortages in downtown Vancouver, the 1940s saw many families moving to Surrey where affordable housing was available, especially in the communities of White Rock and Crescent Beach (Bauerfind, 2019). However, most employment was located North of the Fraser River so most of the population resided North of Surrey (Bauerfind, 2019).

The 1950s saw a rapid growth population in the north end of Surrey especially around Whalley, Fleetwood, Kennedy and Newton (City of Surrey, 2022). These areas had a good road access with Pacific Highway, King George Highway and Scott Road. However, local employment was slow to develop and up to 75% of Surrey workers were employed north of the Fraser River (Bauerfind, 2019). Between 1959 and the 1960s, the completion of the George Massey Tunnel and Highway 99 resulted in a development boom on the west side of Surrey and in South Surrey (Bauerfind, 2019). As well the opening of the Port Mann Bridge in 1964 along with the four lanes of the new Trans-Canada Highway saw the development of the Guildford and Fleetwood areas (Bauerfind, 2019). The development of new roads allowed easier access to jobs north of the Fraser River, however, there was slow progress in developing employment opportunities within Surrey (Bauerfind, 2019).

The 1970s saw continued growth and development and the adoption of the Regional District's plans for Surrey which proposed the development of five town centers (Bauerfind, 2019). Road improvements in the 1980s continued to spur Surrey's growth (Bauerfind, 2019). The widening of King George Highway south of Newton and to 64th Avenue, and the opening of Clover Valley Road as part of Pacific Highway south from Highway 1 to Fraser Highway brought increased development to the Newton District and to east Cloverdale (Bauerfind, 2019). In the 1990s, the focus on the development of town centers continued. On September 11, 1993 Surrey' officially became a city and in 1994, the Sky Train arrived in Whalley (Bauerfind, 2019). The four stations located at Scott Road, Gateway, Central City, and King George provided improved access in the north across the Fraser River (Bauerfind, 2019). This led to a rapid population growth and resulted in new commercial developments outside the traditional town centers (City of Surrey, 2022). It also spurred the need for redevelopment of the commercial cores in Cloverdale, Whalley, Newton, and White Rock (Bauerfind, 2019). The 10 years from 1995 to 2005 saw very rapid growth, specifically residential developments in Guildford, Fleetwood, east and west Cloverdale, west and east Newton, and South Surrey. The percentage change from 1996 to 2001 was 14.2% (City of Surrey, 2022). However, the economic downturn of 2009 slowed growth in Surrey, but population continued to grow at a steady rate (BC Ministry of Finance, 2009).

As for road stocks, there is a steady increase in material stocks between 1997 and 2012, followed by a rapid increase between 2013 and 2015, and reaching a plateau after. In 2014, the City experienced a 1/100-year rainfall which left a significant amount of debris and gravel covering the roads (CTV Vancouver, 2014). As a result, there was a significant amount of road stock that needed to be replaced. The City of Surrey also released a 10-year servicing plan and development between 2014 and 2023 (City of Surrey, 2022). The Plan establishes the City’s capital expenditure plan for the construction of engineering infrastructure to service existing neighbourhoods and to support new growth across the city (City of Surrey, 2022). A majority of the funding, $336,025,000, was allocated to servicing arterial roads, with $75,110,000 allocated to servicing non-arterial roads (City of Surrey, 2022). The Plan also forecasts that 37,100 residential dwelling units will be constructed between 2014 and 2023 and estimates a population increase of 90,700 (City of Surrey, 2022). During this same period, commercial floor space is

expected to expand by 500,000 square feet per year and industrial development by 35 acres per year (City of Surrey, 2022).

Present day, building and road material stocks are accumulated near the edges of the city and near coastal areas. Historically, industrial development was clustered near the Fraser River in the Northern part of Surrey and away from the city center (Bauerfind, 2019). These large industrial buildings remain with large amounts of stock. The development of city centres was more recent, with the construction of high-rise buildings becoming more common in recent years (UrbanSurrey, 2021). For instance, there are seven high rise buildings built after 2010 that are higher than 100 metres (UrbanSurrey, 2021). These buildings also accumulate a high quantity of material stocks. To meet the demands of a growing population, it is likely that the development of more high-rise buildings will be constructed in the future and a greater focus on more sustainable and resilient development (UrbanSurrey, 2021).

4.6.3 Vulnerability of Material Stocks to Flooding and Sea Level Rise

This study quantifies vulnerable building and road material stocks in different return periods and sea level rise scenarios. At a 1/10 return period, the total amount of building material stocks impacted is 87,039.20 kt compared to 87,574.74 kt at a 1/100 scenario. For a 1 metre rise in sea level, the total amount of building material stocks impacted is 1,192,606.43kt compared to 3,445,953.29 kt at a 2.5 metre sea level rise scenario. As for roads, a 1/10 return period had an estimate of 8,209.83 kt impacted compared to 8,232.09 kt at a 1/100 return period. For a 1 metre sea level rise scenario, the total amount of road material stocks impacted was 905,479.07 kt compared to 1,695,985.52 kt at a 2.5 metre sea level rise scenario. A greater quantity of material stocks is impacted from flooding since it considers the accumulation of water downstream, creating inundation areas further into the city. As for the sea level rise assessment, it only accounted for inundated areas that were directly connected to the coast, and there is less land area affected. Buildings and roads located near the coast along with city centres are among the most vulnerable to flooding and sea level rise. The likelihood of flooding occurring in dense urban areas is higher due to the high proportion of paved surfaces. These surfaces limit water infiltration and increase the amount of water running off the ground surface.

In terms of building material stocks, concrete appeared to have the highest quantity impacted to flooding and sea level rise since there is a large accumulation of concrete in residential basements and large industrial buildings. Aggregate had the second highest quantity impacted as large amounts are used when constructing foundation for multiple building types. Timber had the least quantity impacted as it is mainly used for framing and structural purposes. In terms of road material stock, rock appeared to have the highest quantity impacted and aggregate had the least quantity due to the difference in thickness between each layer. Since there are few studies that specifically looked at the impacts of flooding and sea level rise to material stock quantities in a city context, it is difficult to compare the results of this research against. For instance, a study done in Grenada estimated between 135 kt and 216kt of lost timber in buildings from a hurricane. The composition of buildings and geographic differences for a coastal region would indicate differences in the quantity of material stocks impacted. The analysis of potential stock loss scenarios in different geographical contexts can be valuable for informing infrastructure resilience and post-disaster recovery.

4.7 Limitations

This research assessed buildings in a 2D environment which assumes that entire buildings would be impacted to flooding or sea level rise scenarios. Depending on the severity of flooding or sea level rise, only certain heights of buildings may be inundated. The use of LiDAR data can generate accurate building heights and used for 3D modelling of urban areas. 3D modelling can provide simulations of real and accurate effects caused by natural disasters like fires, floods, and earthquakes. It can inform planners of better city management to prevent future disasters and delays in the recovery of the loss due to disaster.

The attribute year of construction for the road network data was missing or inaccurate for a portion of the roads specifically for highways. When examining material stocks over time, it would be more efficient to examine changes on a year-to-year basis, but roads completed prior to 1997 were not indicated. Studies providing accurate temporal overlook of material stock accounts over the years allow for a more in-depth understanding in the flow fluctuations of

materials over time and why they occur. For example, Cheng et al. (2018) found that in Taipei City the total material stock accumulation doubled from 1990 to 2014. Examining these material stocks spatially can help determine where old building clusters exist and enhance the efficiency of predicting future end-of-building life cycle waste flows (Cheng et al., 2018; Stephen & Athanassiadis, 2018).

In terms of the material intensities, this study assumed that buildings within each occupancy class had the same typologies. This is not fully representative, since some homes are constructed differently and can have variable typologies, such as different height basements, roof lines, or exterior building composition. However, it is difficult to provide an accurate prediction of the distribution of different material typologies as it would require verifying each home and its modifications over the years. Therefore, the distributions are estimated quite broadly, but it is important to note that building styles and technology change over time influence construction styles. For future studies, fieldwork can be conducted to obtain a sample estimation and confirm construction styles. More accurate calculation of material stocks will help policy makers and planners understand future resources that can be used for recycling or re-building purposes.

4.8 References

10-year servicing plan. City of Surrey. (2022, April 26). Retrieved October 20, 2022, from https://www.surrey.ca/renovating-building-development/engineering-infrastructure/10-year-servicing-plan#:~:text=The%20Servicing%20Plan%20is%20developed,2021%2D2030)%20Servicing%20Plan.

Bauerfind, D. (2019, September 26). *Hometown Series: A spotlight on Surrey • British Columbia Magazine*. British Columbia Magazine. Retrieved October 20, 2022, from https://www.bcmag.ca/hometown-series-a-spotlight-on-surrey/

Cheng, K.-L., Hsu, S.-C., Li, W.-M., & Ma, H.-W. (2018). Quantifying potential anthropogenic

City of Surrey. (2022, July 25). *About Surrey*. City of Surrey. Retrieved October 20, 2022, from https://www.surrey.ca/about-surrey#:~:text=The%20City%20of%20Surrey%20is,culturally%20diverse%20cities%20in%20Canada.

Fischer-Kowalski, M. (2011). Analyzing sustainability transitions as a shift between sociometabolic regimes. Environmental Innovation and Societal Transitions, 1, 152-159.

Fishman, T., Schandl, H., & Tanikawa, H. (2015). The socio-economic drivers of material stock accumulation in Japan's prefectures. *Ecological Economics*, *113*, 76–84. https://doi.org/10.1016/j.ecolecon.2015.03.001

Fishman, T., Schandl, H., & Tanikawa, H. (2015). The socio-economic drivers of material stock accumulation in Japan's prefectures. Ecological Economics, 113, 76-84.

Fishman, T., Schandl, H., Tanikawa, H., Walker, P., & Krausmann, F. (2014). Accounting for the material stock of nations. Journal of Industrial Ecology, 18(3), 407-420. Fiskel, J. (2006). A framework for sustainable materials management. Global Recycling, 15-22.

Garcia-Torres, S., Kahhat, R., & Santa-Cruz, S. (2017). Methodology to characterize and quantify debris generation in residentiabl buildings after seismic events. Resources, Conservation, and Recycling, 117, 151-159.

Gontia, P., Nageli, C., Rosado, L., Kalmykova, Y., & Osterbring, M. (2018). Material-intensity database of residential buildings: A case-study of Sweden in the international context. Resources, Conservation & Recycling, 130, 228-239. Gordon, R., Bertram, M., &

Graedel, T. (2006). Metal stocks and sustainability. Proceedings of the National Academy of Science, 103(5), 1209-1214

Guo , J., Miatto, A., Shi, F., & Tanikawa, H. (2019). Spatially explicit material stock analysis of buildings in Eastern China metropoles. Resources, Conservation & Recycling, 146, 45-54.

Haberl, H., Wiedenhofer, D., Erb, K.-H., Gorg, C., & Krausmann, F. (2017). The material stockflow-service nexus: A new approach for tackling the decoupling conundrum. Sustainability, 9(1049), 1-19.

Haberl, H., Wiedenhofer, D., Pauliuk, S., Krausmann, F., Muller, D., & Fischer-Kowalski, M. (2019). Contributions of sociometabolic research to sustainability science. Nature Sustainability, 1-12.

IPCC, 2023: Summary for Policymakers. In: Climate Change 2023: Synthesis Report. Contribution of Working Groups I, II and III to the Sixth Assessment Report of the Intergovernmental Panel on Climate Change [Core Writing Team, H. Lee and J. Romero (eds.)]. IPCC, Geneva, Switzerland, pp. 1-34, doi: 10.59327/IPCC/AR6-9789291691647.001

Kapur, A., Keoleian, G., Kendall, A., & Kesler, S. (2008). Dynamic modeling of in-use cement stocks in the United States. Journal of Industrial Ecology, 12(4), 539-556.

Kavgic, M., Mavrogianni, A., Mumovic, D., Summerfield, A., Stevanovic, Z., & DjurovicPetrovic, M. (2010). A review of bottom-up building stock models for energy consumption in the residential sector. Building and Environment, 45, 1683-1697.

Kennedy, C., Cuddihy, J., & Engel-Yan, J. (2007). The changing metabolism of cities. Journal of Industrial Ecology, 43-59. Kleemann, F., Lederer, J., Rechberger, H., & Fellner, J. (2016). GIS-based analysis of Vienna's material stock in buildings. Journal of Industrial Ecology, 21(2), 368-380.

Kleemann, F., Lederer, J., Rechberger, H., & Fellner, J. (2016). GIS-based analysis of Vienna's material stock in buildings. *Journal of Industrial Ecology*, *21*(2), 368–380. https://doi.org/10.1111/jiec.12446

Kohler, N., & Hassler, U. (2002). The building stock as a research object. Building research and information, 30(4), 226-236.

Krausmann, F., & Fischer-Kowalski, M. (2013). In S. Singh, H. Haberl, M. Chertow, M. Mirtl,

& M. Schmid, Long term socio-ecological research: Studies in society-nature interactions across spatial and temporal scales (pp. 339-365). Netherlands: Springer.

Krausmann, F., Gingrich, S., Eisenmenger, N., Erb, K.-H., Haberl, H., & Fischer-Kowalski, M. (2009). Growth in global materials use, GDP and population during the 20th century. Ecological Economics, 2696-2705.

Krausmann, F., Schandl, H., Eisenmenger, N., Giljum, S., & Jackson, T. (2017b). Material flow accounting: Measuring global material use for sustainable development. Annual Review of Environment and Resources, 42, 647-675.

Krausmann, F., Wiedenhofer, D., Lauk, C., Haas, W., Tanikawa, H., Fishman, T., . . . Haberl, H. (2017a). Global socioeconomic material stocks rise 23-fold over the 20th century and require half of annual resource use. Proceedings of the National Academy of Sciences, 114(8), 1880-1885.

Lanau, M., Liu, G., Kral, U., Wiedenhofer, D., Keijzer, E., Yu, C., & Ehlert, C. (2019). Taking stock of built environment stock studies: progress and prospects. Environmental Science and Technology, 53, 8499-8515.

Mesta, C., Kahhat, R., & Santa-Cruz, S. (2018). Geospatial characterization of material stock in the residential sector of a Latin-American city. Journal of Industrial Ecology, 23(1), 280-291.

Miatto, A., Schandl, H., Forlin, L., Ronzani, F., Borin, P., Giordano, A., & Tanikawa, H. (2019). A spatial analysis of material stock accumulation and demolition waste potential of buildings: A case study of Padua. *Resources, Conservation and Recycling*, *142*, 245–256. https://doi.org/10.1016/j.resconrec.2018.12.011

Miatto, A., Schandl, H., Wiedenhofer, D., Krausmann, F., & Tanikawa, H. (2017). Modeling material flows and stocks of the road network in the United States from 1905-2015. Resources, Conservation & Recycling, 127, 168-178.

Muller, E., Hilty, L., Widmer, R., Schluep, M., & Faulstich, M. (2014). Modeling metal stock and flows: A review of dynamic material flow analysis methods. Environmental science and technology, 48(4), 2102-2113.

Padovan, D. (2000). The concept of social metabolism in classical sociology. *Theomai, 2*, Red Internacional de Estudios sobre Sociedad, Naturaleza y Desarrollo. Buenos Aires, Argentina.

Pauliuk, S., & Hertwich, E. (2015). Socioeconomic metabolism as paradigm for studying the biophysical basis of human societies. Ecological Economics, 119, 83-93.

Population Estimates & Projections. City of Surrey. (2022, September 22). Retrieved October 20, 2022, from https://www.surrey.ca/business-economy/business-data/population-estimates-projections

resources of buildings through hot spot analysis. Resources, Conservation and Recycling, 133, 10-20.

Symmes, R., Fishman, T., Telesford, J., Singh, S., Tan, S.-Y., & de Kroon, K. (2019). The weight of islands : Leveraging Grenada's material stocks to adapt to climate change. Journal of Industrial Ecology, 1-14.

Tanikawa, H., & Hashimoto, S. (2009). Urban stock over time: Spatial material stock analysis using 4d-GIS. Building Research & Information, 37(5), 483-502. Tanikawa, H., Fishman, T., Okuoka, K., & Sugimoto, K. (2015). The weight of society over time and space. Journal of industrial ecology, 19(5), 778-791.

Tanikawa, H., Fishman, T., Hashimoto, S., Daigo, I., Oguchi, M., Miatto, A., Takagi, S., Yamashita, N., & Schandl, H. (2021). A framework of indicators for associating material stocks and flows to service provisioning: Application for Japan 1990–2015. *Journal of Cleaner Production*, *285*, 125450. https://doi.org/10.1016/j.jclepro.2020.125450

Tanikawa, H., Fishman, T., Okuoka, K., & Sugimoto, K. (2015). The weight of society over time and space: A comprehensive account of the construction material stock of Japan, 1945-2010. *Journal of Industrial Ecology*, *19*(5), 778–791. https://doi.org/10.1111/jiec.12284

Tanikawa, H., Managi, S., & Lwin, C. M. (2014). Estimates of lost material stock of buildings and roads due to the Great East Japan earthquake and Tsunami. *Journal of Industrial Ecology*, *18*(3), 421–431. https://doi.org/10.1111/jiec.12126

UrbanSurrey. (2021, December 18). *Development*. UrbanSurrey. Retrieved October 20, 2022, from https://urbansurrey.com/category/development/

Van de Voorde, S. (2015, December). *Lightweight Concrete - Post-war building materials*. Post. Retrieved October 20, 2022, from http://postwarbuildingmaterials.be/material/lightweight-concrete/

Weisz, H., & Steinberger, J. (2010). Reducing energy and material flows in cities. Current opinion in environmental sustainability, 2(3), 185-192.

Wiedenhofer, D., Steinberger, J., Eisenmenger, N., & Haas, W. (2015). Maintenance and expansion. Journal of Industrial Ecology, 19(4), 538-551

Zhu, X. (2014). GIS and urban mining. Resources, 3, 235-247.

5.0 Connecting Manuscript 2 and 3

The previous manuscripts (Chapter 2 and 4) focused on the physical implications of flooding and sea level rise on infrastructure, but there are also social factors that impact how communities adapt or persevere against natural disasters. These social factors such as employment, demographic, or household composition are common variables collected in census data. The following manuscript 3 investigates the social resilience to flooding through quantitative assessments and social indicators. Exploring social resilience can improve the insight used to inform efforts to build flood resilience.

6.0 Mapping social resilience to flooding

6.1 Introduction

Resilience takes center stage in disaster management and climate adaptation, given the formidable threats posed to communities by a range of natural disasters, including floods, earthquakes, wildfires, and hurricanes, often resulting in severe consequences. Defined by the Sixth Assessment Report of the Intergovernmental Panel on Climate Change (IPCC) as the capacity of social, economic, and ecosystems to cope with hazardous events or disturbances, resilience involves responding or reorganizing to maintain essential functions, identity, and structure, as well as biodiversity (Intergovernmental Panel on Climate Change, 2023). Resilience extends beyond mere recovery, emphasizing adaptation, learning, and transformation, enabling systems to evolve in the face of changing conditions (Intergovernmental Panel on Climate Change, 2023). Social resilience involves effective disaster response, mutual support, and adaptive measures to minimize harm and facilitate recovery (Cutter et al., 2000, Cutter et al., 2008). This multidimensional concept considers physical preparedness, social connections, community cohesion, and institutional effectiveness (Cutter et al., 2000; Oulahen et al., 2015; Rickless et al., 2019). The focus on resilience has gained prominence in disaster risk reduction and management initiatives, essential for societies grappling with the challenges presented by a shifting climate and an increasingly vulnerable world (Cannon, 1994; Cutter, 1996; Cutter et al., 2003).

Resilience, when applied to a city, usually refers to its ability to “absorb and recover from any shock or stress while maintaining its essential functions, structures, and identity, as well as adapting and thriving in the face of continual change” (ICLEI, 2019). Stresses that cities may face range from high unemployment rate to high risk to flooding. There is an increasing recognition to build resilience by enhancing the capacities of people, communities, and societies to prevent exposure to hazards and increase adaptive and transformational capacities for response and recovery (City of Vancouver, 2019; UNDRR, 2015). Many organizations have dedicated time and resources to measure the resilience of a city and forming strategies to ensure more cities can be resilient in the face of social and environmental challenges. Through the Sustainable Development Goals (SDGs), the United Nations outlines objectives to achieve a better and more

sustainable future. Goal 11, Sustainable Cities and Communities, aims to make cities and human settlements more inclusive, safe, resilient, and sustainable (United Nations, Department of Sustainable Development, 2015). The Rockefeller Foundation, through their 100 Resilient Cities initiative is another large contributor to the research and development of resilient cities (2013). Many other global organizations advocate for resilient cities such as the Organisation for Economic Cooperation and Development, and the Global Facility for Disaster Reduction and Recovery.

The increasing focus on building resilience has led many studies to develop indicators of resilience as well as metrics for quantifying resilience (Cutter et al., 2008; Cutter, 2016; Damude et al., 2015; Morrow, 2008). These studies assess resilience by comparing socioeconomic factors such as housing composition, household income, family structure, and demographic factors against exposure to environmental hazards. Socioeconomic factors can affect the ability of different populations to prepare for, cope with, and recover from, environmental hazards (Berke et al., 2015; Blaikie & Brookfield, 1987; Cannon, 1994; Cutter, 1996; Felsenstein & Lichter, 2014; Hebb & Mortsch, 2007; Sevoyan et al., 2013; Susman et al., 1983; Rickless et al., 2019; Wisner et al., 2004). Understanding the levels of resilience within a city can be used to identify priority areas and inform disaster risk management and climate change policy efforts.

6.1.1 Census Data: Social and Spatial Indicators

Socioeconomic characteristics can be quantified within census data which can be used to investigate the distribution of social and financial resources that may be available in the event of a disaster. Census data contains both attribute and geographic information which allows analysis of both the underlying population characteristics as well as its spatial distribution and patterns. These data may be compiled into aggregation units that represent individual socioeconomic characteristics. Census data is particularly valuable for "... the great spatial detail that is provided – showing how each neighbourhood, each block of streets, each hamlet, differs socially from its neighbours (for every place in the country simultaneously)" (Dorling, 1993, p.167). These data are useful for making inferences about various population characteristics, informing policy and allocation of resources, and examining social trends.

Census data as an area-based indicator has become increasingly prevalent across a number of disciplines, such as for natural hazards (Briguglio, 2003; Cutter et al., 2003; Felsenstein & Lichter, 2014; Oulahen et al., 2015; Rickless et al., 2019), health (Denny & Davidson, 2012; Pampalon et al., 2009; Schuurman et al., 2007), crime (Fabio et al., 2011; Kawachi et al., 1999), and poverty (Prouse et al., 2014; Seguin et al., 2011). Census data are most common as social indicators as large-scale source of information regarding populations and its characteristics (Martin, 1998). For spatial indicators, census data allows investigation of how these characteristics are distributed across space (Dorling, 1993). Spatial analysis is often concerned with spatial patterns because completely random and uniform geographical surfaces in the real world are rare and of little interest (O'Sullivan & Unwin, 2010).

The use of social indices are constrained by data availability and accessibility, which often results in the use of census data as the data source (Briguglio, 2003; Buckle et al., 2000; Cutter et al., 2000; Cutter et al., 2003; Felsenstein & Lichter, 2014; Oulahen et al., 2015; Prouse et al., 2014; Tapsell et al., 2002; Willis & Fitton, 2016). These census variables serve as indicators to postulate the correlation between the measured socioeconomic characteristic and its relevance to social resilience (Birkmann, 2003; Cutter, 2016; Willis & Fitton, 2016). The quantification of social resilience is a relative measure of socioeconomic characteristics between geographic areas. Understanding these relative differences between population subgroups can aid disaster risk management and adaptation planning (Cutter et al., 2000; Cutter et al., 2010; Cutter et al., 2014; Felsenstein & Lichter, 2014; Oulahen et al., 2015; Rickless et al., 2019; Sayers et al., 2017).

For the City of Vancouver and across Canada, Statistics Canada is responsible for conducting and disseminating the census program. The census is conducted once every five years, with the most recent censuses conducted in 2016 and 2011. Census tracts (CTs) are small, relatively stable geographic units that generally have a population between 2,500 to 8,000 people (Statistics Canada, 2012). Dissemination areas (DAs) are the smallest standard census geography units comprising of populations between 400 to 700 people (Statistics Canada, 2012). DAs are contained within CTs, such that their boundaries must respect those of the bounding CT unit (Statistics Canada, 2012).

6.1.2 The Social Resilience Index

A common method to investigate the role of socioeconomic characteristics and the distribution of disaster risk is through the use of indices (Cutter et al., 2000; Cutter et al., 2010; Cutter et al., 2014; Cutter, 2016; Felsenstein & Lichter, 2014; Oulahen et al., 2015; Rickless et al., 2019; Sayers et al., 2017; Tapsell et all., 2002). The purpose of an index is to condense the complexity of multiple quantifiable characteristics into a single numeric value to allow comparison between geographic areas or population subgroups (Briguglio, 2003; Cutter et al., 2003; Cutter, 2016; Oulahen et al., 2015; Rickless et al., 2019).

The Social Resilience Index (SoRI) by Damude et al. (2015) was developed for the City of Surrey to demonstrate the relationship between available census data and population resilience to flooding. The census variables comprising of the SoRI are intended to explain how different socioeconomic characteristics may translate to differences in resilience. The SoRI is comprised of thirteen variables from the Canadian census that are further categorized by a directional component to either increase resilience (+) or decrease resilience (-).

Table 15. Social Resilience Index (SoRI) variables

Indicator	Variable Name	Rationale	+/-
Demographic	Age 65 and over	Decreased mobility and have limited fixed income (Cutter, 2003; Harford, 2015)	-
	No knowledge of official languages	Communication difficulties due to language barrier (Hebb and Mortsch, 2007)	-
	Immigration	Limited opportunity to receive financial aid after a disaster, limited employment opportunities (Cutter, 2003)	-
Economic	Average household income	Having readily available financial assets enhances ability to pay for protection measures or repairs and recovery	+
	Average value of dwellings		+

	Low income	Less financial assets to pay for protection measures or repairs and recovery	-
	Government transfers	Restricted from recovery due to reliance on government aids	-
Household Composition	Single-parent households	More likely to rely on social resources and have less available assets which reduce ability to recover from flooding events	-
	Dwellings major repair	Housing that is older and in a poorer state are more likely to receive greater damage from floods	-
	Mobile homes	Movable dwelling can cause stress personally and financially	-
	Rental property	Populations that rent are less likely to have homeowner's insurance and lack of control over construction quality or repairs	-
	Home ownership	Likely to have homeowner's insurance and financially capable of repairs	+
Employment	Unemployment	Less financial assets to pay for protection measures or repairs and recovery	-

In accordance with Damude et al., the retrieved data were expressed as percentages according to Table 1 and then transformed into z-scores (i.e., mean of 0 and standard deviation of 1) to standardize the raw census data before constructing the index.

6.2 Methodology

This research aims to contribute to current literature on the social aspects of hazards, disasters, and climate change. Inherent and pre-existing social conditions may contribute to how populations perceive risk and what they choose to do about these risks, which ultimately determines their ability and capacity to resist, recover and adapt to potential impacts of environmental hazards (Cutter, 2016).

This study aims to answer the following research question:

How might the social resiliency of communities to flooding be measured? How might this research contribute to creating more sustainable and resilient communities?

This study addresses this research question through:

1. Constructing a social resiliency index (SoRI) for the City of Surrey
2. Mapping the SoRI by dissemination areas (DAs) to visualize spatial patterns of social resilience
3. Mapping the SoRI against flood risk to compare and identify areas of high or low flood risk and corresponding resilience in a community

6.2.1 SoRI scores and principal component analysis

The Social Resilience Index (SoRI) value is computed using a principal components analysis (PCA). This is a multivariate statistical method that reduces the dimensionality of input variables by identifying the principal components (PCs) that capture the most variance within the dataset (Cutter et al., 2003). Damude et al. (2015) advocate for a multi-dimensional approach to social resilience, which encompasses various factors such as community cohesion, social networks, economic resources, and governance structures. This approach highlights the importance of addressing both physical and social vulnerabilities to enhance overall resilience. The analysis used socio-economic and demographic data from the 2022 census year (Statistics Canada, 2022). Data at the dissemination area (DA) scale was utilized to ensure a granular and detailed analysis. Relevant variables that reflect socio-economic and demographic factors highlighted in Table 15, influencing social resilience were selected. These include income levels, employment rates, education levels, age, and housing conditions.

The IBM Statistical Package for the Social Sciences (SPSS) software was used to perform the PCA. SPSS is a robust tool for conducting complex statistical analyses, including PCA. PCA transforms the original variables into a set of uncorrelated components. The first few principal

components capture the most significant variation in the data, simplifying the complexity while retaining essential information. The factor loadings indicate how strongly each variable correlates with the principal components. These loadings help interpret the underlying structure of the data. Scores for each DA were calculated based on their respective principal component values. Since PCA identifies correlations, the directional components may not always represent the variable relationships in reality. Following the original method by Cutter et al. (2003), the sign of each principal component was adjusted based on the nature of the relationships: if the majority of variables correlated to a PC had a negative relationship (i.e., decreases resilience), the sign for that PC was adjusted to be negative. Conversely, if most variables correlated to the PC had a positive relationship (i.e., increases resilience), the sign was adjusted to be positive. If variables with different signs were correlated to the same PC, the absolute value was used. This approach ensures that the SoRI accurately reflects the underlying socio-economic and demographic dynamics. For the purpose of constructing the SoRI, each identified principal component was weighted equally. This approach assumes that all the principal components contribute equally to the overall measure of social resilience, providing a balanced representation of the different dimensions captured in the analysis. The equally weighted principal components were combined to compute the SoRI value. This ensures that no single component disproportionately influences the final index. The SoRI values were normalized and scaled to ensure comparability across different DAs. This step helps in identifying areas with varying levels of social resilience.

6.2.2 Social Resilience Mapping

The results of the SoRI were mapped using the Esri ArcGIS desktop software for each census scale in the three study areas. The maps are represented by quintiles of standard deviation (SD): high (>1.5 SD), medium-high (0.5-1.5 SD), medium (-0.5-0.5 SD), medium-low (-1.5 – (-0.5) SD) and low (<-1.5 SD). Directionality of the standard deviations represents the direction of the mean, where a negative sign indicates a SoRI score below the mean (i.e., low resilience) and a positive standard deviation indicates a SoRI value above the mean (i.e., high resilience). This allows a relative measure between geographic areas in comparison to the city as a whole.

6.2.3 Social Resilience and Flood Risk Matrix

This study assessed the social resilience of communities to flood risk in the City of Surrey by identifying the spatial intersection of the 100-year flood hazard extents, exposure of population, and social resilience. The flood exposure was calculated as the percentage of the total population exposed to flood hazards. By following a GIS-based bivariate choropleth mapping technique, a flood risk assessment matrix is developed. The matrix depicts a spatial relationship between social resilience and flood exposure of population. To represent the spatial distribution of flood risk, the inverted SoRI score and exposure of population (in percentage) were classified into three categories, including Low, Moderate, and High.

Table 16. Flood risk matrix comparing social vulnerability and flood exposure extents

Flood Risk		Social Resilience (SoRI scores)		
		Low	Moderate	High
Flood Exposure	Low			
	Moderate			
	High			

6.3 Results & Findings

The PCA reported differences in the percentage of variance captured for each factor loading. Factor loadings are correlation values between the census variable and the PCs and represents how much each census variable contributes to the overall SoRI value. The results of the PCA are explained in the following sections and the SPSS procedure for the PCA are provided in Appendix B.

6.3.1 City of Surrey

For the City of Surrey, the first principal component (PC1) captured the highest amount of variance possible in the dataset at 22.326%. It reflects the most prominent socio-economic and demographic trends within the City of Surrey. The second principal component (PC2) captured 15.348% amount of variance, the third principal component (PC3) captured 15.258% amount of variance, the fourth principal component (PC4) captured 12.430% amount of variance, and the fifth principal component (PC5) captured 7.830% amount of variance.

Table 17. Summary of PCA results for the City of Surrey

SoRI Census Variable	**Principal Components (PC)**				
	1	2	3	4	5
Age 65 and over		0.979327			
No knowledge of official languages	0.900635				
Immigration	0.940974				
Average household income			-0.73055		
Average value of dwellings			-0.6933		
Low income				0.683933	
Government transfers				0.701913	
Single-parent households	0.520966				
Dwellings major repair			0.645129		
Mobile homes					0.887858
Rental property	0.521893		0.577182		
Home ownership	0.861088				
Unemployment				0.734197	
% Variance	22.326	15.348	15.258	12.430	7.830

73.192

Total % Variance					
Sign Adjustment	-	-	-	-	-

“ * ” indicates variables that were not available at the smaller census unit and values were taken to be equal to the value of the larger unit in which it was contained within and were omitted from the discussion of MAUP effects. “--" indicates factor loadings that are less than 0.5 (i.e., not a significant correlation) and have been supressed 1 “-” indicates negative relationship; “+” indicates positive relationship; “||” indicates absolute value

6.3.1.1 Demographic

The demographic variables considered were age, language skills, and immigrant status. PC1 includes two demographic variables related to language skills and immigrant status. These variables were found to have significant factor loadings, which measure the strength of their association with PC1. The variable language skills reflect the absence of knowledge of official languages, which can be a barrier to accessing services and participating fully in society. The variable of immigrant status indicates the level of immigration, which may be associated with different socio-economic challenges and adaptation issues. Both language skills and immigrant status had factor loadings greater than 0.5 on PC1. Factor loadings quantify the degree to which each variable contributes to the principal component. A loading greater than 0.5 suggests a strong correlation between these variables and PC1, indicating that PC1 effectively captures aspects related to these demographic factors. PC1 captures nearly 8.9% of the overall variability in the socio-economic and demographic data, focusing specifically on the combined effects of language skills and immigrant status.

6.3.1.2 Economic

The economic variables considered were average household income, average value of dwellings, low income, and government transfers received. PC3 and PC4 each capture different aspects of these economic factors. PC3 encompasses two variables that reflect positive economic conditions: higher household income and a higher average value of dwellings. These variables indicate better economic stability and property wealth, contributing to positive socio-economic

resilience. PC3 explains 7.6% of the total variance, highlighting its role in representing economic prosperity. Conversely, PC4 includes two variables that reflect negative economic conditions: low income and the amount of government transfers received. These variables are associated with economic vulnerability and dependency on public assistance, contributing to socio-economic challenges. PC4 accounts for 8.3% of the total variance, indicating its significance in capturing economic difficulties. Together, PC3 and PC4 offer a comprehensive view of the economic factors influencing social resilience, with each principal component emphasizing different aspects of economic well-being and adversity.

6.3.1.3 Household Composition

The household composition variables considered were single parent households, dwellings major repair, mobile homes, rental property, and home ownership. PC1, PC3, and PC5 each capture different aspects of these household composition variables. PC1 includes three variables that reflect negative conditions: single-parent households, rental properties, and home ownership. These variables are associated with challenges such as increased financial pressure and housing instability, which can impact social resilience. PC1 explains 13.4% of the total variance, indicating its significant role in representing these negative household conditions. PC3 focuses on rental property, which also represents a negative effect, contributing to 7.6% of the total variance. Similarly, PC5 captures the negative impact of mobile homes, explaining 7.8% of the total variance. Together, these principal components provide insights into various aspects of household composition and their implications for social resilience, with each component highlighting different dimensions of housing-related challenges.

6.3.1.4 Employment

The employment variable considered was rate of unemployment. PC4 specifically addresses this variable and represents the negative effects associated with high unemployment rates. PC4 captures the impact of unemployment on socio-economic conditions, reflecting how higher unemployment can contribute to economic instability and reduced social resilience. This component explains 4.1% of the total variance, highlighting its role in understanding the contribution of unemployment to overall socio-economic challenges. PC4 underscores the

importance of addressing unemployment as a key factor in enhancing social and economic resilience in the community.

6.3.2 Spatial Distribution of SORI

By joining SoRI scores with the 2016 census subdivisions, a GIS-based choropleth map was produced to visualize local-scale socioeconomic disparities and the extents of social resilience across DAs. The SoRI scores are divided into five categories including Very Low, Low, Average, High, and Very High and represented along a spectral color ramp from red to green. Social resilience is low in North Guildford, parts of City Centre and South Surrey, and throughout Newton and Fleetwood. Social resilience is high in Whalley, North Newton, and most of South Surrey.

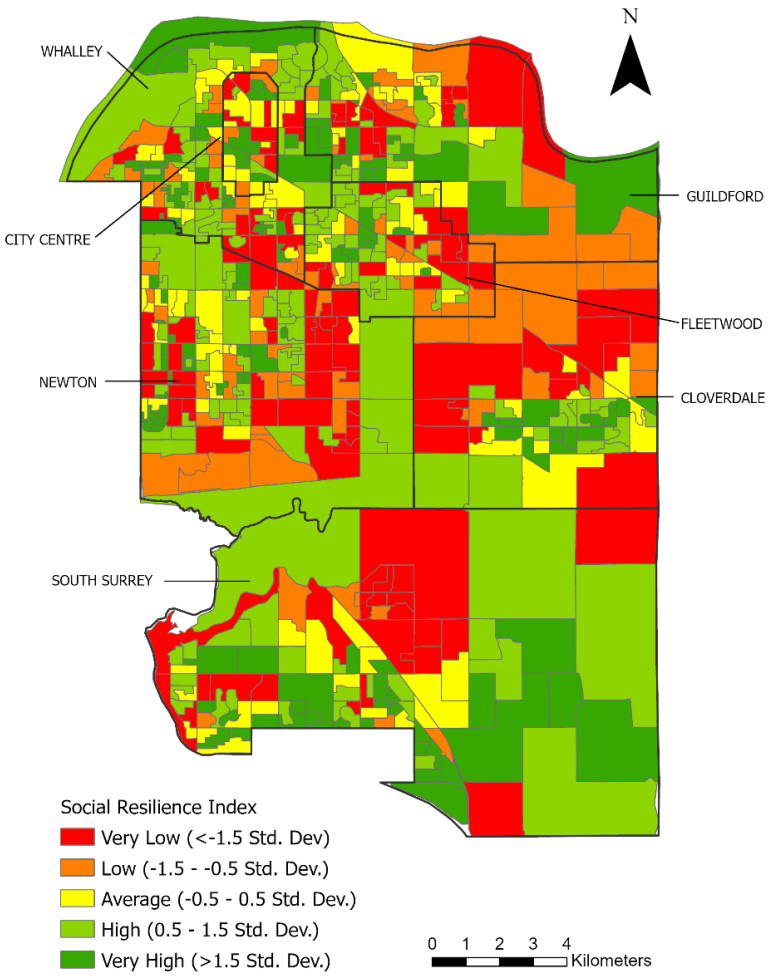


Figure 21. The Social Resilience Index (SoRI) for City of Surrey based on 2016 census data

Figure 21 visualizes the Social Resilience Index (SoRI) across the neighbourhoods and highlights spatial patterns to illustrate disparities in resilience levels throughout the City of Surrey. The figure shows significant variations in social resilience based on different factors, revealing distinct geographic trends. Fleetwood is depicted as experiencing one of the lowest SoRI scores, indicating a high level of vulnerability and lower social resilience in this area. Parts of Guildford, Newton, and City Centre also show notably low SoRI scores, reflecting similar patterns of reduced resilience and increased social challenges.

Figure 22 maps the spatial distribution of the SORI by demographic, household composition, economic, and employment factors across different dissemination areas in the City of Surrey. This analysis reveals varying levels of social resilience based on these factors, with distinct patterns emerging across different neighborhoods.

6.3.2.1 Demographic Factors

Areas with low social resilience are characterized by a higher population of individuals aged 65 and older, higher levels of immigration, and a lack of knowledge of official languages. These demographic characteristics often correlate with increased vulnerability due to potential barriers in accessing services and social integration. In Surrey, such low resilience areas are predominantly found in Newton, Guildford, and Fleetwood. Conversely, areas exhibiting high resilience tend to have a more balanced demographic profile, with lower proportions of elderly residents, lower immigration rates, and better language proficiency. These high-resilience areas are notably located in parts of South Surrey and Whalley.

6.3.2.2 Household Composition Factors

Low resilience in household composition is associated with lower rates of home ownership, homes in need of major repairs, a higher proportion of mobile homes, and a greater percentage of single-parent households. These factors contribute to housing instability and financial stress, which negatively impact resilience. The lowest resilience in this category is observed around City Centre, Cloverdale, and parts of South Surrey and Newton. Areas with high resilience

generally feature higher home ownership rates, well-maintained properties, and fewer single-parent households. Such conditions are typically seen in parts of South Surrey and Whalley.

6.3.2.3 Economic Factors

Economic factors contributing to low resilience include lower household incomes, lower dwelling values, higher rates of low income, and a greater reliance on government transfers. These economic challenges often indicate greater financial instability and reduced capacity for self-sufficiency. Areas with low resilience in this economic category include Cloverdale, parts of Newton, City Centre, and South Surrey. Higher resilience is often found in areas with better economic conditions, including higher household incomes and property values, and lower reliance on government support. Notable high-resilience areas are in Guildford, parts of Whalley, and most of South Surrey.

6.3.2.4 Employment Factors

High unemployment rates are a significant indicator of low resilience, as they reflect economic challenges and reduced job security. Areas with high unemployment and consequently lower resilience are concentrated around City Centre, Whalley, Newton, and parts of Guildford. High-resilience areas generally have lower unemployment rates and better employment conditions, contributing to overall economic stability. These areas are mainly concentrated in South Surrey.



Figure 22. SoRI breakdown by demgraphic, household composition, economic, and employment by dissemination area in Surrey

6.4 Spatial Distribution of Social Resilience to Flood Exposure

By combining social resilience results with flood exposure data for each dissemination area (DA), spatial patterns highlighting the relationship between social resilience and flood risk can be effectively mapped. This integration reveals areas with varying combinations of resilience and flood risk, providing insights into their vulnerability and adaptive capacity.

6.4.1 Low Resilience and Low Flood Risk

Areas with low social resilience but low flood risk are shown in light gray. These regions, including suburbs of Newton, pockets of Fleetwood, and North Guildford, have lower vulnerability to floods but still face challenges due to their low resilience. Despite their reduced flood risk, these areas may struggle with other social or economic factors that impact overall community well-being.

6.4.2 Low Resilience and High Flood Risk

Areas with both low social resilience and high flood risk are indicated in bright red. These regions are characterized by high vulnerability and significant exposure to flooding, suggesting that they face severe challenges in managing flood risks due to their already low resilience. The highest concentrations of these high-risk, low-resilience areas are observed in parts of Cloverdale and South Surrey, but they are also present in segments of other neighborhoods.

6.4.3 High Resilience and Low Flood Risk

Areas that exhibit high social resilience and low flood risk are marked in bright blue. These areas are better equipped to handle both social challenges and flood risks due to their robust resilience and lower flood exposure. South Surrey shows the highest concentration of these high-resilience, low-risk areas, followed by Newton and Fleetwood. These regions benefit from favorable conditions that enhance their capacity to manage and mitigate risks effectively.

6.4.4 High Resilience and High Flood Risk

Areas with high resilience but also high flood risk are of particular interest because they indicate neighborhoods that might have adaptive practices or regulations in place that enhance their ability to cope with flood risks. These areas are indicated in dark red and are primarily located in North Whalley, East South Surrey, and parts of Newton and Guildford. Despite facing significant flood risks, these areas demonstrate a high level of resilience, suggesting they may have implemented effective flood management strategies or possess strong community and infrastructural attributes that improve their risk tolerance.

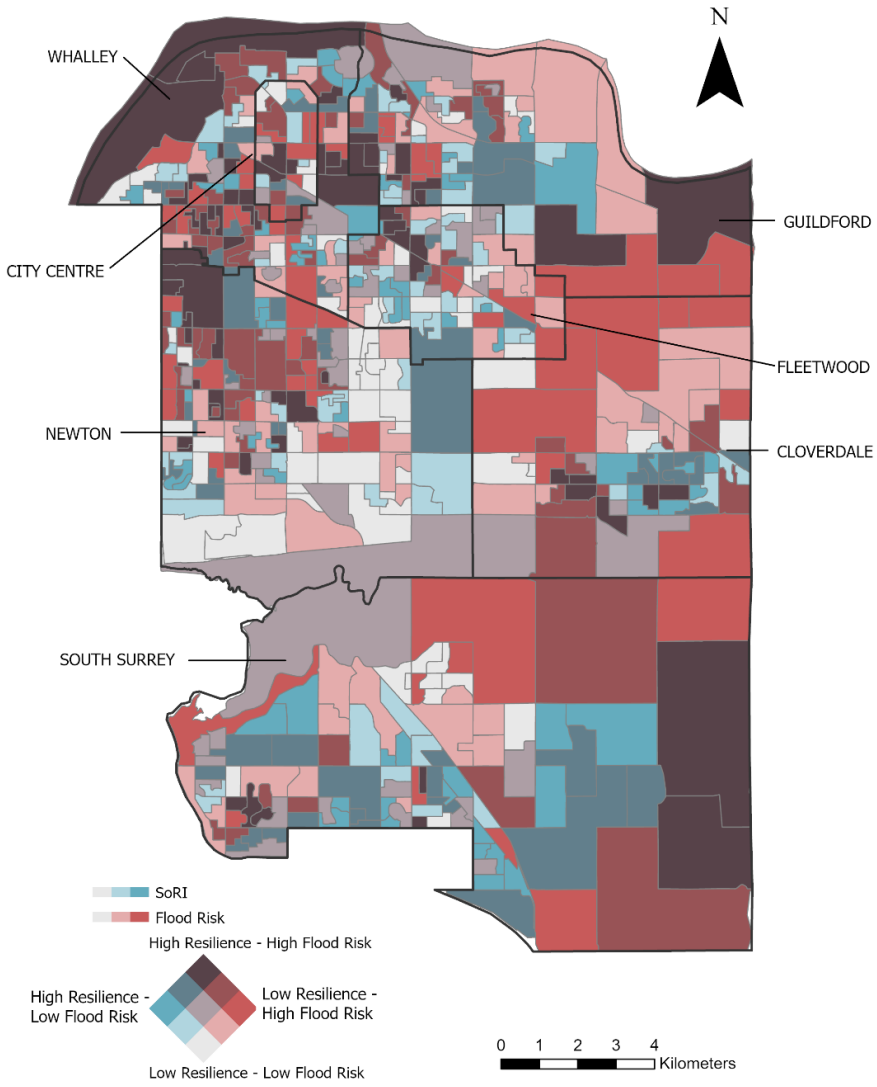


Figure 23. Map of social resilience and flood risk by disemination are in Surrey

Mapping social resilience alongside flood risk provides a comprehensive view of how different areas in Surrey are positioned with respect to their vulnerability and flood exposure. The bright red areas represent the most at-risk zones with low resilience, while bright blue areas signify safer, more resilient regions. Dark red areas highlight communities that, despite their high flood risk, exhibit strong resilience, potentially due to adaptive measures and robust infrastructure. This spatial analysis is crucial for identifying priority areas for intervention and for developing targeted strategies to enhance resilience and flood risk management throughout the city.

6.5 Discussion

The results of this study highlighted areas with a higher population over the age of 65 are less resilient to natural disasters. In Surrey, 14% of the population is 65 years and over, which is 2% higher than in 2011 (Statistics Canada, 2022). In nine B.C. communities, more than one in ten seniors were low-income status in 2015, with seven out of these nine B.C. communities being located in Metro Vancouver (*B.C. Seniors' Poverty Report Card, n.d.)*. Richmond (20.3%), Surrey (16.5%) and Burnaby (16.1%) had the highest seniors' poverty rates of any B.C. community (*B.C. Seniors' Poverty Report Card, n.d.)*. Cutter et al. (2003) stated that children, elderly persons, and handicapped people are the demographic groups most affected by disasters. Elderly may have mobility constraints or mobility concerns increasing the burden of care and lack of resilience. Scherzer et al. (2019) confirmed that people of working age and in good health can evacuate faster in case of emergencies than children or seniors and are also in a better position to assist others during evacuations. Other factors such as social support, government support, governmental social policies, culture, religion and access to health care services can also influence an individuals resilience despite their age.

Surrey is home to the second-largest immigrant population in the Metro Vancouver Region. The total immigration population by percentage from the 2016 census is 43%, with an immigration population growth of 17.2% from 2011. In 2016, over two thirds (68.7%) of Surrey's recent immigrants spoke non-official languages most often at home, compared to 55.3% of its immigrant population. The proportion of Surrey residents whose mother tongue was English declined by 13.6% (61.8% in 2001 to 48.2% in 2016). which is notably lower than Metro Vancouver's regional level which saw a decline of 6.2% over the same period. According to Cutter et al., one's race and ethnicity can impose language and cultural barriers that affect access to post-disaster funding and residential locations in high hazard areas. This makes immigrants less resilient to natural disasters.

Another common demographic indicator of social resilience that wasn't taken into consideration is education. Cutter et al. (2003) noted a positive correlation between level of education and the socio-economic status of a person. A higher level of education often results in

improved lifetime earnings. Educated people might be better able to understand and access warning and recovery information, so that they can better respond and recover from a disruption. Qasim et al. (2016) stated that a greater level of educational attainment strongly increases a community members' disaster preparedness, which in turns contributes to an enhanced resilience.

Socio-economic indicators are among the most frequently mentioned indicators in the social resilience literature (Bolin & Stanford, 1991; Carpenter, 2013; Rufat et al., 2015). They include income, employment, car and home ownership or health insurance. The employment rate grew by 0.8% between 2011 and 2016. A growing employment rate reflects positive economic conditions in the community. Whereas the unemployment rate has declined from 7.9% in 2011 to 6.5% in 2016. Out of the entire population of Surrey, 14.8% are of low income status with 11.5% receiving government transfers. Employment and income seem to be key indicators of the recovery capability of an individual or of a community in the context of damages and losses related to disasters (Rufat et al., 2015). Low-income individuals appear to be less flexible and adaptive during crises than high-income individuals (Marshall, 2007; Van Zandt et al., 2012; Carpenter, 2013; Felsenstein & Lichter, 2014). Home ownership is positively correlated with social resilience. From the Surrey 2016 results, 71.1% of the population are homeowners while 28.8% rent. Asset ownership may increase individual costs resulting from several types of disasters, but these costs often do not erode the entire income of wealthier households. Consequently, their capability to cope with disasters remains rather high (Brouwer et al., 2007; Rufat et al., 2015). Populations that rent are less likely to have homeowner's insurance and lack of control over construction quality or repairs.

Household composition refers to the number and the status of members living in the same household (Orthner et al., 2004). Compared with other demographic and socio-economic characteristics, there are few studies that highlight the importance of family structure and composition in understanding and measuring community resilience (Cutter et al., 2003; Yoon et al., 2016; Parsons et al., 2016). Among these studies the indicators used to describe household composition are single-parent households. In Surrey, 14.5% are single-parent households, with 84% of single-parents having low income status. Studies have shown that families with single-

parent households may have a low level of resilience due to limited financial resources and intense caring responsibilities. This might reduce their adaptive and recovery capabilities during and after a crisis (Cutter et al., 2003). This study also included dwellings with major repair and mobile dwellings. Although the number is few in comparison to the rest of Surrey's population, there are 1345 mobile dwellings and 7045 dwellings under major repair. Movable dwelling can cause stress personally and financially. Housing that is older and in a poorer state are more likely to receive greater damage from floods (Cutter et al., 2010).

6.6 Limitations

Due to data constraints of the census, certain SoRI variables were chosen. However, the literature reveals that other factors such as social capital is also important for measuring social resilience (Adger, 2003; Norris et al., 2008; Aldrich & Meyer, 2014; Cheung et al., 2017). Putnam defined social capital as a 'feature of social life — networks, norms and trust — that enable participants to act together more effectively to pursue shared objectives' (1995, p.664). Similarly, Lin (2002) described social capital as 'resources embedded in social networks accessed and used by actors for actions' (Lin, 2002, p.25). More generally, social capital refers to a set of adaptive networked capacities, which allows members of a social to use their social resources towards solving problems and achieving a shared goal (Mayunga, 2007; Norris et al., 2008). The connectedness of social networks are seen as a significant element of social capital that allows bonding, linking, and bridging (Ahmed et al., 2004; Magis, 2010; Aldrich & Meyer, 2014; Patel et al., 2017).

Other studies from the literature also reference social cohesion, social networks, community knowledge, skills and awareness as variables influencing social resilience. The desire of individuals to contribute and be involved in local events with other members of the same community, is often proposed as an indicator to characterise social networks (Carpenter, 2013; Scherzer et al., 2019). Community engagement can enhance a communities' readiness for future disasters and to allow for a better recovery after a disaster (Arbon et al., 2016). Community knowledge, skills and awareness are considered as important since they represent a community's potential to activate competences to cope with catastrophic events (Norris et al., 2008; Zakour &

Gillespie, 2013; Saja et al., 2018). Knowledge and understanding of local risks as well as diversity skills and trained personnel are also important. Patel et al. (2017) argued that the short- and long-term effects of disasters can be mitigated effectively if a community understands its own risks and vulnerabilities. If vulnerabilities can be identified and addressed before disasters occur, this will help to build resilience within a community. Kwok et al. (2016) found that increasing a community's risk awareness helps to increase its resilience. According to Maclean et al. (2014), a high level of resilience requires a variety of different skills to cope with unexpected changes. Such skills would include governance skills as well as business and financial management skills (Maclean, 2014).

Race or ethnicity as an indicator was considered but not included as a factor in resilience assessments as it could unintentionally lead to stigmatization or reinforce stereotypes. Race and ethnicity intersect with many other factors that influence resilience, including socio-economic status, access to resources, and social networks. These intersections can complicate the interpretation of resilience if not carefully managed. Using race or ethnicity data in resilience assessments requires careful consideration of ethical implications and data privacy. There is a risk of misuse or misinterpretation of such sensitive information, which could have unintended consequences for the communities being assessed.

Several other indicators have been discussed in the literature, though less frequently, which could provide a more nuanced understanding of social resilience. These include social beliefs and cultural practices, which influence how communities cope with crises through shared values and norms. Faith and spirituality also play a critical role, as religious and spiritual organizations often provide emotional support and resources that can enhance community resilience. Measures of community inclusiveness and equity are essential for understanding how well different groups are integrated and supported, as high levels of inclusiveness and equitable access to resources contribute to greater resilience. Additionally, community processes and plans, such as emergency preparedness and risk management strategies, are crucial for effective resilience. Crime and social safety also impact resilience; high crime rates and safety concerns can undermine community cohesion, while safer environments foster a more supportive community atmosphere.

To gain a clearer picture of social resilience, future research should consider incorporating these additional variables. Relying solely on census data may offer a limited perspective, as it captures only broad, aggregate measures without delving into the complexities of community dynamics. Incorporating direct data collection methods, such as surveys and interviews, can provide richer insights into community-specific factors and lived experiences. Engaging with community members and stakeholders helps capture local knowledge and perceptions that are not always reflected in standard census data. By broadening the scope of indicators and adopting a more participatory approach, future studies can develop a more accurate and comprehensive understanding of social resilience, leading to better-targeted policies and interventions that enhance community capacity to withstand and recover from various challenges.

6.7 References

B.C. Seniors' Poverty Report Card - Sparc.bc.ca. (n.d.). Retrieved August 27, 2022, from https://www.sparc.bc.ca/wp-content/uploads/2018/07/B.C.-Seniors-Poverty-Report-Card.pdf

Copeland, S., Comes, T., Bach, S., Nagenborg, M., Schulte, Y., & Doorn, N. (2020). Measuring social resilience: Trade-offs, challenges and opportunities for indicator models in transforming societies. *International Journal of Disaster Risk Reduction*, *51*, 101799. https://doi.org/10.1016/j.ijdrr.2020.101799

Cutter, S. L., 1996. Vulnerability to environmental hazards. Progress in Human Geography, 20(4), pp. 529-539.

Cutter, S., Mitchell, J. & Scott, M., 2000. Revealing the Vulnerability of People and Places: A Case Study of Georgetown County, South Carolina. Annals of the Association of American Geographers, 90(4), pp. 713-737.

Cutter, S. L., Boruff, B. J., & Shirley, W. L., 2003. Social Vulnerability to Environmental Hazards. Social Science Quarterly, 84(2), pp. 242-261.

Cutter, S., L., Barnes, L., Berry, M., Burton, C., Evans, E., Tate, E. & Webb, J., 2008. A place-based model for understanding community resilience to natural disasters. Global Environmental Change, 18, pp. 598-606.

Cutter, S. L., Burton, C. G. & Emrich, C. T., 2010. Disaster Resilience Indicators for Benchmarking Baseline Conditions. Journal of Homeland Security and Emergency Management, 7(1), Article 51.

Cutter, S. L., Boruff, B. J., & Shirley, W. L. (2003). Social vulnerability to environmental hazards*. *Social Science Quarterly*, *84*(2), 242–261. https://doi.org/10.1111/1540-6237.8402002

Cutter, S. L., Ash, K. D. & Emrich, C. T., 2014. The geographies of community disaster resilience. Global Environmental Change, 29, pp. 65-77. Cutter, S. L., 2016. The landscape of disaster resilience indicators in the USA. Natural Hazards, 80, pp.741-758.

Damude, K., Mortsch, L. & Joakim, E., 2015. Draft Report: Methods for Quantifying Social Resilience in Metro Vancouver, Canada. Ontario: Coastal Cities at Risk (CCaR) Project.Government of Canada, S. C. (2021, October 27).

Census profile, 2016 census Surrey, City [Census Subdivision], British Columbia and British Columbia [province]. Census Profile, 2016 Census - Surrey, City [Census subdivision], British Columbia and British Columbia [Province]. Retrieved August 27, 2022, from https://www12.statcan.gc.ca/census-recensement/2016/dp-pd/prof/details/page.cfm?Lang=E&Geo1=CSD&Code1=5915004&Geo2=PR&Code2=59&Data=Count&SearchText=surrey&SearchType=Begins&SearchPR=01&B1=All&TABID=1

Fabio, A., Tu, L.-C., Loeber, R. & Cohen, J., 2011. Neighbourhood Socioeconomic Disadvantage Immigration, Refugees, and citizens Canada. (2018). *Immigrant demographics surrey, B.C.* New To BC. Retrieved August 27, 2022, from https://newtobc.ca/wp-content/uploads/2021/02/Surrey-Immigrant-Demographic-Profile-2018-2.pdf

Kwan, C., & Walsh, C. A. (2017). Seniors' disaster resilience: A scoping review of the literature. *International Journal of Disaster Risk Reduction*, *25*, 259–273. https://doi.org/10.1016/j.ijdrr.2017.09.010

Mendelson, R., 2001. Geographic Structure As Census Variables: Using Geography to Analyse Social and Economic Processes. Statistics Canada Geography Working Paper Series Catalogue no. 92F0138MIE. Ottawa: Statistics Canada. [online] Available at: [Accessed 19 April 2019].

Openshaw, S., 1984. The Modifiable Areal Unit Problem. Concepts and Techniques in Modern Geography No. 38 ed. Norwich: GeoBooks.

Openshaw, S. & Taylor, P., 1979. A million or so correlation coefficients: three experiments on the modifiable areal unit problem. In: Wrigley N. ed. 1979. Statistical applications in the spatial sciences. London: Pion.

Rickless, D. S., Yao, X. A., Orland, B. & Welch-Devine, M., 2019. Assessing Social Vulnerability through a Local Lens: An Integrated Geovisual Approach. Annals of the American Association of Geographers, 0(0), pp. 1-20.

Statistics Canada. 2022. (table). *Census Profile*. 2021 Census of Population. Statistics Canada Catalogue no. 98-316-X2021001. Ottawa. Released September 21, 2022. https://www12.statcan.gc.ca/census-recensement/2021/dp-pd/prof/index.cfm?Lang=E (accessed October 20, 2022). Timalsina, R., Songwathana, P., & Sae-Sia, W. (2021). Resilience and its associated factors among older disaster survivors. *Geriatric Nursing*, *42*(6), 1264–1274. https://doi.org/10.1016/j.gerinurse.2021.08.008

United Way. (n.d.). *Supporting the non-medical needs of older adults in B.C.* Better at Home RSS. Retrieved August 27, 2022, from https://betterathome.ca/

7.0 Conclusions

This thesis applied a geospatial approach to investigate the impacts of flooding and sea level rise on critical infrastructure and further quantifies in-use material stocks that would be vulnerable. Beyond conducting a vulnerability assessment, this thesis also analyzed how resilience varies with respect to different social and geographic factors. The first manuscript focuses on modelling flood and sea level rise scenarios to estimate the impacts on buildings and roads. The second manuscript focuses on quantifying total building and road material stocks while estimating and geographically locating materials that would be most vulnerable in different scenarios. The third manuscript explores the social resilience to flooding through evaluating social indicators and spatially representing resilience on a scale of low to high risk. This chapter summarizes the findings and overall contributions of this research.

7.1 Development of a GIS-based Method to Evaluate Flood Risk and Sea Level Rise Impacts

The first study applied a GIS-based bluespot model to model flood and sea level rise scenarios in the City of Surrey. The vulnerability of buildings and roads to these potential scenarios were also assessed. At a 1/10 year scenario, 12.59% of buildings and 27.17% of roads would be at risk to flooding. This is compared to a 1/100 scenario, where 14.82% of buildings and 28.87% of roads would be at risk to flooding. As for sea level rise, at a 1m SLR scenario, 1.87% of buildings and 6.39% of roads would be at risk to flooding. This is compared to a 2.5m SLR scenario, 3.72% of buildings and 12.11% of roads would be at risk to flooding. The results indicate that most buildings built after 2000s would likely be impacted by flooding. This is concerning as it indicates a lack of improvement in building more resilient buildings and roads. When mapped, most buildings and roads that are at high risk to flooding are located along the Fraser River in the northern part of Surrey. Central Surrey which is comprised mainly of agricultural land is highly susceptible to flooding. Although there are dyking infrastructure in place, about 48.65% of dykes are considered to be vulnerable today and located in bluespots that are greater than 2 metres in depth. If the government does not implement any adaptation plans or coastal protection measures, when the global mean sea level rises by 1.0 m or even 2.0 m by the end of this century, most of the building and road stocks along the coastline will be flooded.

7.2 Accounting for building and road material stocks for the City of Surrey, British Columbia

The second study applied a GIS-based bottom-up approach to model in-use building and road material stocks in the City of Surrey and assessed the vulnerability of material stocks to potential flooding and sea level rise scenarios. The building stock accounting yielded a total stock of 115.17 t/capita given that year's population. Concrete accounted for the largest share of MS at 54% or 61.85 t/capita. The total MS is largely dominated by residential buildings, accounting for 59% of the total MS. The road stock accounting yielded a total stock of 117.61 kt/capita. The quantity of soil is the highest, totalling 9.81 kt/capita and accounts for 42% of the road stocks. This is followed by asphalt at 30%, then aggregate at 28%. The amount of building stock affected during the most severe return period scenario is 87,574.74 t/capita at a 1/100 scenario and 5,940.89 t/capita at a 2.5m SLR scenario. The amount of road stock affected during the most severe return period scenario is 8,232.09 t/capita at a 1/100 scenario and 5,940.89 t/capita at a 2.5m SLR scenario. For building material stock, concrete appeared to have the highest quantity impacted to flooding and sea level rise since there is a large accumulation of concrete in residential basements and large industrial buildings. Timber had the least quantity impacted as it is mainly used for framing and structural purposes. In terms of road material stock, rock appeared to have the highest quantity impacted and aggregate had the least quantity due to the difference in thickness between each layer. The analysis of potential stock loss scenarios is valuable for informing infrastructure resilience and post-disaster recovery.

7.3 Mapping social resilience to flooding

The third study constructed a Social Resilience Index (SoRI) for the City of Surrey using statistical analysis and GIS. A principal components analysis was conducted using census variables that are intended to explain how different socioeconomic characteristics may translate to differences in resilience. There were thirteen variables used that were categorized into four types: demographic, economic, household composition, and employment. It was found that areas with low resilience were attributed to a population with ages 65 and older, high immigration status, no knowledge of official languages, low home ownership, homes requiring major repair, be a mobile home, have greater percentage of single parent households, lower household income,

and greater percentage of government transfers. Areas with high resilience were attributed to high household income and high value of dwelling. Social resilience is low in North Guildford, parts of City Centre and South Surrey, and throughout Newton and Fleetwood. Social resilience is high in Whalley, North Newton, and most of South Surrey. Areas that have low resilience and high flood risk had the highest concentration in Cloverdale and South Surrey has the highest concentration. Areas with high resilience and low flood risk had the highest concentration in Newton and Fleetwood. Combining the SoRI and flood analysis offers a reliable method for identifying priority areas (i.e., areas of low resilience) that can inform planning and policy efforts.

7.4 Contributions of the study

This research significantly advances the understanding and management of flooding and material stocks in urban environments, specifically in the City of Surrey. As the first study in Surrey to map and quantify material stocks in buildings and roads, the study provides a detailed inventory crucial for assessing flood and sea-level rise impacts. The study improves upon previous methodologies by incorporating building design and floor plans and provides a framework for road stock accounting applicable to other North American cities. This empirical application of material stock analysis, combined with flood risk assessment, offers a comprehensive understanding of the city's vulnerability to environmental hazards. Moreover, the study enhances DEM accuracy for flood mapping using high-resolution LiDAR data and constructs a Social Resilience Index to assess and map community resilience to flooding.

7.4.1 Advancing Sustainable Development Goals through Urban Resilience and Material Stock Analysis

A central focus of the United Nations 2030 Agenda for Sustainable Development is to empower action towards social, economic, and environmental sustainability. The integration of different sustainable development goals can alleviate the impacts of climate change and advance the development of more sustainable infrastructure and resilient communities. SDG 13.1 aims to strengthen resilience and adaptive capacity related to climate hazards and natural disasters. On the same track, SDG 11 is to “make cities and human settlements inclusive, safe, resilient and

sustainable". The flood analysis and social resilience index conducted for the City of Surrey contributes to the achievement of both these goals by identifying the resilience of communities to climate hazards. Furthermore, the accounting of material stocks across the City of Surrey contribute to SDG 9.1 which aims to develop sustainable and resilient infrastructure. The impacts of future flood scenarios on material stocks provides insight into which construction materials would be most vulnerable and guides future research to look into more resilient materials to replace current ones. This research provides insight into construction materials most vulnerable to flooding and informs future research in resilient and sustainable construction materials.

7.4.1 Utilization of Material Stock Analysis by Urban Planners

This research provides significant contributions to understanding the interplay between flooding, material stocks, and urban planning. By mapping and quantifying the current material stocks contained in buildings and roads within the City of Surrey, the study establishes a comprehensive baseline for assessing how material assets interact with flood risks. The integration of material stock analysis with flood risk assessment offers a novel empirical method to evaluate the resilience of urban infrastructure in the face of climate change and rising sea levels. This approach not only identifies vulnerable areas and infrastructure but also highlights the potential for post-disaster material recovery and recycling, thus supporting sustainable urban redevelopment. By focusing on the actual material composition and distribution of urban assets, this research provides actionable data that can be used to enhance the durability and adaptability of urban environments.

Urban planners can leverage material stock analysis results in several ways to inform decision-making and enhance resilience in urban environments. The detailed material stock analysis offers valuable insights into the quantity, condition, and spatial distribution of buildings and roads, enabling planners to prioritize investments and optimize resource allocation for maintenance, repairs, and upgrades. By understanding the vulnerability of various infrastructure components to flooding and other hazards, planners can develop targeted mitigation strategies to enhance urban resilience. The research also informs land use planning by identifying areas with high concentrations of vulnerable buildings and infrastructure, guiding zoning regulations,

building codes, and development policies to minimize exposure to risks and promote sustainable urban growth. Furthermore, the integration of social resilience mapping with flood risk and material stock data allows for a holistic approach to resilience planning. Planners can use this comprehensive data to engage with communities, raise awareness of vulnerability issues, and ensure that resilience strategies are inclusive and informed by local knowledge and priorities. Overall, this research provides a robust framework for urban planners to build more resilient, adaptive, and sustainable urban environments.

7.4.2 Insights for Policy-Making and Planning

The research findings identifies key determinants of resilience, informing policy decisions and investments in disaster risk reduction and climate adaptation. Policymakers can use this information to develop targeted interventions that address the specific needs of vulnerable areas, ensuring that resources are allocated efficiently and effectively. The study also highlights the importance of community engagement in resilience-building efforts. By communicating research findings to local communities and stakeholders, policymakers can foster inclusivity and ensure that resilience strategies are informed by local knowledge and priorities.

7.5 Future Study Directions

This section reflects on the results and limitations and provides some general recommendations for policy makers and practitioners on future material stock (MS) modelling, analysis, management, and protection.

This study focused on mapping the physical impacts of flooding such as exposure of buildings and roads. Flood exposure maps with spatial variability can help inform community planners to effectively allocate resources. It can also provide emergency management agencies with a better understanding and background before taking action, setting priorities, and developing long-term risk reduction strategies. However, it is also important to incorporate social factors that contribute to vulnerability. Social vulnerability is a socially constructed phenomenon attributed to changes in the biophysical and built environment. It depends on the susceptibility of a society to external threats which can be attributed to demographic and socioeconomic inequalities among social groups within societies. Flood impacts are not equally distributed

among different groups of people due to their differential exposure and socioeconomic characteristics. Flood exposure is often higher for socially vulnerable populations, specifically those who exhibit poor socio-economic characteristics such as financial issues or are socially isolated. Future studies could identify these susceptibilities through surveying communities to understand where assistance and planning can be prioritized. Combining social vulnerability and geospatial analysis is important to evaluate the extent to which a system is exposed to floods, and its susceptibility in conjunction with its ability to cope, recover, or basically adapt.

Accounting for in-use material stock for Surrey could be improved in several aspects. An accurate and comprehensive material stock account is important to understand the status of material stock accumulation and better manage materials throughout their life cycle which includes import, reuse, recycle, and disposal. This study only took building and road stocks into consideration, but other infrastructures, such as dams and utility infrastructure also protect or can become vulnerable to flooding and were not included. This study could be improved upon by expanding the scope of the material stock account. In addition, the buildings and road classification system and material stock typologies used in material stock accounting should be validated via on-site survey and adjusted to improve the accuracy of material stock estimation. GIS can play a role in managing and tracking materials throughout its lifecycle. This also includes employing building information modelling through computer-aided software such as AutoCAD where quick calculations of building composition can be made (Wong & Zhou, 2015). Integration of LIDAR data can help improve accounting of material stocks through records of more in-depth attributes such as year of construction and accurate height information.

Large amounts of material stocks may become lost as waste due to flooding or sea level rise and would require additional materials to replace what was lost. As well, roads in Canada require much maintenance as harsh winters make them more susceptible to cracks and potholes. This contributes to materials lost as waste and new materials used during maintenance. Sustainable maintenance and protection of material stocks are necessary for building Surrey's sustainable and resilient socio-ecosystem. Material stock accounting could be used to estimate and manage construction and demolition (C&D) waste. Additionally, C&D waste could have high recycling potentials if they are properly managed. However, mismanagement would lead to C&D waste discarded back to nature, and negatively impacting the natural environment as well

as losing its economic value (Fu et al., 2021; Miatto et al., 2019). Surrey's material stock account developed in this study could be used for estimating potential C&D waste. The calculation of C&D waste will require a detailed investigation of construction technologies and a deep understanding of construction lifespan.

This study used quantitative metrics to distinguish levels of resilience amongst populations based on socioeconomic indicators, called social resilience (Cutter et al., 2008; Damude et al., 2015; Morrow, 2008). These indicators are used to represent financial and social capital that can affect resilience in the event of a flood (Cutter et al., 2008; Damude et al., 2015; Joakim et al., 2015; Jones & Tanner, 2017; Morrow, 2008). These socioeconomic indicators are often retrieved through census data, which represents individual-level characteristics as aggregate census units (Mendelson, 2001; Prouse et al., 2014). However, policy and planning that is based solely on quantitative analyses at the aggregate level may not fully address the underlying issues affecting resilience at the individual level (Jones & Tanner, 2017; Jones et al., 2018). While a number of efforts have developed quantitative metrics to measure and model resilience using aggregate indicators, there is a gap in understanding how flood resilience is perceived and implemented at the individual-level. At the individual-level, the "subjective" assessments of how people perceive their own capacities and the types of actions that they might take against flood hazards may be critical for building resilience, particularly through policy and planning initiatives. Future studies can investigate the local contexts in different study areas through surveys to identify local perspectives towards flood hazards and their preparedness. Another avenue of research could be to further explore qualitative perspectives and local contexts from experts and practitioners to verify the input variables in identifying resilience and the final mapped results. The use of qualitative information may present alternate patterns of flood resilience, which may differ from the information from quantitative metrics. Understanding these qualitative aspects can provide a more holistic understanding of flood resilience and contribute to the development of more targeted approaches for building flood resilience.

Appendix A. Supplementary Information for the City of Surrey Study Data Sources

A.1 Classification of Building Codes

100 – Institutional code buildings
200 – Commercial code buildings
300 – Residential code buildings
400 – Tourism code buildings
500 – Cultural code buildings
600 – Transportation code buildings
700 – Storage code buildings
800 – Agricultural code buildings

Table A.1: Domain codes for each building occupancy class

Code	Building Occupancy Classes		
110	Church	323	Townhouse
121	Educational Campus Building	324	Rowhouse
122	Educational Elementary/Secondary School	330	Mobile House
131	Health Related	331	Boat House
140	Government Office	340	Detached Garage
141	Fire Station	341	Coach House
142	Post Office	410	Hotel
210	Commercial	510	Park Facility
211	Commercial (Office)	520	Recreational Centre
212	Commercial (Non-Office)	521	Community Centre
213	Commercial Mall	522	Library
214	Automotive Services	531	Art Gallery
220	Urban-area mixed commercial	532	Museum
230	Industrial	610	Port
231	Assembly	620	Airport
232	Retail	630	Transit Station
233	Manufacturing	711	Garage
241	Lumber Yard	712	Parking Garage
242	Rail Yard	713	Warehouse
311	One Family Dwelling	714	Storage
312	Two Family Dwelling	810	Agricultural
321	Low Rise Apartment	811	Farm Building
322	High Rise Apartment	812	Greenhouse

A.2 Building Types

Residential Homes: Foundation without reinforced concrete: Residential homes with concrete structure basements, timber framed, timber framed roof, different exterior wall materials A. Stucco, B. Brick, C. Wood Siding









Concrete Structure 1: A concrete structure typically under 4 storeys or 12 metres, Concrete block with a concrete or aggregate roof and Stucco or block exterior no basement just slab on grade. Typically, commercial, etc









Concrete Structure 2: *Concrete Structure a.* A concrete structure typically under 4 storeys or 12 metres, concrete block walls (fire walls) /timber frame with a timber roof, stucco or block wall exterior. *Concrete Structure 2b. Brick exterior*





Concrete Structure - Steel reinforced: Typically, higher than 4 storeys or 12 metres and therefore reinforced. High-rises.





Steel Structure – Concrete Foundation: Typically, industrial warehouses and 1 or 2 storeys. Large





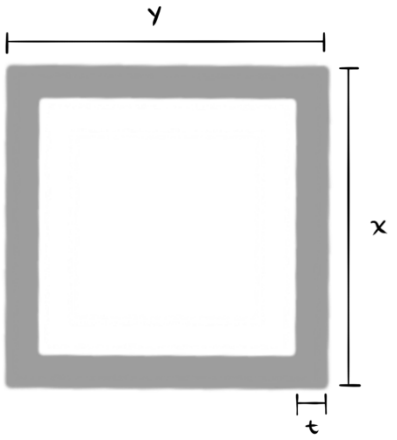


Table A.2 Material Constants

Constant	Value	Source
C_1 (Concrete constant weight)	2400 kg/m^3	https://www.inchcalculator.com/concrete-weight-calculator/
T_1 (Wood/Timber Constant weight)	422 kg/m^3	https://www.canadianwood.com.vn/en/canadian-wood-types/
S_1 (Steel Constant weight)	7848 kg/m^3	https://www.canadianplate.com/metal-weight.html
A_1 (Aggregate Constant weight)	1400kg/m^3	https://www.homedit.com/civil-engineering/materials/concrete/density-of-aggregate/
B_1 (Brick Constant weight)	1922 kg/m^3	https://www.simetric.co.uk/si_materials.htm
G_1 (Glass Constant weight)	2579 kg/m^3	https://www.simetric.co.uk/si_materials.htm

A.3 Equations for measuring material intensities

Concrete Amount: Foundation Footing



No. of Floors Supported	Minimum Width of Strip Footings, mm	
	Supporting Exterior Walls[2]	Supporting Interior Walls[3]
1	250	200
2	350	350
3	450	500

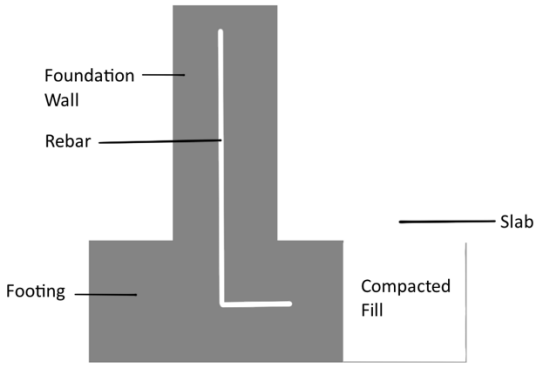
Total footing volume = $(x*y*z_f) – ((x-2(t))* ((y-2(t))*z_f$

Total volume intensity of footing = $\frac{\text{Total footing volume}}{(GV\ (gross\ volume\ of\ home\ (x*y*z)}$

Material Intensity [kg/m^3] = (Total volume intensity of footing) * C_1 (constant concrete weight)

Note z_f – need to contact construction home builders

Concrete Amount: Foundation – Slab
Standard slab size is typically 4 inches



Z_{slab} 4 inches = 0.1016 m

Total slab volume = ($x*y*z_{slab}$)

Total volume intensity of footing = $\frac{\text{Total slab volume}}{(GV\ (gross\ volume\ of\ home\ (x*y*z)}$

Steel Amount: Foundation – Slab

Standard residential rebar size is ½ inch and placed every 36 inches in a concrete slab (in any direction)

- 36 inches = 0.9144 m
- ½ inch = 0.0127 m

Total volume intensity of rebar for slab =

$$\frac{(((\text{Width}/0.9144)\ *\ (\text{Length}*(0.01272)*\pi)\ +\ ((\text{Length}/0.9144)\ *\ (\text{Width}*(0.01272)*\pi))}{(GV\ (gross\ volume\ of\ home\ (x*y*z)}$$

Material Intensity [kg/m^3] = (Total volume intensity of footing) * S_1 (constant steel weight)

Steel Amount: Foundation – Wall

Standard residential rebar size is ½ inch and placed every 24 inches horizontally and 36 inches vertically if in wall

- 36 inches = 0.9144 m
- 24 inches = 0.6096
- ½ inch = 0.0127 m

Total volume intensity of rebar for slab =

$$\frac{\begin{array}{c}((((\text{Height of basement wall}/0.6096)*\ (\text{Length}*(0.01272\text{^}2)*\pi))\ + \\ (((\text{Height of basementwall}/0.9144)*\ (\text{Width}*(0.01272\text{^}2)*\pi))+ \\ (((Length/0.9144)*Height\ of\ basement\ wall)*\ ((0.01272^2)*\pi))+ \\ (((Width/0.9144)*Height\ of\ basement\ wall)*\ ((0.01272^2)*\pi)))*2\end{array}}{(GV\ (gross\ volume\ of\ home\ (x*y*z)}$$

Material Intensity [kg/m^3] = (Total volume intensity of footing) * S_1 (constant steel weight)

Exterior Wall Materials
Wood Siding or Concrete/Stucco

Different type of exterior wall material thickness:
Thickness of Wood siding – ½ inch = 0.127 m
Thickness of Stucco – ½ inch = 0.127 m
Thickness of Brick – 0.1125 m

Brick Total volume intensity of outside wall material =

Stucco:

$$\frac{(\text{Height} * \text{Length} * 0.1125) + (\text{Height} * \text{Width} * 0.1125) * 2}{(GV\ (gross\ volume\ of\ home\ (x * y * z)}$$

Wood Siding:

$$\frac{(\text{Height} * \text{Length} * 0.0127) + (\text{Height} * \text{Width} * 0.0127) * 2}{(GV\ (gross\ volume\ of\ home\ (x * y * z)}$$

Material Intensity [kg/m^3] = (Total volume intensity of footing) * $_1$ (constant weight)

A.4 Material Intensity Summary

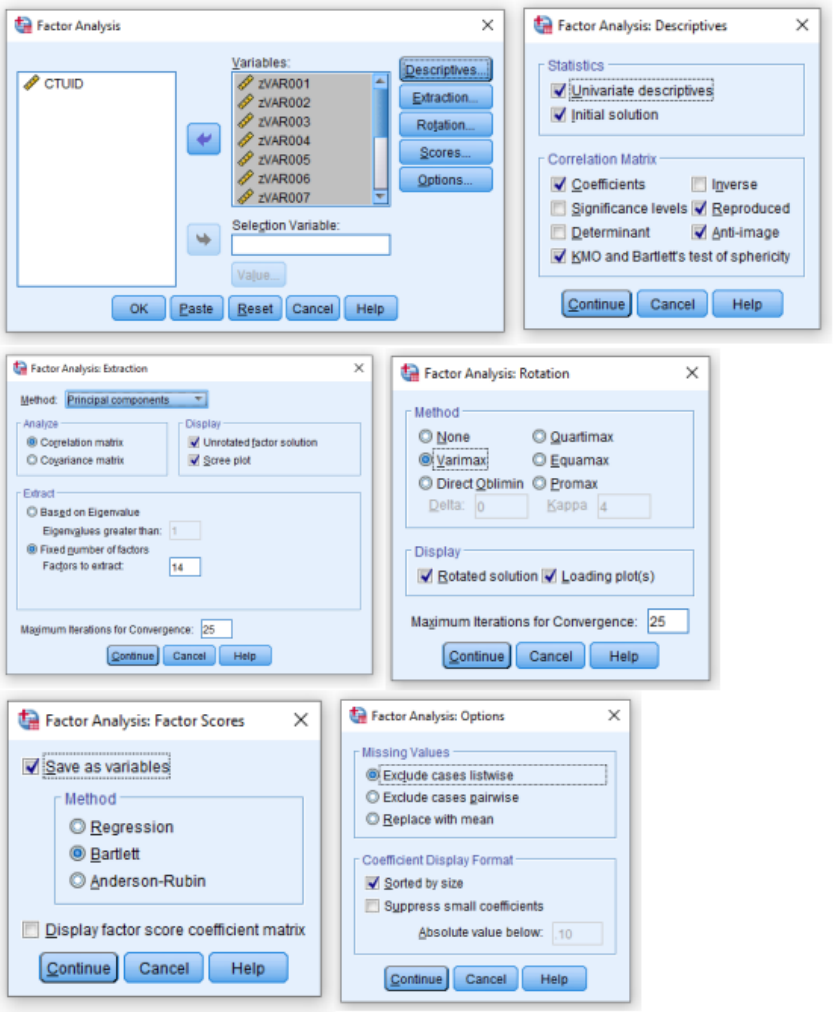
Calculations were automated in excel for each residential home to calculate an average of kg/m^3 intensity. This was done for all single family homes, duplexes, and townhomes. There were 67, 516 homes that fell within this category.

	Aggregate	**Concrete**	**Timber**	**Steel**	**Masonry (Brick)**
Foundation with reinforced concrete					
Foundation - Strip Footings	-	11.7	-	-	-
Foundation - Ground Slab	52.89	44.86	-	1.81	-
Floors	-	-	1.24	-	-
Walls (2 types: red (brick exterior), vinyl (nothing added))	-	45.59 (basement wall)	25.57	6.12	
Roof- Frame	-			-	-
Roof – Covering	-			-	-
Total a. (brick exterior)					
Total b. (vinyl exterior)					-

Appendix B Principal Components Analysis (PC) Procedure

The principal components analyses (PCA) were conducted using the IBM Statistics Package for the Social Sciences (SPSS) Version 26 software. The procedure and settings for running the PCA is detailed below.

1. Run SPSS Factor Analysis Tool Toolbar: Analyze > Dimension Reduction > Factor…
2. Apply the following settings from the "Factor Analysis" window:



B.1 Suitability of PCA

The Kaiser-Meyer-Olkin (KMO) test and Bartlett's test of sphericity are diagnostic measures used to evaluate the suitability of a PCA for a dataset. The KMO test measures the proportion of

variance in the variables that may be caused by underlying factors; strength of relationships among variables; indication of whether PCA will yield distinct and reliable components (Coleman, 2012; Oulahen et al., 2015). The KMO measure ranges from 0 to 1, with higher values (i.e., closer to 1), indicating a higher suitability of a PCA for the dataset. 0.6 is a suggested minimum (Coleman, 2012). Bartlett's test of sphericity is a statistic that measures whether the variables in the dataset are related such that the PCA would be suitable for structure detection (Coleman, 2012; Oulahen et al., 2015). The null hypothesis is that the correlation matrix is an identity matrix – each variable is not correlated to any other variable except for itself. A highly significant test statistic ($p < 0.001$) that rejects the null hypothesis indicates that the PCA is an appropriate procedure for the dataset. The results of the KMO test and Bartlett's test for each census scale and study area are summarized below.

KMO Test	0.650
Bartlett's test	0.000

The results from both statistics indicate that the PCA is an appropriate procedure for computing the SoRI with the available census data.